KU Leuven
Biomedical Sciences Group
Faculty of Medicine
Department of Chronic Diseases,
Metabolism and Ageing

KU LEUVEN

DOCTORAL SCHOOL
BIOMEDICAL SCIENCES

NEURO-IMMUNE INTERACTION IN THE ENTERIC NERVOUS SYSTEM FROM EARLY DEVELOPMENT TO AGING

Maria Francesca Viola

Jury:

Supervisor: Prof. Dr. Guy Boeckxstaens
Co-supervisor: Prof. Dr. Pieter Vanden Berghe
Chair examining committee: Prof. Dr. Patrick Callaerts
Chair public defence: Prof. Dr. Kristin Verbeke
Jury members:
Prof. Dr. Myriam Baes
Prof. Dr. Schalk Van Der Merwe
Prof. Dr. Martin Guilliams
Prof. Dr. Kiavash Movahedi
Prof. Dr. Elvira Mass

Dissertation presented in partial fulfilment of the requirements for the degree of Doctor in Biomedical Sciences

November 2022

Table of Contents

Chapter 1: General Introduction 7
1.1 Introduction 8
1.2 Origin of Intestinal Resident Macrophages 8
1.3 The macrophage niche 11
1.3.1 Niche requirements 11
1.3.2 Niche accessibility and niche availability 13
1.4 Functional heterogeneity of niche-specific macrophages in health and disease 15
1.5 Lamina propria macrophages: the classical view 17
1.6 The enteric nervous system and neuron-associated macrophages 21
1.6.1 Submucosal Neuron-Associated Macrophages 23
1.6.2 Muscularis Neuron-Associated Macrophages 24
1.7 Blood Vessel-associated macrophages 26
1.8 Additional macrophage niches within the intestine 30
1.8.1 Crypt-associated macrophages 30
1.8.2 Peyer's Patch-Associated Macrophages 31
1.9 Concluding Remarks 31

Chapter 2: Objectives and Aims 33

Chapter 3: Development and maintenance of the enteric nervous system orchestrated by dedicated resident macrophages 37
3.1 Abstract 38
3.2 Introduction 38
3.3 Results 40
3.3.1 MMϕ refine the ENS during early postnatal development 40
3.3.2 MMϕ function differs according to the developmental stage of the gut 43
3.3.3 Gene expression profiling revealed transcriptomic adaptation of MMϕ 44
3.3.4 Distinct MMϕ subsets are located in different subtissular niches 47
3.3.5 ENS-derived TGFβ Instructs MMϕ to Adopt a Neuron-Associated Phenotype 51
3.4 Discussion 55
3.4.1 Remodelling of the ENS by MMϕ 55
3.4.2 ENS-MMϕ Relationship in Adulthood 56
3.4.3 The ENS-MMϕ Niche 56
3.4.4 Functional Plasticity of MMϕ 57

3.4.5 Paralleled Role for Macrophages/Microglia in the Central and Enteric Nervous System 57
3.5 Acknowledgements 58
3.6 Author Contributions 58
3.7 Declaration of interests 58
3.8 Data Availability 58
3.9 Materials and Methods 59
3.9.1 Mice 59
3.9.2 Histology and immunofluorescence 59
3.9.3 Ex-vivo live imaging 59
3.9.4 Quantification of synaptic volume and synaptic engulfment 60
3.9.5 Analysis of MMϕ morphology 60
3.9.6 Tissue harvest for single cell suspensions 60
3.9.7 Flow cytometry 60
3.9.8 Sorting of live cells confocal imaging 60
3.9.9 Depletion of muscularis macrophages 61
3.9.10 Whole Gut Transit Time 61
3.9.11 scRNAseq library preparation 61
3.9.12 scRNAseq analysis 61
3.9.13 Ex-vivo phagocytosis assay 63
3.9.14 RNA Isolation and qRT-PCR 63
3.9.15 Sorting of live cells for gene expression analysis 63
3.9.16 Hybridization Chain Reaction (HCR) 63
3.9.17 Structured illumination microscopy (SIM) 64
3.9.18 BMDM experiments 64
3.9.19 Enteric denervation using Benzalkonium Chloride (BAC) 64
3.9.20 AAV9 Transfection Experiments 65
3.9.21 Tamoxifen treatment 65
3.9.22 Statistics 65
3.10 Supplementary Information 66

Chapter 4: Loss of Neuron-Associated Macrophages Promotes Neurodegeneration and Constipation in Aging Female Mice 73
4.1 Introduction 74
4.2 Results 75
4.2.1 Female mice develop constipation with age 75

4.2.2 Characterisation of MMΦ in the aging muscularis externa 78
4.2.3 Gender-specific changes in MMΦ in the aging muscularis externa 81
4.2.4 Insoluble protein aggregates do not cause neurodegeneration in the muscularis externa 84
4.3 Discussion 86
4.3.1 Single-Cell RNA sequencing reveals gender-specific transcriptional shifts in aging MMΦ 86
4.3.2 The role of insoluble protein aggregates in neurodegeneration 87
4.3.3 The role of gender in age-related neurodegeneration 88
4.3.4 Conclusions and future prospects 88
4.3.5 Acknowledgements 89
4.3.6 Author Contributions 89
4.3.7 Declaration of interests 89
4.4 Materials and Methods 90
4.4.1 Mice 90
4.4.2 Whole Gut Transit Time 90
4.4.3 Faecal Output and Faecal Water Content 90
4.4.4 Muscle Strip Organ Bath Experiments 90
4.4.5 Histology and immunofluorescence 91
4.4.6 Ussing Chambers 91
4.4.7 Tissue harvest for single cell suspensions 91
4.4.8 scRNAseq library preparation 92
4.4.9 scRNAseq analysis 92
4.4.10 Flow cytometry 92
4.4.11 Injection of Preformed Fibrils (PFFs) 93
4.4.12 Statistics 93
4.5 Supplementary Information 94

Chapter 5 Conclusions 99
5.1 Muscularis Macrophages From Development to Aging: Common Mechanisms of Neuro-Immune Interaction in the Gut and in the Brain? 100
5.1.1 Macrophages prune synapses and refine myenteric neurons during early postnatal development, thereby contributing to the functional maturation of the ENS (Chapter 3) 102
5.1.2 At weaning, a developmental switch occurs which leads to a shift of muscularis macrophage (MMΦ) transcriptome and function (Chapter 3). 102

5.1.3 Developmental maturation of MMΦ is orchestrated by myenteric neurons, that via production of TGFβ imprint a neuron-associated MMΦ (NA-MMΦ) phenotype; loss of these NA-MMΦ in adulthood leads to neurodegeneration and delayed intestinal transit (Chapter 3). 103

5.1.4 In female mice, aging is characterised by neurodegeneration and constipation, which is accompanied by the loss of NA-MMΦ (Chapter 4). 104

5.1.5 Conclusions and Future Prospects 105

Chapter 6 Scientific Summary 107

Bibliography 110

Personal Contribution and Conflict of Interests 123

Acknowledgements 124

Curriculum Vitae 127

Publication Record 128

Chapter 1

General Introduction

Adapted from:

Niche-specific functional heterogeneity of intestinal resident macrophages

Maria Francesca Viola[1] and Guy Boeckxstaens[1].

Gut 70:1383-1395, 31st of December 2020.

doi: 10.1136/gutjnl-2020-323121.

and

Intestinal neuro-immune interactions: focus on macrophages, mast cells and innate lymphoid cells

Nathalie Stakenborg[1], Maria Francesca Viola[1], Guy E. Boeckxstaens[1]

Current Opinion on Neurobiology 2020, 62:68–75, published online 18th of December 2019.

doi: 10.1016/j.conb.2019.11.020.

1.1 Introduction

The first studies on macrophages revealed the potent ability of these cells to scavenge and phagocytose, and they were rapidly identified as cells crucial to host defence and tissue homeostasis. As macrophage populations were progressively discovered in most tissues, these cells became known as "house-keepers", cells whose purpose is to clear apoptotic cells and defend the host from pathogen invasion. In the intestine, the most characterised macrophage population resides in the lamina propria, interspersed within the villi, in prime position to engulf and clear pathogens and dietary antigens that breach the intestinal barrier. The constant exposure to the content of the lumen, and the low-grade inflammation generated by exposure to commensal microbes, promotes a rapid turnover of lamina propria macrophages, which require continuous replenishment by monocytes circulating in the bloodstream. While in other organs macrophages were shown to derive mainly, if not exclusively, from self-maintaining macrophages that colonise the embryonic tissue, similar studies in the intestine revealed that macrophages seeded embryonically had been replaced by incoming monocytes at around 3 weeks of age, and that the macrophage pool within the intestine relies solely on replenishment by circulating monocytes[1]. For many years, this dogma held true, and intestinal macrophages were frequently cited as being the 'ontological exception', as the only tissue-resident macrophages deriving exclusively from circulating monocytes. Using fate-mapping techniques, we and others demonstrated that the intestine also harbours self-maintaining macrophages that reside in specific anatomical locations within the intestinal wall. These macrophages interact closely with surrounding cells and carry out specific functions, suggesting that they receive cues from the surrounding environment, a concept otherwise known as the macrophage "niche"[2]. Here, I will discuss the recent novel insights in the role of these specialised macrophage populations and speculate how these subsets may be implicated in gastro-intestinal disease.

1.2 Origin of Intestinal Resident Macrophages

Since their first description by Nobel Prize laureate Elie Metchnikoff in 1878, subsequent research uncovered that tissue resident macrophages throughout different organs have similar morphological and functional characteristics, suggesting that they share a common progenitor. This led to the introduction of the mononuclear phagocyte system (MPS) in the 1970s, which postulated that all tissue resident macrophages derive from monocytes circulating in the bloodstream migrating into intestinal tissue where they undergo further differentiation [3,4]. However, the advent of fate-mapping technologies and parabiosis experiments have largely refined this hypothesis. It is now clear that most tissue resident macrophage populations originate largely, if not exclusively, from precursors seeded embryonically and are able to self-maintain within the tissue[5–7]. Resident macrophages can only be

replaced by circulating haematopoietic monocytes under specific conditions, such as depletion or disappearance over time. Thus, macrophage pools in different tissues constitute a heterogeneous population with varying contributions of macrophages of embryonic and haematopoietic origin (Figure 1). Macrophages within the central nervous system represent one extreme of this ontological spectrum, as they are almost exclusively derived from embryonic progenitors that give rise to an adult macrophage pool that self-maintains throughout adulthood without contribution of circulating monocytes, with exception of choroid plexus macrophages[8]. In other organs, such as skin, heart, pancreas and the liver, embryonic precursors and circulating monocytes both give rise to the resident macrophage pool, although the contribution of monocytes tends to increase over time [9–13].

Embryonic precursors of macrophages are seeded before birth and derive from either yolk-sac erythro-myeloid progenitors (EMPs) or fetal-liver precursors. In mice, embryonic hematopoiesis occurs in three sequential waves and begins at E7.0 (seventh day of embryonic life) with the primitive wave in the yolk sac, which gives rise to erythroblasts, megakaryocytes and macrophages[14–17]. Of note, microglia are the only macrophage population known to derive directly from primitive myeloid progenitors that arise in the yolk sac before E8.0[18,19]. Once the blood circulation is established at E8.5, a second wave of EMPs migrates from the yolk sac to the fetal liver, where EMP-derived fetal monocytes will give rise to tissue-resident macrophages[20]. From E10.5, the third and final wave starts, giving rise to fetal hematopoietic stem cells for lifelong haematopoiesis, which eventually seed the bone marrow at E17.5[21]. However, the exact contribution of each wave of embryonic precursors to the different mature macrophage pools in the adult is subject to intense debate as yet, not all transcription factors involved have been identified. Within the intestinal lamina propria, initial studies revealed that, although the intestine is seeded by embryonic precursors from E8.5 onwards, these cells do not persist to adulthood and they are replaced by incoming bone marrow-derived monocytes around the time of weaning[1]. Recently, however, using murine fate-mapping models, we and others were able to show that in the gut, as in other organs, embryonic progenitors give rise to a subset of macrophages that are able to self-maintain and persist into adulthood[22,23]. These long-lived, self-maintaining macrophages occupy well-defined niches within the gut wall, notably the submucosal and myenteric plexus, intestinal crypts and vasculature (Figure 1).

In humans, there is also mounting evidence that points towards a similar mixed ontogeny for tissue resident macrophages. Studies in sex-mismatched organ transplantation enable the assessment of longevity/self-maintenance of donor-derived tissue-resident macrophages and their replenishment by circulating monocytes of the recipient. In some organs, such as the derma, donor-derived tissue resident macrophages are rapidly replaced by circulating monocytes of the host, whereas in other organs, such as the lung and heart, a population of donor-derived tissue resident macrophages persists through local proliferation and is not replenished[24–26]. A similar transplantation study in the intestine by Bujko and

colleagues elegantly showed that macrophage subsets are replaced at differing rates by circulating cells, suggesting that a similar ontological heterogeneity exists also within the human intestine[27]. These studies suggest that in human tissues, mature resident macrophage pools can be replenished by circulating cells, but that there is likely also a population of self-maintaining resident macrophages. Further evidence for self-maintaining resident macrophages derives from several reports of patients with congenital monocytopenia in which the number of tissue-resident macrophages in various organs was not affected[28,29]. These findings support the hypothesis that also in humans, resident macrophages are able to develop and maintain in the absence of monocytes, likely through self-maintenance. In line with murine findings, this study revealed that these long-lived macrophage subsets tend to occupy specific niches and may be functionally distinct from their incoming counterparts.

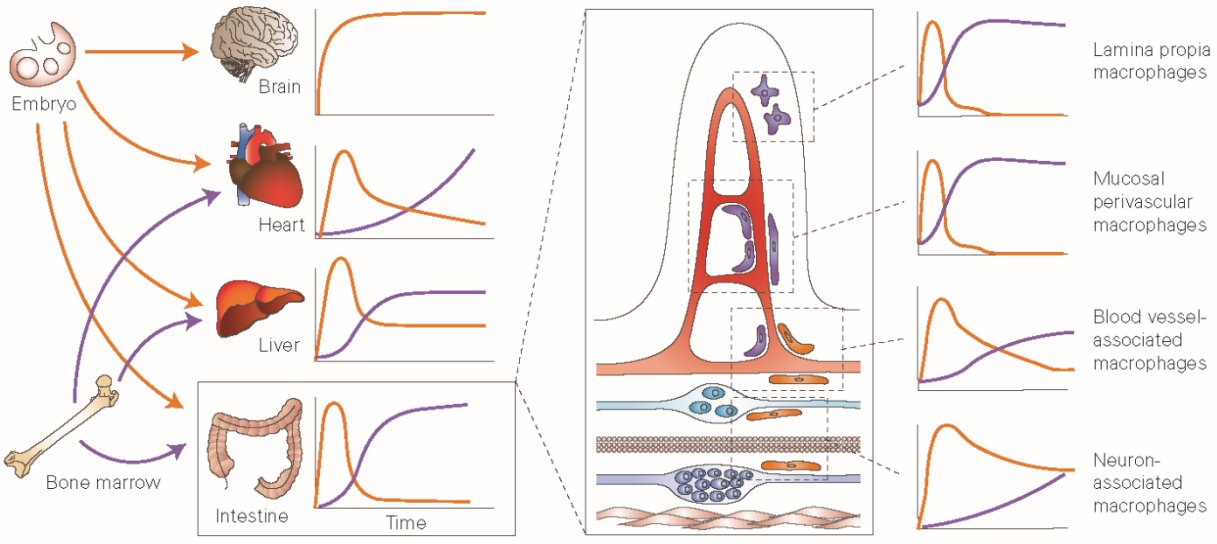

Figure 1: Ontogeny of tissue resident macrophages. Most organs contain a heterogeneous mix of bone marrow derived macrophages and macrophages deriving from embryonic progenitors; however, in the brain, the resident macrophage population (microglia) derives solely from the proliferation of progenitors seeded in the embryo. Of note, the two first embryonic waves are represented together in this figure, for simplicity. Within the intestine, the large majority of macrophages derive from the bone-marrow, however a small population of macrophages derives from embryonic progenitors and is able to self-maintain in adulthood. These self-maintaining macrophage populations colonise specific niches in close proximity to the vasculature in the submucosa, and enteric neurons. Other macrophage populations, located in the villi and surrounding the mucosal vascular network, derive entirely from precursors that originate in the bone-marrow. Adapted from Ginhoux and Guilliams, Immunity 2016[13].

1.3 The macrophage niche

1.3.1 *Niche requirements*

Although macrophages have been studied for over a century, advances in RNA sequencing and single-cell RNA sequencing have only recently revealed highly specialised macrophage populations, insight that has led to the introduction of the concept of macrophage niche. In recent years, studies have uncovered populations such as immunoregulatory neuron-associated macrophages in the lung, collagen-degrading Lyve1^{+} macrophages associated with blood vessels, lipid-associated macrophages regulating adipocyte size and metabolic homeostasis in adipose tissue, and many more[30–32]. These macrophage subsets occupy distinct anatomical locations and perform unique functions, suggesting that the surrounding cells participate in the instruction of macrophages to imprint functions specific to the niche (Figure 2). Furthermore, when circulating cells of hematopoietic origin differentiate into tissue-resident macrophages, they acquire a similar phenotype, functional specialisation and, often, ability to self-maintain as their embryonic resident counterparts[33]. The concept that macrophages adapt functionally to the niche in which they reside implies the existence of a combination of trophic factors, signalling molecules and physical scaffolding present within a specific tissue that is able to imprint this precise function and phenotype on the macrophage[2]. In turn, it is likely that the adopted phenotype of the macrophage is of benefit, or may even be critically important, to the imprinting niche, as illustrated by the examples above.

Macrophages depend on a continuous supply of trophic factors such as colony stimulating factor 1 (CSF1 or M-CSF), colony stimulating factor 2 (CSF2 or GM-CSF) and IL-34 for their development and maintenance, and express the corresponding receptors Csf1r or Csf2r[34–39]. Csf1r is required for the development, proliferation, survival and recruitment of tissue resident macrophages in most organs, whereas Csf2r deficiency mainly affects lung macrophages[40–43]. Intestinal macrophages express Csf1r and depend on CSF1 to differing levels, as Csf1$^{op/op}$ mice present almost complete loss of macrophages in the muscularis externa, and only a reduction of macrophages in the lamina propria [44–46]. Within the intestine, neurons and interstitial cells of Cajal produce CSF1 to maintain the macrophage population within the muscularis externa[45,47]. However, while Csf1r-expressing macrophages are present within the lamina propria and are ablated upon Csf1r blockade, CSF1 production has so far only been reported by unidentified cells located at the base of intestinal crypts, most likely Paneth cells, and by epithelial cells located at the base of gastric pyloric glands [46,48–50].

Additional signalling molecules may be involved in the niche-specific instruction of the macrophage, as shown for Transforming Growth Factor beta (TGFb) in the case of microglia and colonic macrophages, TGFb and bone morphogenetic protein 7 (BMP7) for mucosal Langerhans cells and TGFb, BMP9 and

desmosterol for liver Kupffer cells[51–55]. Further programming of macrophages may also occur through phagocytosis of specific metabolites. This process occurs in red pulp macrophages in the spleen, which upon phagocytosis of aged erythrocytes sense heme and upregulate transcription factor Spi-C, which controls iron-recycling in macrophages (Figure 2)[56]. Thus, imprinting of specific functions within the niche can occur due to cell-to-cell interaction via secreted molecules, or engulfment of metabolites that can activate transcriptional programming.

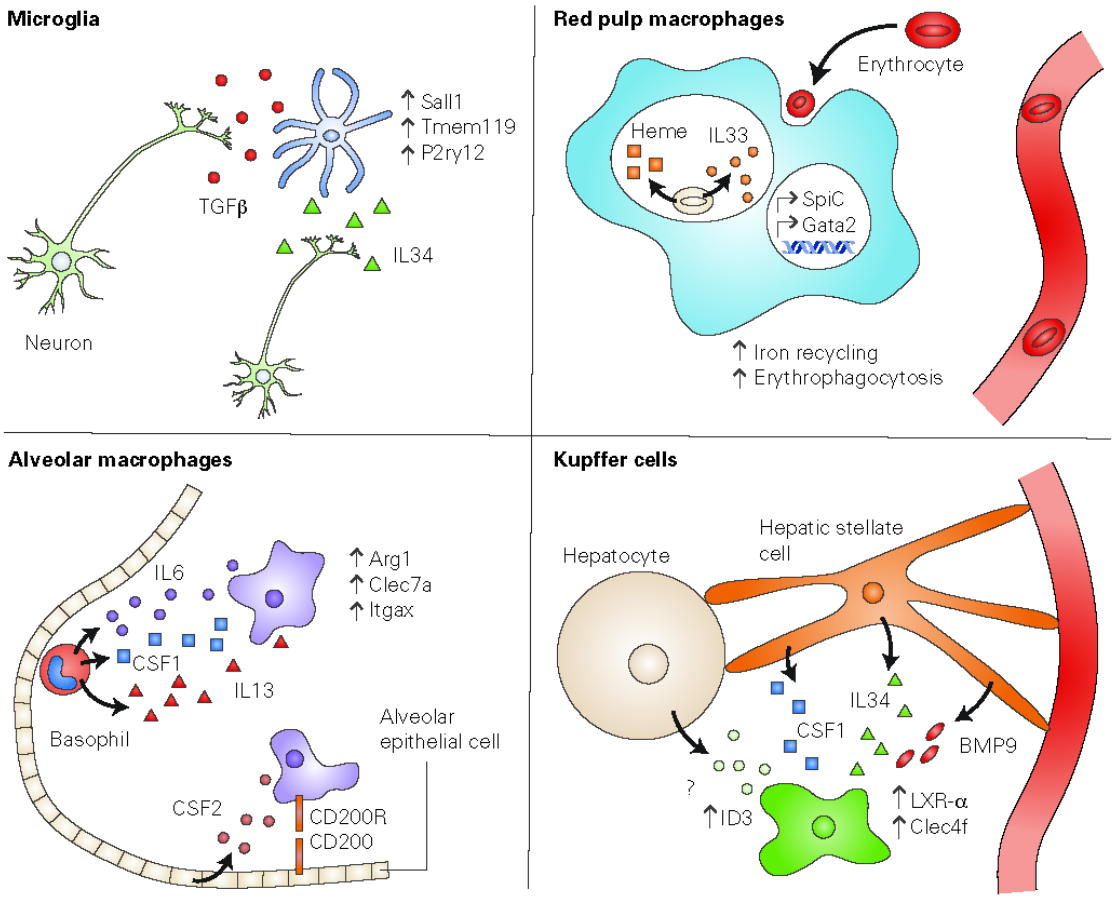

Figure 2: Local signals imprint macrophage phenotype. The local cellular environment produces signals which are able to activate specific transcriptional profiles within tissue resident macrophages, conferring a niche-specific phenotype or function to the macrophage. In the brain, neurons produce Il34, a growth factor required for the survival and proliferation of macrophages. In addition, neurons produce TGFβ, which has been shown to induce the expression of microglia-specific genes. In the spleen, red pulp macrophages clear aged erythrocytes via phagocytosis (erythrophagocytosis). The phagocytosed erythrocytes release mediators that upregulate transcription factors including SpiC and Gata2, leading to an increase of iron recycling and further erythrophagocytosis. Alveolar macrophages in the lung interact with alveolar epithelial cells via CD200-CD200R interaction. Epithelial cells are also a critical source of CSF2, a growth factor necessary for alveolar macrophage survival. Furthermore, basophils produce a variety of signalling molecules which are critical for the transcriptional signature of alveolar macrophages. Finally, Kupffer cells in the liver require multiple signalling molecules produced by hepatic stellate cells to upregulate Kupffer cell-specific genes, including Clec4f. Furthermore, hepatocytes seem to be necessary for the upregulation of ID3, another Kupffer cell specific gene, however the mechanism through which this signalling occurs is unknown. Kupffer cell panel adapted from Bonnardel et al., Immunity 2020 [53].

1.3.2 *Niche accessibility and niche availability*

Colonisation of a specific niche is determined largely by niche accessibility and niche availability, which regulate the contribution of circulating cells to the niche[57]. *Niche accessibility* is determined by the presence of a barrier and whether it impedes the passage of circulating cells to the niche. Microglia, for example, being isolated from the blood stream by the blood-brain barrier, are uniquely of embryonic origin, whereas spleen, peritoneal and liver macrophages, which are more readily accessible from the blood stream, receive a progressively higher input by circulating cells with age (Figure 3)[58]. *Niche availability*, on the other hand, is determined by whether there are empty niches that can be colonised, due to neonatal tissue growth, for example, or loss of resident cells due to inflammation (Figure 3). Finally, engraftment by circulating cells is subject to competition from the presence of local resident self-maintaining macrophages, which are able to proliferate, differentiate in response to local signals, and occupy the niche. In most tissues, in the absence of inflammation, maintenance of the local tissue-resident macrophage pool occurs through self-maintenance. However, inflammation can lead to loss of resident macrophages and render the niche accessible to blood monocyte engraftment. It can induce a rapid and substantial recruitment of monocytes**,** triggered by the release of chemokines. These monocytes must first differentiate into macrophages before they compete with resident proliferating cells for the available niche. The role of inflammation in facilitating engraftment of monocytes may be the reason why macrophages in the lamina propria of the intestine are so readily replaced by circulating cells, whereas their counterparts deeper within the gut wall are not readily replaced, as will be discussed in further detail in the following paragraph. The lamina propria is continuously exposed to the contents of the intestinal lumen and the microbiota, which has been proposed to constitute a source of permanent 'physiologic' or 'controlled' inflammation[59]. Similarly, in organs where monocyte engraftment increases progressively with age, it is possible that low-grade inflammation associated with aging ('inflamm-aging') or metabolic stress, in addition to a potential loss of self-renewal capacity of resident cells, may drive infiltration of incoming monocytes [60,61].

The fact that resident macrophages proliferate when a niche becomes available implies that macrophages possess the ability to sense loss of their counterparts. Furthermore, tissue-resident macrophages tend to display a regular pattern and distribution within the tissue, suggesting that they can detect, and are potentially repelled by, neighbouring cells[62,63]. This phenomenon is somewhat reminiscent to quorum-sensing, the system that bacteria use to regulate population density. The mechanisms underlying macrophage quorum sensing are unknown, however availability of trophic factors may be involved [57]. Indeed, low levels of CSF1 are necessary for macrophage survival while high

levels are able to induce macrophage proliferation[64–66]. Macrophages, as the predominant cell type that express Csf1r, consume available CSF1, thereby keeping CSF1 levels low and thus inhibiting macrophage proliferation. Upon loss of resident macrophages, unconsumed CSF1 leads to a rise in CSF1 levels, thereby unlocking macrophage proliferation (Figure 3). Furthermore, CSF1 may also regulate monocyte replenishment, as increased CSF1 leads to monocytopenia in the circulation, and recruitment of monocytes to the tissue through induction of CCR2 ligands[64,66,67].

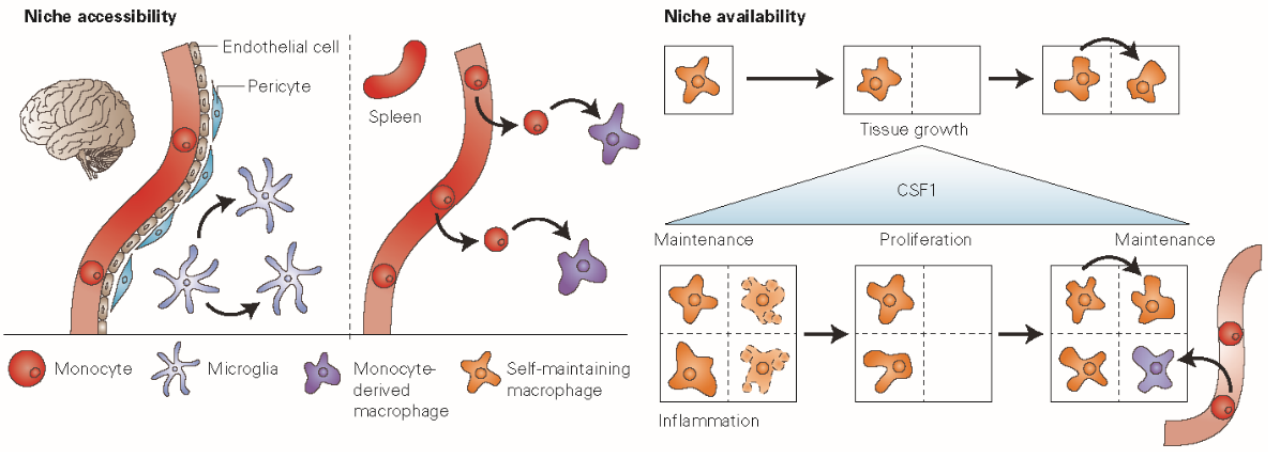

Figure 3: Accessibility and availability of the macrophage niche. The colonisation of a macrophage niche by self-maintenance of resident cells or incoming monocytes that differentiate into macrophages depends on niche accessibility and niche availability. *Niche accessibility*: In the brain, the blood brain barrier made up of endothelial cells, pericytes and astrocytes (not shown) impedes the egression of monocytes, therefore maintenance of tissue resident macrophages (microglia) occurs solely through local proliferation. In organs such as the spleen, where no vascular barrier is present, monocytes can easily leave the blood stream and differentiate to macrophages within the tissue. *Niche availability*: a macrophage niche may become available due to tissue growth, leading to the proliferation of local macrophages that then occupy the open niche. If a macrophage niche becomes available due to inflammation and loss of macrophages (represented here using a dotted line), there may be engraftment of monocytes that differentiate to macrophages. It is plausible that the regulation of macrophage numbers may be determined by the levels of available CSF1, which has been shown to promote macrophage maintenance and proliferation.

1.4 Functional heterogeneity of niche-specific macrophages in health and disease

Macrophages can be found throughout the gastrointestinal tract, where they occupy distinct niches and carry out a variety of functions. The most abundant macrophage population is represented by the lamina propria macrophages that reside within the villi. Lamina propria macrophages are crucial for host defence and intestinal homeostasis and require constant replenishment by circulating cells. In addition, we recently demonstrated that deeper within the gut wall, there are several populations of macrophages that are able to self-maintain, and derive partially from precursors seeded embryonically[22,23]. To demonstrate this, we made use of a murine fate-mapping model, which enables irreversible labelling of Cx3cr1^{+} cells present at the time of tamoxifen administration. Using this approach, we were able to demonstrate that a subset of intestinal macrophages, labelled at 4-6 weeks of age, retained labelling even 35 weeks after tamoxifen administration[22]. Furthermore, by administering tamoxifen to pregnant dams, we were able to demonstrate that a population of macrophages seeded within the embryo persists until adulthood. These findings clearly demonstrate that a subset of intestinal macrophages is able to self-maintain within the tissue and does not require replenishment from circulating monocytes. Interestingly, when studying the anatomical location of self-maintaining macrophages in the intestine, we observed that these cells occupy specific areas within the gut wall, distant from the lumen, and in close proximity to the enteric neurons and blood vessels found in the submucosa and muscularis externa, and Paneth cells. Using single-cell RNA sequencing, we showed that these subpopulations are transcriptionally distinct, suggesting that they receive imprinting from the surrounding cells. It is thus clear that, in addition to short-lived lamina propria macrophages, specialised macrophage subsets subject to reduced turnover and self-maintaining, occupy specific niches within the gut (Table 1). In the following paragraphs, I will discuss the functional specialisations of these different subsets and speculate on how they may be implicated in gastro-intestinal disease.

Niche	Location	Marker	Function	Notes	Key reference
Blood Vessel	Small Intestine	Adamdec1†	Vascular integrity maintenance	• Self-maintaining	De Schepper et al., Cell 2018 [22]
Neuron	Small Intestine	Fcrls†	Required for the survival of enteric neurons	• Self-maintaining	De Schepper et al., Cell 2018 [22]
Unknown	Small Intestine, Colon	Tim4 CD4	Unknown	• Self-maintaining	Shaw et el., JEM 2018 [23]
Blood Vessel/ Crypt	Small Intestine, Colon	CD169	Monocyte recruitment in colitis		Asano et al., Nature Communications 2015 [68]
Crypt	Small Intestine	Unknown	Unknown	• Self-maintaining	De Schepper et al., Cell 2018 [22]
Peyer's Patch	Small Intestine	Tim4 CD4	$Tim4^+$: Phagocytosis $Tim4^-$: Microbial defense	• Tim4 expression discriminates subsets with distinct location and function	Bonnardel et al., Cell Reports 2015 [69]
Blood Vessel	Small Intestine	Unknown	Regulation of bacterial translocation to blood	• Microbiota-dependent • Monocyte-derived	Honda et al., Nature Communications 2020 [62]
Epithelium	Colon	Cd11c Cd121b	Unknown	• Microbiota-dependent	Kang et al., Mucosal Immunology 2020 [70]

Table 1: Overview of macrophage populations present within the intestine, with details regarding niche, location, markers and function where known. Markers included are either surface markers, or proposed gene markers derived from single-cell RNA sequencing experiments (labelled with †). Further comments on longevity and microbiota-dependence, in addition to the key reference, are also included.

1.5 Lamina propria macrophages: the classical view

The most abundant and amply characterised macrophage population within the GI tract resides within the intestinal mucosa and villi. Lamina propria macrophages are positioned in the first line of defence to respond to bacteria and food antigens that breach the intestinal barrier and are thus crucial for maintaining the delicate balance between pathogen defence and oral tolerance (Figure 4). Lamina propria macrophages are highly phagocytic; however, upon ingestion of food antigens or harmless commensal bacteria, they do not release pro-inflammatory mediators or nitric oxide, thereby preventing the influx of other immune cells (that might conceivably induce collateral damage) and maintaining tissue homeostasis[71–73]. In addition, lamina propria macrophages participate in oral tolerance via the presentation of trapped antigens to $CD103^{+}$ dendritic cells, which then migrate to mesenteric lymph nodes to induce antigen-specific regulatory T cells[74–76]. Conversely, the expansion within the intestine of $FoxP3^{+}$ regulatory T cells, which are involved in oral tolerance to dietary antigens, relies on IL-10. IL-10 is produced by lamina propria macrophages in the presence of microbiota. However, macrophage-derived IL-10 is dispensable for oral tolerance and regulatory T cell maintenance, whereas IL-10 produced by the regulatory T cells themselves is critical for oral tolerance[77–79]. These findings, in addition to contradicting reports regarding the importance of Cx3cr1-expressing macrophages in the establishment of oral tolerance, suggest that our understanding of how macrophages may participate in oral tolerance is incomplete and warrants further investigation. $Cx3cr1^{high}$ macrophages may participate in antigen presentation also by luminal sampling, as these cells extend dendritic projections through the epithelium to capture antigens within the lumen[80,81]. Projection of dendrites is enhanced by lactic acid and pyruvic acid, two common microbial metabolites, via GPR31 in $Cx3cr1^{high}$ macrophages[82]. Finally, lamina propria macrophages help to preserve epithelial integrity by phagocytosing apoptotic cells in the intestinal epithelium, and this is illustrated by *Csf1* deficient mice, which display impaired epithelial differentiation and renewal[83,84]. Interestingly, a recent single-cell RNA sequencing study uncovered a novel population of CD121b+ macrophages located close to the tips of the villi, thereby in close proximity to apoptotic cells of the epithelium and intestinal microbes[70]. In line with this finding, this population was greatly reduced in germ-free mice, further supporting a role of the intestinal microbiota in shaping the phenotype of intestinal macrophage populations.

As will be discussed in the following paragraphs, there is compelling evidence for the existence of specialised niches within the lamina propria, such as crypt-associated macrophages. However, it is a subject of debate whether the macrophage population that is located within the villi (and is dedicated to host defence and phagocytosis), truly represents a differentiated niche. While these cells present a certain degree of functional specialisation, the pool of macrophages in the lamina propria requires a

high level of replenishment by bone marrow-derived monocytes. Parabiosis and bone-marrow chimera experiments have demonstrated that circulating donor cells will readily engraft within the gut wall and contribute to the lamina propria macrophage pool[1,5]. Once within the tissue, newly recruited monocytes rapidly undergo differentiation to adopt a mature macrophage phenotype through a series of well-defined intermediate stages, a process otherwise known as the monocyte to macrophage waterfall (Figure 4)[1,85]. In this process, which depends on the transcription factor *Nr4a1*, newly recruited cells rapidly acquire major histocompatibility complex (MHC) type II (MHCII) expression, downregulate Ly6C and extravasation genes, and finally upregulate Cx3cr1 to acquire a mature macrophage phenotype[51,62,71,85]. The acquisition of the mature Cx3cr1^{high} MHCII^{high} Ly6C^{-} phenotype occurs in 5-6 days and is paralleled by significant changes in gene expression, most notably genes involved in phagocytosis, genes of the complement pathway and Il-10[51]. Newly recruited macrophages, however, still differ transcriptionally from their resident counterparts 12 days after engraftment, and likely continue to undergo further differentiation with time. Interestingly, the dynamics of differentiation of engrafted cells appears to diverge between the small and the large intestine, suggesting that the environmental cues, such as the microbiome, imprinting incoming macrophage cells may be region-specific[86]. A monocyte-to-macrophage "waterfall" has also been described in the human intestinal mucosa, in which CD14^{hi} CCR2^{+} CD11C^{hi} monocytes transition through intermediate populations, giving rise to mature CD14^{lo} CCR2^{-} CD11C^{lo} macrophages (Figure 4)[27,71,87]. In contrast to murine intestinal macrophage maturation, however, human monocytes downregulate CX3CR1 as they differentiate into macrophages[87].

The high turnover and dependence of lamina propria macrophages on circulating monocytes argues against the lamina propria constituting a niche. However, it is possible that lamina propria macrophages merely require such a high rate of replenishment and replacement due to the permanent 'physiologic' inflammation generated by exposure to commensal microbiota and dietary antigens. This hypothesis is supported by the fact that lamina propria macrophages themselves upregulate monocyte chemoattractants such as CCL7, CCL8 and CCL12 as they differentiate from monocytes[51,59]. This continuous inflammatory stress may drive premature macrophage death, in addition to providing the inflammatory stimuli for the recruitment of incoming cells. In line with this hypothesis, replenishment of lamina propria macrophages by circulating monocytes occurs at a much slower rate in germ-free or antibiotic-treated mice[1,23,88]. There is little evidence, however, to support the notion that there are self-maintaining macrophages within the lamina propria pool. In mice lacking the C-C motif chemokine receptor 2 (CCR2), which controls Ly6C^{hi} monocyte egress from the bone marrow, and mice in which monocytes are depleted, lamina propria macrophages are significantly reduced[71,89,90]. Furthermore, upon thermal injury, local Cx3cr1^{+} macrophages surrounding the injury site did not proliferate and the

injury site was replenished by $CCR2^+$ monocytes, which then differentiated into $Cx3cr1^+$ macrophages[62]. Replenishment of the injury site by monocytes also occurred in antibiotic-treated mice, albeit at a slower rate, further supporting the notion that inflammatory stimuli generated by the presence of the microbiota favours monocyte engraftment, and that the lamina propria may not harbour resident cells capable of self-maintenance. However, experiments employing depletion of lamina propria macrophages, followed by adoptive transfer of labelled monocytes, demonstrated that monocyte-derived macrophages in the lamina propria can proliferate within the niche[91]. Although these experiments were carried out in an arguably artificial setting, they do demonstrate that monocyte-derived macrophages are able to proliferate and colonise a niche, if the niche is empty. It is plausible that self-maintaining macrophages alone may not be sufficient to guarantee host defense at the mucosal barrier, and that only a continuous supply of newly differentiated macrophages is able to protect the lamina propria from bacterial invasion.

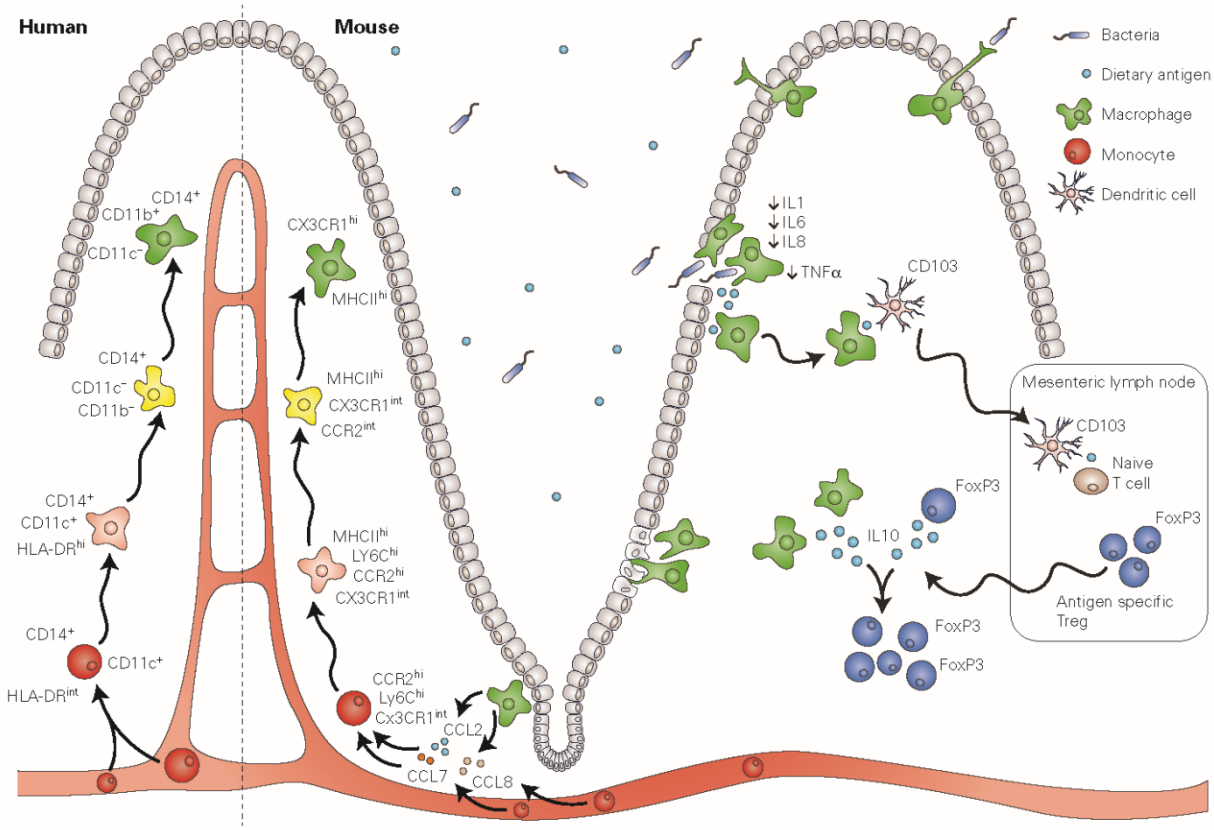

Figure 4: Lamina propria macrophages in mouse and in human: The classical view. The pool of macrophages located within the lamina propria requires a high level of replenishment by circulating monocytes, which upon egression from the blood stream rapidly undergo a series of well-defined steps (known as the monocyte to macrophage 'waterfall') to differentiate into macrophages. This process has been extensively studied within mouse, however studies suggest that a similar process is present also within the human lamina propria. Fully matured lamina propria macrophages are play a major role in host defense and are responsible for the phagocytosis of bacteria and dietary antigens which breach the mucosal barrier. Upon ingestion, lamina propria macrophages downregulate the expression of pro-inflammatory cytokines and mediators, thereby promoting oral tolerance. Lamina propria macrophages have also been implicated in the development of oral tolerance, as they have been shown to present trapped antigens to dendritic cells, which then migrate to the mesenteric lymph nodes to induce antigen-specific regulatory T cells. Antigen-specific regulatory T cells then migrate to the intestine, where their expansion is mediated by IL-10 produced by lamina propria macrophages and the regulatory T cells themselves.

1.6 The enteric nervous system and neuron-associated macrophages

The gastrointestinal tract receives extrinsic input by the peripheral nervous system, which together with intrinsic enteric neurons coordinates intestinal functions including smooth muscle contractility, intestinal secretion and blood flow[92]. The peripheral nervous system consists of the sympathetic nervous system, of which the main neurotransmitter is norepinephrine, and the parasympathetic nervous system, whose primary neurotransmitter is acetylcholine. Together the sympathetic and parasympathetic nervous systems (i.e. vagus nerve) provide the extrinsic neural control of vital gut functions including regulation of smooth muscle contractility, blood flow and fluid secretion. Besides this efferent brain-to-gut communication, peripheral information is conveyed to the central nervous system through vagal afferent neurons of the nodose ganglion and via nociceptive and visceroceptive splanchnic and pelvic afferents originating from the thoracolumbar and lumbosacral dorsal root ganglions, respectively. In general, vagal afferents provide information about physiological processes including hunger and satiety, whilst spinal afferents inform the brain about pain and discomfort. Indeed, splanchnic afferents express voltage-gated sodium channels such as $Na_v1.8$ and $Na_v1.9$, purinoceptors and transient receptor potential (TRP) channels involved in pain perception, whilst vagal afferents are activated by hunger/satiety-related peptide hormones (i.e. cholecystokinin and leptin) released by enteroendocrine cells. Of note, both types of afferents also express receptors for pro-inflammatory mediators released by immune cells. Upon their activation, the afferent neurons will transmit information to the brain to modulate tissue inflammation accordingly.

The GI tract itself is also under control of the intrinsic enteric nervous system (ENS), which consists of an extensive network of interconnected neurons and glia and is capable of functioning autonomously from the central nervous system. The ENS develops from progenitors of the neural crest, which colonise the gastrointestinal tract prior to birth in a process that is extremely fine-tuned in time and space, and is orchestrated by an interplay between signalling molecules and receptors that ensures complete innervation of the gut[93]. While the process of colonisation by progenitors terminates prior to birth, neuronal subtypes develop at differing rates, and the full range of neuronal differentiation is only reached after birth[94]. In the gut, neurons arrange themselves into interconnected ganglia that occupy distinct sub-anatomical layers; the submucous plexus that lies deep in the submucosa, and the myenteric plexus, located between the two muscle layers that compose the *muscularis externa.* These two layers are interconnected, and equipped with a non-myelinating population of enteric glia that provide protection and are crucial for the maintenance of homeostasis.

The ENS is equipped with sensory (i.e. primary afferent), motor and interneurons. Neurons in the submucous plexus control fluid secretion and transport, nutrient absorption and blood flow, whereas

myenteric neurons mainly coordinate gut muscle contractility. Although most enteric neurons are cholinergic, other types of neurons communicate via the release of neurotransmitters and neuropeptides such as nitric oxide (NO), adenosine triphosphate (ATP), vasoactive intestinal peptide (VIP) and calcitonin gene-related peptide (CGRP). In addition to communicating with other neurons and enteric glia, there is also an intense crosstalk between enteric neurons and immune cells, in particular macrophages, mast cells and innate lymphoid cells, which is critical for the maintenance of homeostasis[95]. In particular macrophages have been shown to be critical for the function of enteric neurons, and using a fate-mapping model, we recently identified populations of self-maintaining neuron-associated macrophages critical for neuronal survival in both the myenteric and the submucosal plexus (Figure 5)[22].

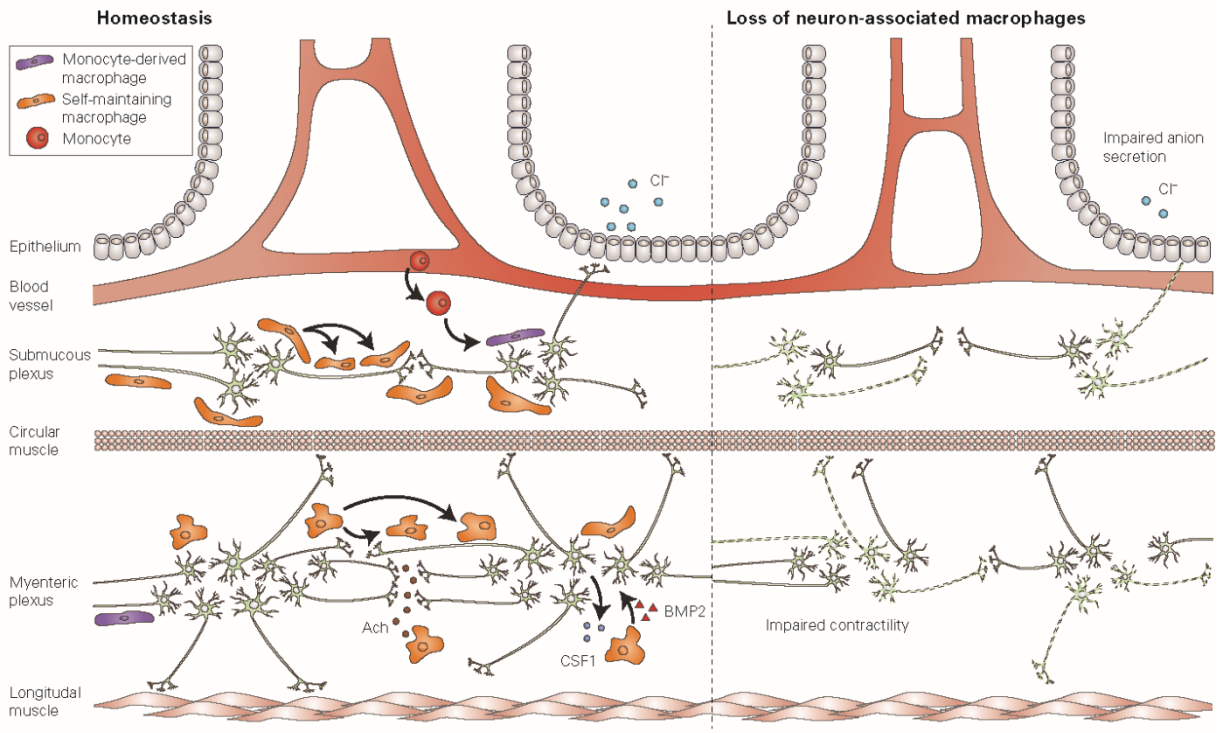

Figure 5: Neuron-associated macrophages. Neuron-associated macrophages are located in close proximity to enteric neurons within the submucous plexus and the myenteric plexus, located deep within the gut wall. Neuron-associated macrophages are largely self-maintaining and receive little input from circulating cells. Neurons in the myenteric plexus maintain the macrophage population via production of CSF-1, which is necessary for macrophage survival. Furthermore, acetylcholine released from enteric neurons can modulate the phenotype of macrophages in the context of intestinal inflammation. Conversely, macrophages within the muscularis externa produce BMP2, which is critical for peristalsis. Selective depletion of neuron-associated macrophages leads to a loss of enteric neurons in both the myenteric and submucosal plexi, leading to impaired intestinal contractility and impaired anion secretion.

1.6.1 *Submucosal Neuron-Associated Macrophages*

The submucosal plexus, also known as Meissner's plexus, is situated in the submucosal region between the circular muscle and mucosa. In close association to the neurons of the submucous plexus, there is a population of macrophages that is primarily self-maintaining, as over 90% of cells located in this niche is derived from macrophages that were present, and labelled, at birth. Submucosal neuron-associated macrophages occupy a niche that is relatively distant from the intestinal lumen, food antigens and bacteria, and are thus characterised by a distinct transcriptome and turnover compared to lamina propria macrophages. Single-cell RNA sequencing of all self-maintaining macrophages revealed a subpopulation of macrophages that upregulate neuron-associated genes, and can be localized to the submucosal plexus via in-situ hybridization[22]. These neuron-associated macrophages upregulate genes which have been reported to be enriched in microglia, including *Fcrls*, *Mef2a*, *Hexb* and *Gpr34*, suggesting that they receive predominant imprinting from neuronal signals, as occurs for microglia in the brain. In line with this concept, a similar imprinting of a 'microglia-like' signature has recently been reported in neuron-associated macrophages in peripheral nerves located throughout the body[96]. Wang and colleagues studied macrophages associated to dorsal root ganglia, vagal nerve, subcutaneous fascial nerves and sciatic nerves and found a core 'microglia-like' expression signature, characterised by genes such as *Tmem119*, *P2ry12*, *Siglech*, *Trem2* and *Olfml3*[96]. However, a recent study profiling sciatic nerve associated macrophages found these cells to be rather more similar to border-associated macrophages, that represent a macrophage population in the brain distinct from microglia[97]. Furthermore, microglia express the unique transcription factor Sall1, that is not expressed in other tissue-resident macrophages, suggesting that the distinct embryonic origin of microglia is able to confer a specific transcriptional profile that cannot be fully recapitulated by tissue resident macrophages located in proximity to nerve fibers[98,99]. It is thus clear that ontogeny plays a part in defining transcriptional identity, in addition to further imprinting by local, niche-specific signals.

Neuron-associated macrophages within the submucous plexus are crucial for neuronal survival, as their selective depletion leads to apoptosis of submucosal neurons mediated by Caspase-3, and impaired neuron-evoked intestinal anion secretion (Figure 5)[22]. Intestinal anion secretion is crucial for increase in luminal fluid and propulsion of intestinal content, and dysfunction of submucous neurons may underlie delayed transit as in slow transit constipation. Indeed, loss of submucous neurons has been described in patients with slow transit constipation[100,101]. Given the relatively recent discovery of neuron-associated macrophages, no data are available on these cells in the context of slow transit constipation. However, these recent advances warrant further exploration of their potential role in gastro-intestinal disorders with delayed transit.

1.6.2 *Muscularis Neuron-Associated Macrophages*

A similar neuron-associated macrophage population is located in the muscularis externa, in close association to the enteric neurons of the myenteric plexus. Using a fate-mapping model which labels Cx3cr1^{+} macrophages at 3 weeks of age, we showed that over 80% of macrophages in the myenteric plexus retained labelling after 35 weeks, suggesting that this niche receives little input from circulating monocytes, and consists largely of self-maintaining cells of embryonic origin[22]. Indeed , monocytes could only be detected at very low levels within the muscularis externa at steady state conditions[102,103]. However, upon selective depletion of self-renewing macrophages, the myenteric plexus was repopulated by bone marrow-derived macrophages [22]. It is most likely that these incoming cells gain the neuron-associated phenotype imprinted by signals from the neuronal niche. Indeed, bulk RNA sequencing of long-lived, self-maintaining macrophages and newly recruited macrophages revealed few differentially expressed genes, suggesting that incoming cells are efficiently imprinted by the niche and are able to adopt a neuron-associated phenotype[22]. It is as yet unclear which molecular cues produced by myenteric neurons are responsible for the imprinting of neuron-associated macrophage phenotype; however, it has been shown that neurons are a source of CSF-1, which is critical for macrophage survival[104]. Furthermore, in the context of inflammation, it was showed that vagus nerve stimulation reduced intestinal inflammation by activating cholinergic enteric neurons in close proximity to macrophages expressing the α7 nicotinic acetylcholine receptor[105,106]. These findings were recapitulated in patients undergoing abdominal surgery, where activation of cholinergic enteric neurons using the 5-HT4 agonist prucalopride reduced the inflammatory response and improved clinical recovery[105]. These studies suggest that neuronal signalling is able to polarise macrophage phenotype and inflammatory response, a finding that is further supported by recent work in the context of infection-induced inflammation, where macrophages in the myenteric plexus were shown to respond to β2-adrenergic signalling via an Arginase 1-polyamine neuroprotective pathway, thereby limiting loss of enteric neurons[107]. Taken together, these findings clearly demonstrate that neurons are able to imprint a specific phenotype to the macrophages present within the niche, and that, in response to inflammation or infection, neuronal signalling is able to instruct macrophages so as to preserve the neuronal network.

Neuron-associated macrophages in the myenteric plexus are crucial for the survival of myenteric neurons, as their depletion leads to Caspase-3-mediated apoptosis and loss of over 50% of neurons in the myenteric plexus, with consequent impaired peristalsis and prolonged intestinal transit (Figure 5)[22]. Furthermore, macrophages associated to neurons in the myenteric plexus have been shown to produce Bone Morphogenetic Protein 2 (BMP2), which is critical for the regulation of peristalsis[104]. Finally, in Csf1$^{op/op}$ mice where macrophages are completely absent, the myenteric plexus is disorganized and neuronal density is increased, suggesting that macrophages may also participate in shaping connectivity

in the enteric nervous system[45]. Taken together, these findings demonstrate that neuron-associated macrophages are crucial for the maintenance of the neuronal population in the myenteric plexus and may play a critical role in disorders of the gastrointestinal tract characterised by altered or delayed gastrointestinal transit accompanied by neurodegeneration, as occurs in diabetes or aging. The increasing prevalence of these chronic conditions in the western society underscores the urgent need for therapeutic options, and neuron-associated macrophages may represent a novel and exciting target.

In diabetes, neuropathy occurs in up to 50% of patients, and can affect the gastro-intestinal tract, leading to vomiting, constipation, diarrhoea, and most notably, gastroparesis[108–111]. Delayed gastric emptying is attributed to loss of gastric nitrergic neurons and ICCs both in patients and in animal models of diabetes[112–116]. However, neurodegeneration in the context of diabetes is not limited to the stomach, as the number in cholinergic, nitrergic and total neurons is also reduced in the colonic myenteric plexus of animal model of diabetes[117]. Similarly, in patients with diabetes, apoptosis and loss of colonic myenteric neurons with consequent impaired contractile and inhibitory responses have been observed[118]. While the role of macrophages in diabetic neuropathy of the colon has not been explored, macrophages are known to play a crucial role in diabetic gastroparesis. In animal models, loss of $CD206^+$ macrophages in the gastric muscularis externa has been linked to the loss of neuronal nitric oxide synthase-expressing neurons, increased oxidative stress and pro-inflammatory cytokine levels, and the development of delayed gastric emptying[119,120]. In line with these findings, $CD206^+$ macrophages are reduced in the gastric antrum of patients with diabetic gastroparesis, a finding that correlates with loss of ICC[112]. In mice with diabetic gastroparesis, macrophages were found to express higher levels of inflammatory genes, including *IL-6* and *iNOS*, and lower levels of anti-inflammatory genes such as *HO-1*, *Arg1* and *Fizz1*[121]. In the complete absence of muscularis macrophages, as in $Csf1^{op/op}$ mice, mice do not develop gastroparesis following induction of diabetes, and replenishment of macrophages after diabetes induction led to development of delayed gastric emptying and ICC damage[121,122]. These data suggest that macrophage polarisation is central to the development of diabetic gastroparesis. On the one hand, loss of $CD206^+$ macrophages is instrumental to ICC damage and long-standing diabetes in the absence of gastroparesis is associated with high levels of *CD206* and *HO-1*. On the other hand, mice lacking macrophages are protected from gastroparesis[123]. It is plausible that loss of a neuroprotective population of macrophages may drive neuropathy in the stomach, although it is unclear whether the $CD206^+$ macrophage population described above corresponds to a neuron-associated population. Whether neuron-associated macrophages are lost or adopt an altered phenotype remains to be studied; however, findings support the hypothesis that in the context of diabetes, the gastric muscularis externa niche is altered and unable to imprint a neuro-supportive phenotype to macrophages. The effect of diabetes on the macrophage niche and the signalling molecules involved are, to this date unknown, and

warrant further study as they represent an intriguing and promising target for therapeutic intervention in the context of diabetic gastroparesis.

1.7 Blood Vessel-associated macrophages

The vasculature represents an additional example of highly specialised niche, and vasculature-associated macrophages have been identified in the heart, adipose tissue and the dermis[124,125]. Macrophages associated to the blood vessels are exposed to particulate material flowing in the blood stream and may thus act as immune sentinels at the interface between the organ and the rest of the body. Also within the intestine, several specialised populations of blood-vessel associated macrophages have been described. While these populations share common features, it is unclear whether these populations represent a single population or whether distinct subpopulations are present within the intestine. In the following paragraph, I will summarise recent findings on blood vessel-associated macrophage populations in the intestine.

We recently described a specialised population of self-maintaining macrophages in the lamina propria that is closely associated to the vascular plexus, where large veins and arteries give rise to the capillary bed of the mucosa (Figure 6)[22]. These macrophages present a distinct transcriptome, as revealed by single-cell RNA sequencing, and upregulate genes involved in angiogenesis, such as *Ecm*, *Tnfaip2*, *Anpep*, *Hif1a*, *Mmp2* and *Mmp14*, in addition to candidate marker gene *Adamdec1*. Depletion of self-maintaining blood-vessel associated macrophages led to loss of VE-cadherin^{+} blood vessels and increased vascular leakage (Figure 6)[22]. These findings suggest that blood-vessel associated macrophages are essential for vascular integrity and may be critical in preventing dissemination of luminal microbes to the blood stream. In light of these findings, it is plausible that blood vessel-associated macrophages contribute to the recently described gut-vascular barrier, a barrier similar to the blood-brain barrier, that is crucial to prevent dissemination of intestinal microbes to the liver and the bloodstream[126,127].

Intriguingly, a recent study identified macrophages intimately associated to the blood-vessels within the villi[62]. Using advanced *in vivo* imaging technology, Honda and colleagues showed that these mucosal perivascular macrophages form an interdigitated network surrounding the microcirculation, and that in the absence of microbiota these cells retracted, leaving large portions of the circulation uncovered. Furthermore, the consequence of this retraction was shown to be increased dissemination of intestinal pathogens to systemic sites, suggesting that these macrophages act to support and protect the gut vascular barrier within the villi (Figure 6). Perivascular mucosal macrophages derive from circulating monocytes and their differentiation was shown to depend on the transcription factor *Nr4a1* and the

presence of the microbiota. It is plausible that these cells are functionally specialised due to the close proximity to blood vessels, in a similar manner to the self-maintaining blood vessel-associated population of the submucosa; however, they require a high turnover due to their anatomical location and the constant exposure to luminal contents. In line with this hypothesis, these cells displayed delayed turnover in antibiotic-treated mice.

In addition to the self-maintaining blood-vessel associated macrophages and the mucosal perivascular macrophages described above, another specialised, CD169$^+$ macrophage population in close association with the vasculature and lymphatics of the intestine has been described. CD169, or sialoadhesin, is expressed by macrophage populations localized at the boundary between tissues and circulating fluids throughout a variety of organs, in particular spleen, the subcapsular and medullary sinus of the lymph node, and in the small intestine along the length of the central lacteal and lymphatic vessel at the base of the villi[68,128]. Notably, CD169$^+$ macrophages were initially described to be associated to intestinal crypts, however increasing evidence points towards an intimate association of these cells to vessels, and therefore this population has been included in this paragraph[70,128]. It may be, however, that CD169$^+$ macrophages also associate to intestinal crypts, and that the latter may represent a distinct population.

CD169$^+$ macrophages capture particulate materials including apoptotic cells, viruses and immune complexes, and are implicated in the development of tolerance to circulating antigens[128,129]. It is thus likely that the exposure of CD169$^+$ macrophages to the circulating fluid drives the imprinting of a specific function. However, it is unclear whether within the intestine this population represents a distinct macrophage population to the self-maintaining population described above, as these cells have not been transcriptionally defined. Furthermore, while circulating monocytes are able to engraft in the pool of CD169$^+$ macrophages, it is unclear whether embryonic progenitors give rise to this population, and whether these cells are able to self-maintain[68]. Further research is certainly warranted on the ontogeny and transcriptome of intestinal CD169$^+$ macrophages; however, compelling evidence has already been provided to suggest a functional specialisation of these cells and that they play a crucial role in murine models of colitis[68].

Intestinal CD169$^+$ macrophages have been shown to be critical in promoting infiltration of monocytes via CCL8 expression in experimental models of colitis, a mechanism dependent on the CD169$^+$ macrophage transcription factor *Maf* (Figure 6)[68,129]. In addition to regulating CCL8 expression, *Maf* also appears to repress cytoprotective genes downstream of the anti-oxidative transcription factor *Nrf2*, suggesting it acts as a molecular switch governing the phenotype of CD169$^+$ macrophages[129]. In mice, selective depletion of CD169$^+$ macrophages, or anti-CCL8 treatment, ameliorated disease progression, suggesting that CCL8-mediated monocyte recruitment is central in initiating mucosal inflammation[68].

Following the initial pro-inflammatory response, CD169^{+} macrophages subsequently downregulate *Maf* expression, leading to a progressive upregulation of *Nrf2*-dependent genes and downregulation of CCL8 during resolution of inflammation. Thus *Maf* expression appears to govern the functional and phenotypical response of CD169^{+} macrophages to environmental cues, further illustrating the plasticity of macrophages in adapting to the niche and surrounding environmental cues. Future studies should elucidate the signals that regulate *Maf* expression in CD169^{+} macrophages, and how this signalling pathway could be targeted for therapeutic intervention during colitis. Furthermore, it is unclear whether a comparable population is present in human, and whether a similar mechanism is present in inflammatory bowel diseases (IBD).

It is crucial to increase our understanding of the role of blood vessel-associated macrophages in maintaining intestinal blood vessel integrity, as this subpopulation may be implicated in diseases characterised by gut vascular barrier dysfunction and bacterial translocation. High levels of endotoxemia can be detected in patients with IBD and liver cirrhosis, suggesting that in these diseases, the intestinal vascular barrier is impaired[130–132]. In mice it has been demonstrated that the establishment of the mucosal perivascular macrophage network relies on the presence of the microbiota, and upon antibiotic treatment mice showed reduced vascular adhesion by perivascular macrophages and increased systemic bacterial dissemination, leading to a reduction in survival and impaired vascular healing in the context of colitis[62]. Intriguingly, in colitis, antibiotic-treated mice showed impaired differentiation of monocytes to macrophages compared to untreated controls. As stasis of immature monocytes has widely been described in patients with inflammatory bowel disease, these new findings shed light on the role of the microbiota in promoting the differentiation of monocytes to mucosal perivascular macrophages, in addition to providing a mechanism through which impaired macrophage differentiation could promote endotoxemia in colitis[71,133–135]. Furthermore, the finding that the microbiota is crucial for vascular protection by mucosal perivascular macrophages to prevent systemic dissemination of intestinal pathogens, becomes highly relevant when considering that paediatric patients are more susceptible to *S. aureus* colonization following a course of antibiotics[62,136]. Uncovering the mechanisms through which the microbiota contributes to regulating macrophage phenotype and function will be critical to exploit these novel findings and therapeutically target blood-vessel associated macrophages in the context of IBD.

Also in liver disease, gut microbiota and bacterial translocation play an important role in the pathogenesis of non-alcoholic or metabolic-associated fatty liver disease (NAFLD/MAFLD) and steatohepatitis (NASH.) In NAFLD patients and high-fat diet (HFD) mouse models, gut vascular barrier dysfunction has been observed leading to increased bacterial translocation to systemic sites[127,137]. Whether HFD drives dysfunction of blood vessel-associated macrophages is as yet unknown, however

it has been shown to promote accumulation of pro-inflammatory macrophages in the colon, suggesting that local inflammation may affect local macrophage phenotype imprinting[138]. Further research should focus on the effect of HFD on specific macrophage populations within the intestine, as therapeutic interventions preventing bacterial dissemination may be key to reducing systemic low-grade inflammation and metabolic endotoxemia.

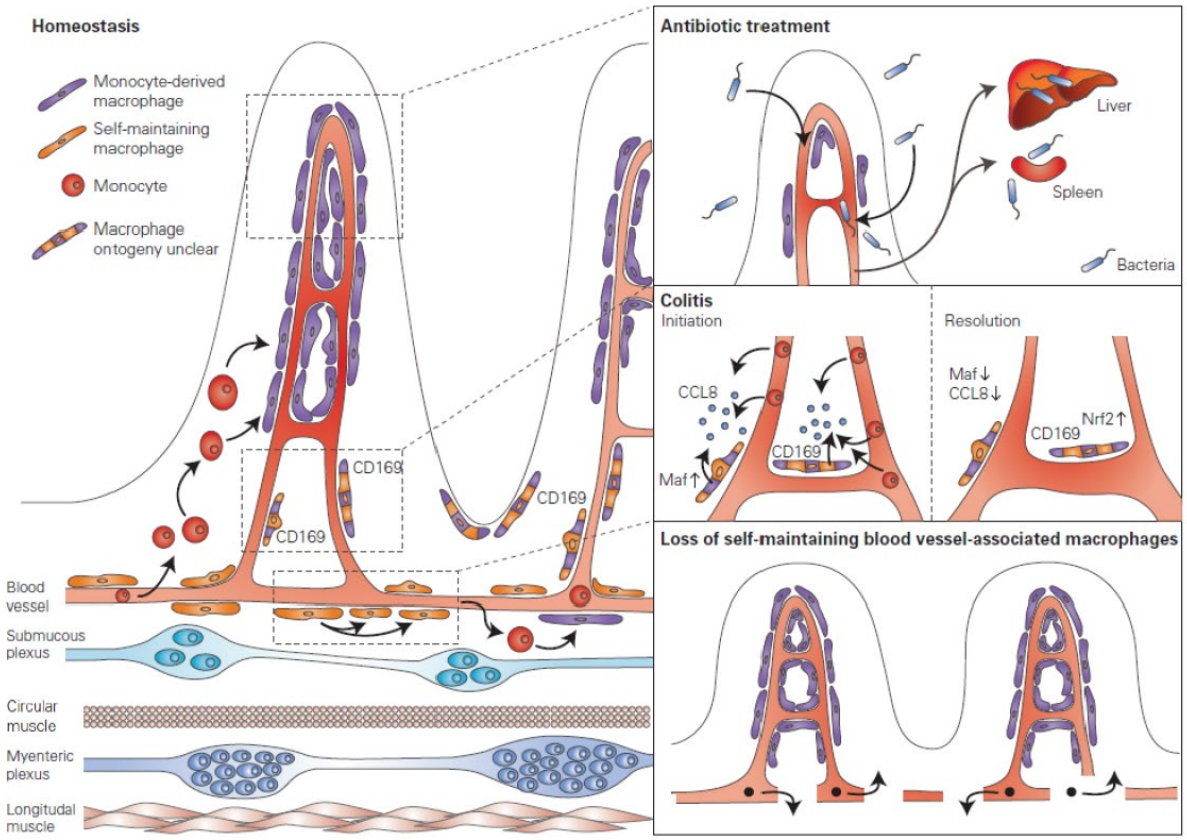

Figure 6: Blood vessel-associated macrophages. Various populations of blood vessel associated macrophages have been identified within the intestine. Mucosal perivascular macrophages in the villi derive from monocytes and form an interdigitated network surrounding the blood vessel. Antibiotic treatment reduces the population of mucosal perivascular macrophages, thus impairing the perivascular network and leading to bacterial translocation to the liver and the spleen. Furthermore, a population of $CD169^{+}$ macrophages which appears to be associated to the vasculature and lymphatics, distant from the epithelial border, was identified. While the ontogeny of this population remains to be defined, these macrophages were shown to be critical in the initiation phase of colitis, where upregulation of the transcription factor *Maf* leads to upregulation of CCL8 and recruitment of monocytes. Conversely, in the later stages of colitis, these macrophages downregulate *Maf* and CCL8, leading to an upregulation of *Nrf2*-dependent genes that favour the resolution of inflammation. Finally, we identified a population of self-maintaining macrophages that are associated to the vascular plexus located at the base of the villi. These macrophages were shown to regulate blood vessel integrity, as their selective depletion led to loss of blood vessels and increased vascular leakage.

1.8 Additional macrophage niches within the intestine

1.8.1 *Crypt-associated macrophages*

The intestinal crypt is a highly specialised environment, harbouring intestinal stem cells for epithelial regeneration, Paneth cells for antimicrobial defence, and mucus-producing goblet cells. This unique niche is also supported by macrophages, and recent studies have shed light on a population of CSF1R-dependent macrophages intimately associated with the crypt epithelium[46]. Depletion of these macrophages led to a reduction of $Lgr5^+$ intestinal stem cells, and aberrant differentiation of Paneth cells and goblet cell density. Furthermore, single-cell RNA sequencing revealed a population of self-maintaining macrophages expressing typical Paneth cell markers, such as *Itln1* and *Defa,* suggesting physical interaction between these macrophages and Paneth cells[22]. Paneth cells produce antimicrobial compounds, such as α-defensins and lysozyme, in addition to Wnt3, which is critical for $Lgr5^+$ intestinal stem cell maintenance[139]. The antimicrobial products secreted by Paneth cells prevent bacterial translocation across the gut epithelium, and the reduction of lysozyme release observed upon loss of crypt-associated macrophages may promote intestinal dysbiosis and intestinal expansion of *Escherichia coli*[140]. Intriguingly, as Paneth cells have been reported to produce CSF-1, it is possible that Paneth cells maintain the local macrophage subset in a similar manner as neurons in the myenteric plexus[48]. Future studies should focus on unravelling the communication between macrophages, intestinal stem cells and Paneth cells, to identify the molecular mechanisms provided by macrophages that are crucial for stem and Paneth cell homeostasis, in addition to defining whether crypt-associated macrophages represent a transcriptionally distinct subset of macrophages. In an experimental model of colitis, it was shown that macrophages are essential for the regeneration of the damaged epithelium. Indeed, during the regenerative response, there was an upregulation of macrophage activation genes such as chemokines, chemokine ligands and Interferon response genes in the crypt niche[141]. Macrophages were shown to extend processes to directly contact colonic epithelial stem cells near the crypt base, and in the absence of macrophages, epithelial proliferation was impaired[141]. Similarly, in a murine model of epithelial damage, $Trem2^+$ macrophages were shown to promote wound healing via IL-4 and IL-13[142].

The crypt-associated macrophage niche has not yet been well-defined; however, considering the critical role of macrophages in promoting wound healing and epithelial regeneration, these cells may be important in the context of colonic dysplasia and carcinoma. Indeed, dysregulated wound healing and epithelial regeneration are known to promote colorectal cancer[143].

1.8.2 *Peyer's Patch-Associated Macrophages*

A distinct population of macrophages can be found located in Peyer's patches. It has been shown that Peyer's patch-associated macrophages derive from $CCR2^{+}$ monocytes and fail to express typical macrophage markers such as CD64, F4/80 and CD206[69]. Instead, $Tim4^{+}$ and $Tim4^{-}$ $CD4^{+}$ macrophage subsets have been defined within the Peyer's patch niche. Peyer's patch-associated macrophages have been shown to efficiently phagocytose particles and apoptotic cells, and present an antimicrobial and antiviral gene signature[69]. In line with these findings, single-cell RNA sequencing revealed a population of macrophages upregulating B cell genes, including *CD79a*, *CD79b* and *Ms4a1,* further supporting the hypothesis that Peyer's patch-associated macrophages play an important role in the clearance of apoptotic cells[22].

1.9 Concluding Remarks

While intestinal macrophages were long considered the house-keepers of the intestinal mucosa, it has become clear that these cells carry out a plethora of additional functions vital to the correct functioning and homeostasis of the gastrointestinal tract. The proof that also within the intestine, macrophage subsets are able to self-maintain and do not only derive from circulating monocytes, sets the stage for differentiated and specialised macrophage subsets. Furthermore, the concept that surrounding cells imprint specific functions on the resident macrophage (the macrophages niche) further highlights the functional plasticity of macrophages and opens the possibility of the existence of additional macrophage niches within the intestine that have yet to be described. We have only scratched the surface of the true diversity and importance of intestinal macrophages, and the coming years we will see a major overhaul in our understanding of the role of these cells in both intestinal homeostasis and disease.

Chapter 2

Objectives and Aims

The field of macrophage biology has seen, in recent years, major advances in terms of our understanding of macrophage heterogeneity within tissues and the role of the local microenvironment, ie., the macrophage niche, in determining macrophage phenotype and function. These advances have led to the description of niche-specific macrophage subtypes, characterised by a specific transcriptome and function, throughout tissue and organs, including the gastro-intestinal tract. Indeed, our group recently described long-lived, self-maintaining sub-population of macrophages that lies in close association to enteric neurons (neuron-associated macrophages; NA-MMΦ) in the submucous and myenteric plexi. These NA-MMΦ were characterised by a distinct transcriptome and were critical for function and the survival of enteric neurons in adulthood[22].

While niche-specific macrophage specialisation has largely been accepted and the literature is awash with reports detailing the transcriptome of various macrophage subtypes, often the cues underlying such differential specialisation remain unclear. In the liver, a recent report elegantly described the molecular mediators involved in shaping resident macrophage identity from monocyte to mature Kupffer cell; this process required an elaborate sequential cascade of signalling from hepatocytes that induced ID3 expression, and induction of LXR-α via NOTCH-BMP signalling mediated by endothelial cells and stellate cells[55]. Similarly, TGFβ1 signalling is critical for microglia differentiation in the brain [144]. However, in addition to molecular cues deriving from surrounding cells, macrophage function may also be determined by developmental programming. Macrophages in the kidney, heart and in the brain display a significant developmental plasticity, and can adapt their function, their phenotype and their transcriptome to the age-specific requirements of the tissue[145–147]. In the brain, microglia undergo a stepwise differentiation program from postnatal development to adulthood, which is accompanied by significant shifts in function and transcriptome, in addition to undergoing further transcriptional changes later in life during aging[146]. Whether intestinal macrophages display such developmental plasticity is unknown, and the molecular mediators involved in instructing specific macrophage subsets remain to be elucidated. In Chapter 3 of this thesis, I will explore the developmental plasticity of NA-MMΦ in the myenteric plexus, and elucidate the molecular mediators involved in shaping their phenotype in adulthood. In particular, I will assess whether the neuron-macrophage relationship changes with developmental stage, and investigate whether macrophages may participate in shaping the ENS during early postnatal development. Next, using single-cell RNA sequencing of macrophages during development and adulthood, I will investigate whether macrophage transcriptome and function can adapt to the evolving needs of the tissue. Finally, I will investigate the molecular mediators involved in imprinting the mature NA-MMΦ phenotype in the adult myenteric plexus.

While developmental plasticity may represent a critical determinant in adapting macrophage function to the evolving needs of the tissue, developmental reprogramming that accompanies aging may

represent a counter-productive evolution of macrophage phenotype as a response to the aging tissue. Indeed, aging is generally accompanied by low grade inflammation (*inflamm-aging*) and increased oxidative stress, which lead to a decline in tissue function and homeostasis over time[148,149]. Macrophages display age-associated alterations, with decreased chemotaxis, reduced phagocytic capacity and altered cytokine production[150–152]. In the brain, aging is associated with the emergence of a subset of microglia that activate transcriptional profiles similar to those of microglia described in neuro-degenerative disorders, also referred to as disease-associated microglia (DAMs)[153,154]. However, it is as yet unclear whether these altered macrophage states that occur with aging are a consequence, or drivers themselves, of age-related inflammation and increased oxidative stress.

In the gut, aging is accompanied by gastro-intestinal complaints, most commonly constipation, which affects up to 40% of geriatric patients[155]. While gastro-intestinal dysfunction may arise as a consequence of medication, or other age-related diseases, increasing evidence suggests that functional changes observed with advanced age can be attributed to age-related neurodegenerative changes in the ENS. In line, morphological studies have demonstrated the loss of enteric neurons in both submucosal and myenteric plexuses in humans and in rodents, affecting mainly the cholinergic population that modulates ascending contractions during peristalsis[156,157]. However, the mechanisms underlying such age-related neurodegeneration remain to be elucidated. As we recently described a NA-MMΦ population in the gut that is critical for the function and the survival of enteric neurons, and it is known that macrophages may undergo age-related changes in phenotype and function, in Chapter 4 I hypothesize that these NA-MMΦ lose their neuroprotective properties with aging resulting in *neurodegeneration and constipation*. To this end, I will first evaluate the number of neurons in the myenteric plexus and gastro-intestinal transit in male and female mice of 3 and 20 months to assess the onset and severity of age-related neurodegeneration. Next, I will explore changes in macrophage phenotype and function with age and will attempt to dissect the mechanisms that contribute to neurodegeneration in the aging myenteric plexus. Taken together, these findings will provide crucial understanding of the role of macrophages during ENS development, homeostasis, and age-related neurodegeneration and constipation. ENS function is critical for survival, therefore it is of vital importance to further our understanding of macrophages as key players in maintaining ENS homeostasis, with the goal of harnessing the therapeutic potential of these cells for intervention in neurodegenerative disorders of the GI tract. Finally, the ENS, as 'brain of the gut', may mirror the CNS in homeostasis and in disease, and may thus offer an unexploited snapshot of ongoing pathological processes in the brain.

Chapter 3

Development and maintenance of the enteric nervous system orchestrated by dedicated resident macrophages

Maria Francesca Viola[1], Marta Chavero-Pieres[1], Elodie Modave[1], Nathalie Stakenborg[1], Marcello Delfini[1], Naomi Fabre[1], Iris Appeltans[1], Tobie Martens[2], Katy Vandereyken[3,4], Jens Van Herck[3$], Philippe Petry[5], Simon Verheijden[1#], Sebastiaan De Schepper[1†], Alejandro Sifrim[4,6], Katrin Kierdorf[5,7], Marco Prinz[5,7,8], Pieter Vanden Berghe[2], Thierry Voet[3,4] and Guy Boeckxstaens[1,4]

Affiliations

[1] Laboratory for Intestinal Neuro-Immune Interaction, Translational Research Center for Gastrointestinal Disorders (TARGID), Department of Chronic Diseases and Metabolism (ChroMeta), KU Leuven, Belgium
[2] Laboratory for Enteric NeuroScience (LENS), Translational Research Center for Gastrointestinal Disorders (TARGID), Department of Chronic Diseases and Metabolism (ChroMeta), KU Leuven, Belgium
[3] Laboratory of Reproductive Genomics, Department of Genetics, KU Leuven, Leuven, Belgium.
[4] Leuven Institute of Single Cell Omics (LISCO), KU Leuven, Leuven, Belgium
[5] Institute of Neuropathology, Faculty of Medicine, University of Freiburg, Freiburg, Germany; Faculty of Biology, University of Freiburg, Freiburg, Germany
[6] Laboratory of Multi-Omic Integrative Bioinformatics (LMIB), Department of Genetics, KU Leuven, Leuven, Belgium; Leuven AI Institute, KU Leuven, Leuven, Belgium
[7] Centre for Integrative Biological Signalling Studies, University of Freiburg, Germany; Center for Basics in NeuroModulation (NeuroModulBasics), Faculty of Medicine, University of Freiburg,, Germany
[8] Signalling Research Centres BIOSS and CIBSS, University of Freiburg, Freiburg, Germany
[#] Current affiliation: Janssen R&D BE, Turnhoutsweg 30, 2340 Beerse, Belgium
[†] Current affiliation: UK Dementia Research Institute, UCL Queen Square Institute of Neurology, Faculty of Brain Sciences, University College London, London
[$] Deceased

Under revision in *Nature*

3.1 Abstract

Correct development and maturation of the enteric nervous system (ENS) is critical for survival as it coordinates gut motility, nutrient absorption and intestinal secretion. At birth, the ENS is immature and requires significant refinement in order to exert its functions in adulthood. Here, we demonstrate that resident macrophages of the muscularis externa (MMϕ) refine the ENS early in life by pruning synapses and phagocytosing abundant enteric neurons. Depletion of MMϕ prior to weaning disrupts this process and results in abnormal intestinal transit. After weaning, MMϕ continue to closely interact with the ENS and acquire a neuro-supportive phenotype. This neuro-supportive phenotype is instructed by TGFβ produced by the ENS; chemical depletion of the ENS and disruption of TGFβ signalling results in a decrease of neuron-associated MMϕ. The latter is associated with a loss in enteric neurons and altered intestinal transit. These findings introduce a novel reciprocal cell-cell communication responsible for the maintenance of the ENS and indicate that the ENS, similar to the brain, is shaped and maintained by a dedicated population of tissue resident macrophages, that adapts its phenotype and transcriptome to the timely needs of the ENS niche.

3.2 Introduction

In mammals, gut function is largely controlled by the enteric nervous system (ENS), a complex and vast collection of neurons organized in two plexuses, the myenteric and submucous plexus. Even in the absence of input from the central nervous system (CNS), the ENS efficiently coordinates a plethora of vital functions including nutrient absorption, peristalsis and intestinal secretion[158]. It has been estimated that the adult human ENS contains over half a billion neurons, and therefore is often referred to as the "brain of the gut". Diseases of the ENS range from limiting life-quality to lethal, and can arise during early development or manifest as neurodegeneration later in life[159–161].

The ENS develops from progenitors of the neural crest, which colonise the gastrointestinal tract prior to birth in a process that is extremely fine-tuned in time and space, and is orchestrated by an interplay between signalling molecules and receptors that ensures complete innervation of the gut[93]. While the process of colonisation by progenitors terminates prior to birth, neuronal subtypes develop at differing rates, and the full range of neuronal differentiation is only reached after birth[94]. In the ENS, neuronal maturation persists after birth, with changes in neurochemical composition, soma size and synaptic input reported to occur between early postnatal life and adulthood[162]. In line, the randomly occurring contractions required for motility only appear several days after birth, and reach a mature frequency and amplitude after weaning[163]. This maturation pattern appears to mirror the developing need of the

intestine to first propel liquid, and only subsequently solids, through the gastrointestinal tract. Indeed in mouse, experiments show that the intestine is able only after postnatal day (P) 14 to expel beads, and the speed at which this occurs increases significantly from P14 and P21[163]. These findings suggest that the ENS undergoes significant maturation in early postnatal life, however the mechanisms involved in this process have yet to be elucidated.

Tissue-resident macrophages are highly specialized phagocytes that actively contribute to immune defence but also to tissue homeostasis of their host organ[14,164]. They play a key role in supporting the tissue in which they reside by secreting growth factors and responding to tissue damage, in addition to carrying out unique, tissue-specific functions. To perform these specialized functions, tissue-resident macrophages are characterized by a distinct phenotype and transcriptome that is imprinted by surrounding cells via secreted mediators or cell-to-cell contacts, also referred to as the local 'niche'[2]. This understanding has led to the description of the instructing niche for various specialised tissue resident macrophage subtypes; for example, Kupffer cells in the liver require interactions with stellate cells, hepatocytes, and endothelial cells to acquire their specific transcriptomic identity; in the brain, microglia require TGFβ produced by astrocytes and neurons to acquire their neuroprotective phenotype[55,144].

In the gut, tissue-resident macrophages are present throughout its different layers, where they carry out distinct functions according to their anatomical location[165]. We recently identified a subpopulation of long-lived resident macrophages in the muscularis externa located in close proximity to the myenteric plexus, an organised layer of enteric neurons embedded within the muscle layer that is responsible for the coordination of gastrointestinal motility[6,22,45]. These muscularis macrophages (MMϕ) colonise the gut prior to birth, however it is unclear whether they participate in the extensive remodelling of the ENS early in life[166]. In adulthood, MMϕ are characterised by a distinct transcriptome and play an essential role in neuronal survival and function, as their depletion leads to neurodegeneration, delayed intestinal transit, impaired intestinal motility and colonic dilation[22,45]. The establishment and maintenance of this neuro-supportive MMϕ population is therefore critical for gut health and function, nevertheless the cells composing this specialised macrophage niche and the molecular mediators involved remain to be elucidated[22,104]. Here, we show that MMϕ, similar to microglia in the CNS parenchyma, contribute to the maturation of the ENS early in life. Furthermore, we identified the time of weaning as crucial 'tipping-point' for macrophage function, at which MMϕ shift their role from neuronal refinement to neuronal support. This shift is accompanied by profound transcriptional and phenotypic maturation imprinted by transforming growth factor β (TGFβ) produced by the ENS, introducing a novel cell-cell circuit responsible for the maintenance of the neuron-associated MMϕ niche in the gut. Taken together,

these findings support a common evolutionary mechanism of neuronal refinement shared by the CNS and the ENS, and suggest that the ENS, as 'brain of the gut' may mirror the CNS in homeostasis and disease.

3.3 Results

3.3.1 *MMϕ refine the ENS during early postnatal development*

Previous reports have suggested that the ENS undergoes remodelling during early postnatal development, including changes of soma size, organization of ganglia and synaptic density[162,163]. To carefully define these age-related changes in ENS architecture, we first assessed neuronal density during early postnatal development (P10 and P14), at weaning (P21) and during adulthood (P56). At P10, neuronal cell bodies were abundant throughout the plane between the circular and longitudinal muscle layers, loosely organised into ganglia that run parallel to the circular muscle layer, while delimitations between ganglia were ill-defined and interconnecting fibres were disorganised (Figure 1A). Density of enteric neurons, ganglia and single extra-ganglionic neurons dynamically decreased from postnatal development to adulthood, also when tissue growth was taken into account (Figure 1A-D, S1A-C). These changes were accompanied by a decrease in interconnecting fibres (Figure 1E). Density of the presynaptic marker Synapsin I was measured at P7, P14, P21 and P56, with a significant increase at P14 compared to younger (P7) and older (P21, P56) timepoints (Figure 1F)[162]. These findings suggest that the early postnatal phase prior to weaning represents a dynamic phase for the remodelling and the refinement of the enteric neuronal network.

We hypothesized that MMϕ, like microglia in the CNS, refine the ENS during development and closely interact with enteric neurons. To assess neuron-MMϕ interaction, we generated mice expressing tdTomato in enteric neurons and green fluorescent protein (GFP) in Cx3cr1^{+} macrophages, including MMϕ, (*Cx3cr1*$^{GFP/WT}$ *Wnt1*$^{CRE/WT}$ *Rosa26*$^{tdT/WT}$). Using ex-vivo live-imaging of the muscularis externa at P14, we observed that Cx3cr1^{high} MMϕ extend and retract dendrites towards neurons (Figure 1G + supplementary videos 1 and 2). At P56, MMϕ processes appeared more ramified and elongated towards adjacent enteric neurons, compared to the processes of MMϕ at P14, where phagocytic cups, phagosomes and vesicles were evident (Figure 1G). In line, analysis of MMϕ morphology revealed a significant increase in filopodia length and number of dendrites at P56 compared to P14, while no changes in cell body volume were observed (Figure S1D-G).

As we showed that MMϕ indeed dynamically interact with enteric neurons, we next investigated whether MMϕ prune synapses in the ENS. Synaptic engulfment was assessed using Synapsin-I immunostaining and confocal imaging, followed by digital reconstruction as previously described[167]

(Figure S1H). At P14 MMϕ engulfed significantly more Synapsin I^{+} puncta compared to P21 and P56 (figure 1H-K, S1I-K). Of note, engulfed synapses could be observed within CD68+ lysosomes (Figure 1L, S1J). In addition to the engulfment of synapses, MMϕ could also be observed engulfing neuronal bodies at P14, but not anymore at P56 (Figure S1L-M). Using ex-vivo live imaging in *Cx3cr1*$^{GFP/WT}$ *Wnt1*$^{CRE/WT}$ *Rosa26*$^{tdT/WT}$, we observed the engulfment of neural tdTomato+ debris that was internalised via phagosomes, and was digested until loss of fluorescence (Figure 1M, S1N, Supplementary Video 3). To further validate whether MMϕ may also be engulfing neurons or ENS debris, in addition to synapses, we made use of *Cx3cr1*$^{GFP/WT}$ *Wnt1*$^{CRE/WT}$ *Rosa26*$^{tdT/WT}$ mice, and determined neural tdTomato within Cx3cr1^{+} MMϕ via flow cytometry. The percentage of Cx3cr1^{GFP} positive MMϕ containing ENS-derived tdTomato^{+} was significantly higher at P14 compared to P56 (figure 1N, S1O). To distinguish between engulfment occurring in vivo, and engulfment occurring ex vivo during enzymatic cell isolation, we repeated this experiment and combined tissue from a wildtype mouse with that of *Cx3cr1*$^{GFP/WT}$ *Wnt1*$^{CRE/WT}$ *Rosa26*$^{tdT/W}$ mouse ex vivo, and analysed the percentage of tdTomato^{+} GFP^{-} MMϕ. Of all tdTomato+ MMϕ 15% were GFP- while the remainder 85% were GFP+ MMϕ (Figure S1P) indicating that MMϕ ingest neuronal debris in vivo. Finally, we sorted tdTomato^{+} GFP^{+} MMϕ for confocal microscopy and showed that the tdTomato signal is indeed localized inside the cell (Figure 1O, S1Q). Taken together, these findings suggest that early postnatal development is a period of dynamic neuronal refinement in the ENS, and MMϕ actively participate in the remodelling of the ENS via contacting adjacent neurons and engulfment of neuronal bodies and synapses.

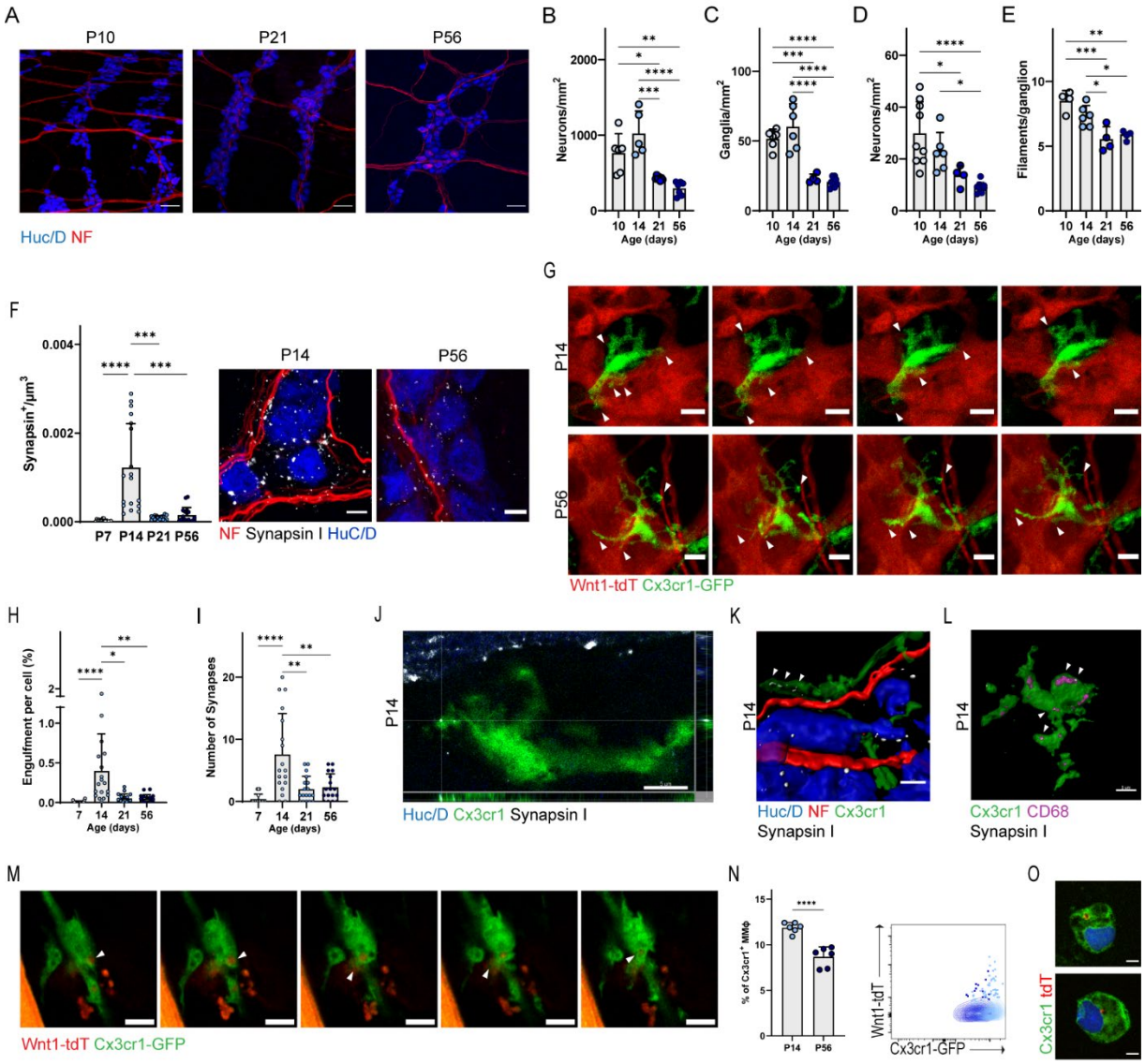

Figure 1: MMϕ prune synapses and engulf neurons during early postnatal development. (**A**) Representative confocal images of the myenteric plexus at P10, P21 and P56. Scale bar is 50µm. Quantification of neuronal density (**B**), density of ganglia (**C**), single extra-ganglionic neurons (**D**) and interconnecting fibre bundles (**E**) in the myenteric plexus at P10, P14, P21 and P56. (**F**) Quantification of the volume of Synapsin-I per µm^3. Representative confocal image of myenteric neurons at P14 and P56. Scale bar is 5µm. (**G**) Time-lapse stills taken from ex vivo live-imaging of the muscularis externa of 14 and 56 day-old Wnt1$^{Cre/WT}$ Rosa26$^{tdT/WT}$ Cx3cr1$^{GFP/WT}$ mice. Arrows indicate phagocytic cups and filopodia of MMϕ extending and retracting towards neural cells. Scale bar is 10µm. (**H**) Percentage of synaptic engulfment per cell, determined as volume of Synapsin$^+$ volume/MMϕ volume. (**I**) Number of Synapsin I+ puncta engulfed by MMϕ, determined via digital reconstruction (Imaris). (**J**) Orthogonal view depicting MMϕ engulfing synaptic machinery at P14. Scale bar is 5 µm. (**K**) Digital reconstruction (Imaris) depicting engulfment of synapses by MMϕ. White arrowheads indicate engulfed synapses. Scale bar is 5 µm. (**L**) Digital reconstruction (Imaris) depicting synapses engulfed by MMϕ located within CD68+ lysosomes. White arrowheads indicate engulfed synapses. Scale bar is 5 µm. (**M**) Time-lapse stills taken from ex vivo live-imaging of the muscularis externa of 14 day-old Wnt1$^{Cre/WT}$ Rosa26$^{tdT/WT}$ Cx3cr1$^{GFP/WT}$ mice. Arrows indicate engulfed tdTomato+ debris within MMϕ phagosomes. Scale bar is 10µm. (**N**) Quantification via flow cytometry of percentage of MMϕ engulfing neural cells (Wnt1-tdTomato$^+$), and representative dotplot of Wnt1-tdTomato signal in MMϕ. (**O**) Confocal images of FACS-sorted tdTomato+ MMϕ showing engulfed neuronal debris. Scale bar is 5 µm. Data are shown as Mean ± SD, analysed using t-test, ANOVA (followed by Tukey's multiple comparisons) or Kruskal-Wallis (followed by Dunn's multiple comparisons). Data are representative from at least 2 independent

experiments, apart from experiments shown in F, H, I, M and N. N=4-7 mice per experiment, apart from data in G and M. * $p < 0.05$; ** $p < 0.01$; *** $p < 0.001$; **** $p < 0.0001$.

3.3.2 *MMϕ function differs according to the developmental stage of the gut*

In adulthood, we previously demonstrated that enteric neurons rely on MMϕ for their survival, as indicated by the observation that depletion of neuron-associated MMϕ leads to neurodegeneration[22]. Whereas we demonstrated above that MMϕ refine the ENS early in life, rather than already providing trophic support, we hypothesized that MMϕ depletion during the early postnatal phase might have consequences for the development and the maturation of the ENS. To test this hypothesis, mice received 2 injections of a depleting αCSF1r 3 days apart, either during postnatal development (at P3 or at P10), at weaning (P21), or in adulthood (P56), and were analysed 7 days after the first injection (Figure 2A). Treatment with αCSF1r led to a significant reduction in MMϕ but did not alter other immune cell populations in the muscularis externa, including B cells and T cells (Figure S2A-B). In line with our previous findings, depletion of MMϕ during adulthood led to a significant reduction in neuronal density compared to controls[22] (Figure 2B-C). In contrast, if MMϕ were depleted at P10, neuronal density was found to be significantly increased in treated mice compared to controls (Figure 2B,C). Strikingly, ganglia maintained the morphological appearance characteristic of P10, with ill-defined ganglia and reduced distance between them, while in control mice, maturation of ganglia had continued and appeared more organized resembling ganglia at P21 (Figure 2B, C). In line, depletion of MMϕ at P10 also led to increased synaptic density (Figure 2D-E). The effect of MMϕ depletion on neuronal density in early postnatal life was restricted to P10-P21, as depletion of MMϕ from P3-P10 did not affect neuronal density (Figure 2B-C). Depletion of MMϕ at weaning (P21) led to no significant changes in neuronal density or morphology of ganglia (Figure 2B-C). It should be noted that despite previous reports stating that using a low dose of αCSF1r preserves lamina propria macrophages[45], we observed a significant reduction in lamina propria macrophages using this protocol (Figure S2C). However, given the anatomical separation between these two compartments, we do not expect loss of lamina propria macrophages to impact neuronal density in the myenteric plexus.

As we observed synaptic engulfment by MMϕ during early postnatal life, we assessed synaptic density in mice treated with αCSF1r at P10. In line with a role of synaptic refinement by MMϕ at P10, we observed an increase in synaptic density in αCSF1r-treated mice compared to controls (Figure 2D-E). Finally, to assess the functional implications of neuronal refinement by MMϕ during postnatal development, we depleted MMϕ from P10 until P24, and assessed whole-gut transit time at P56 (Figure 2F). Strikingly, depletion of MMϕ during postnatal development led to accelerated transit in adulthood (Figure 2G). In line, density of neurons was increased in αCSF1r-treated mice, suggesting that neuronal refinement by MMϕ during development is required for normal peristalsis in adulthood (Figure 2H-I).

Taken together, our findings support a role in MMϕ in neuronal refinement during early postnatal life. Furthermore, we confirmed again the neuro-supportive role of MMϕ in adulthood, suggesting that the neuron-MMϕ interaction within the niche differs significantly at distinct stages in development.

3.3.3 *Gene expression profiling revealed transcriptomic adaptation of MMφ*

To investigate potential differences in the transcriptional signature underlying the functional transition of MMϕ prior to and after weaning, Cx3cr1^{+} MMϕ were FACS sorted from Cx3cr1$^{GFP/WT}$ mice at P10 and P56 and further used for single-cell RNA sequencing using the smartSEQ2 platform (Figure S2D). We intended to use this sequencing protocol rather than the commonly used 10x Genomics Chromium platform in order to acquire high transcriptomic coverage[168]. Following quality control, we obtained a total of 353 cells, of which 169 were from P10 mice and 184 from P56 mice (Figure S2E). Unbiased hierarchical clustering revealed 5 transcriptionally distinct cellular subpopulations, which were all classified as macrophages based on their expression of signature genes including *Ptprc*, *Csf1r* and *Adgre1* (F4/80) (Figure S2E,F). Expression of monocyte markers such as *Ccr2* or *Ly6c2* was low or not detected (Figure S2F). One cluster, comprising 34 cells and present almost exclusively in the P10 samples, contained a high amount of transcripts of extracellular matrix genes, including *Col3a1* and *Dcn*, suggesting potential contamination of their transcriptional signatures due to phagocytosis of cells depositing the extracellular matrix (Figure S2G). At P10, some MMϕ were indeed embedded within the extracellular matrix, which expressed the identified markers such as *Dcn* (Figure S2H). As these findings suggest that these cells clustered separately due to the contamination by transcripts of phagocytosed cells, we excluded this cluster from further analysis (Figure 2J).

Before performing cluster annotation, we assessed global differential gene expression changes between the P10 and the P56 sample (Figure S2I). Interestingly, in the P10 samples we observed upregulation of genes involved in phagocytosis and endocytosis (*Snx9*, *Cd36, Clta, Itgb1*), cell cycle and replication (*Top2a*, *Mki67, Smc2, Smc4*) (Figure S2I). In contrast, P56 MMϕ upregulated genes involved in immune surveillance and antigen presentation (*H2-Ab1*, *H2-Aa*, *Cd74*, *Cd14*) and genes involved in macrophage activation or differentiation (*Socs3*, *Stat3*, *Sbno2*) (Figure S2I).

We next annotated the clusters using the integrated dataset. The most abundant cluster was characterised by an upregulation of *Lyve1* and genes implicated in phagocytosis, including *Lyz2*, *Apoe* and *Ctsd,* and we thus named this cluster 'Lyve1^{+} MMϕ' (Figure 2K, S2J). The second cluster consisted of proliferating MMϕ, and was characterised by the upregulation of cell cycle genes, including *Mki67, Top2a, Cdkn1a, Smc4* and *Tubb* (Figure 2K, S2J). The third cluster was composed of MMϕ undergoing differentiation, as it was characterised by the upregulation of several transcription factors involved in terminal macrophage differentiation including *Etv3*, *Socs3* and *Irf1*, and transcriptional co-regulators

such as *Sbno2* (Figure 2K, S2J). The fourth cluster was characterised by the expression of genes considered to be microglia signature genes, including *Hexb, Ctss*, *Tmem119*, *F11r, Olfml3, Sema4d, Cx3cr1* (Figure 2K, S2J). Upregulation of microglia signature genes has been described in macrophages associated to peripheral nerves, so we named this cluster neuron-associated MMϕ (NA-MMϕ)[96,97].

When the abundance of each identified cluster was assessed by age, we found that the P10 sample comprised of mainly Lyve1^{+} MMϕ and proliferating MMϕ (Figure 2L). In the adult (P56) sample, cells were either undergoing terminal differentiation, or had acquired a NA-MMϕ transcriptional signature (Figure 2L). These findings suggest that the change in function of MMϕ is based on a profound shift in transcriptomic signature of MMϕ from postnatal development to adulthood.

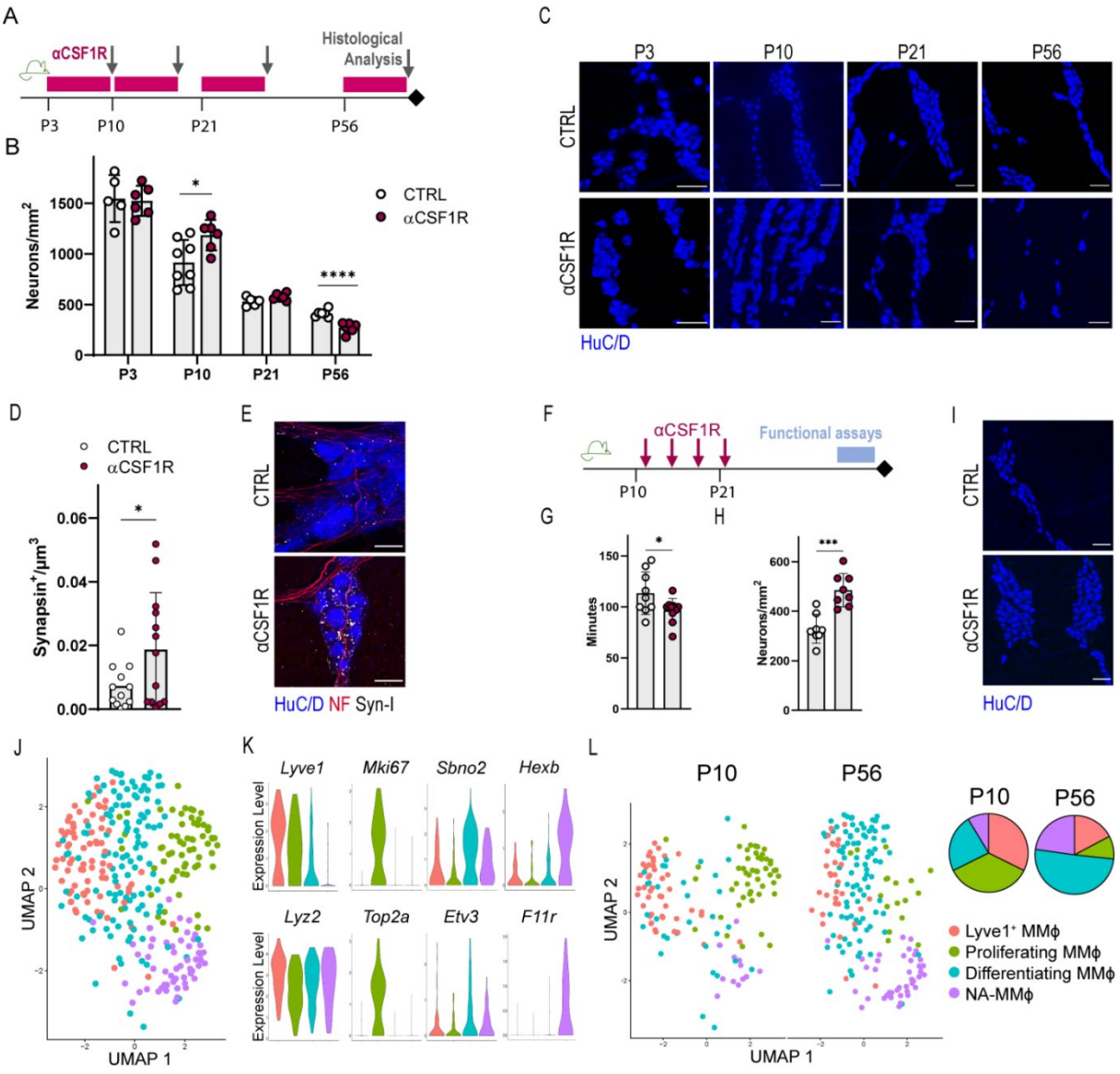

Figure 2: MMϕ undergo functional and transcriptional shifts from early postnatal development to adulthood. (**A**) Diagram to illustrate the treatment of mice with two injections of αCSF1R, to deplete MMϕ for the duration of 7 days, during either postnatal development, weaning or adulthood. (**B**) Neuronal density in αCSF1R-treated mice and controls. Pooled data from 2 experiments. (**C**) Representative confocal images of the myenteric plexus in αCSF1R-treated mice and controls. (**D**) Synaptic density assessed in mice treated with αCSF1R or control at P10 as detailed in 2A. (**E**) Representative confocal images of the myenteric plexus in mice treated with αCSF1R or control. Scale bar is 20µm. (**F**) Experimental protocol of αCSF1R antibody treatment to deplete MMϕ throughout postnatal development. (**G**) Whole gut transit time assessed in 8 week-old mice treated with αCSF1R or control antibody throughout postnatal development. (**H**) Neuronal density as assessed via histological analysis in 8 week-old mice treated with αCSF1R or control antibody throughout postnatal development. (**I**) Representative confocal images of the myenteric plexus of 8 week-old mice treated with αCSF1R or control antibody throughout postnatal development. (**J**) UMAP dimensionality reduction and clustering analysis of SMARTSeq2 scRNAseq data (n=319 cells) reveals four subpopulations of MMϕ, colour coded on the UMAP plot. (**K**) Violin plots displaying expression distributions of individual genes in cells grouped by cluster identified in D. (**L**) UMAPs by age, with colour coding reflecting the clusters identified in the integrated dataset. Scale bar is 50µm unless otherwise indicated. Data are shown as Mean ± SD and were analysed using T-tests. N=5-10 mice per experiment, apart from scRNAseq data (L-O). * $p < 0.05$; *** $p < 0.001$; **** $p < 0.0001$.

3.3.4 *Distinct MMφ subsets are located in different subtissular niches*

Next, we sought to validate our scRNAseq findings and investigated whether the identified subclusters may occupy specific niches and carry out specialised functions. First, we quantified the Lyve1^{+} MMϕ cluster via flow cytometry in MMϕ isolated at P10 and P56. We observed significantly more Lyve1^{+} MMϕ at P10 than at P56 (Figure 3A). As recently described, a Lyve1^{hi}MHCII^{lo} macrophage subtype resides within numerous organs, including the intestine, and is associated to vasculature[124]. The Lyve1^{+} cluster identified here resembles the Lyve1^{hi}MHCII^{lo} cluster transcriptionally, with upregulation of *Fcna*, *Lyve1*, *Cbr2*, *Cd209f*, *Ninj1* and *Hmox1* (Figure S3A). Similarly, these cells could be found either associated to VE-Cadherin^{+} blood vessels within the myenteric plexus, or closely associated to capillaries located within the serosa, but not within the muscle layer (Figure 3B-C). A similar anatomical distribution was observed at both P10 and P56, however Lyve1^{+} MMϕ were less abundant in the myenteric plexus at at P56 (Figure 3B-C). As this cluster upregulated genes involved in phagocytosis, including *Apoe* and *Lyz2*, we hypothesised that Lyve1^{+} MMϕ may be specialised in phagocytosis. Phagocytic capacity of MMϕ was assessed via an ex-vivo phagocytosis assay using fluorescently labelled dextran. Lyve1^{+} MMϕ had a significantly higher phagocytic index than the other identified MMϕ subtypes at P56, suggesting that this cluster represents MMϕ specialised in phagocytosis and engulfment (Figure 3D, S3B-C). In line, Lyve1^{+} MMϕ were enriched in CD68+ lysosomes compared to their NA-MMϕ counterparts (Figure S3D). We thus investigated whether Lyve1^{+} MMϕ were responsible for the engulfment of neuronal debris early in life, and found that Lyve1^{+} MMϕ were the predominant tdTomato^{+} MMϕ subtype in the neuronal engulfment assay detailed in Figure 1N (Figure S3E). Taken together, these results suggest that Lyve1^{+} MMϕ may be responsible for the engulfment of synapses and neuronal debris during early postnatal life.

The second cluster most abundant cluster at P10 was composed of proliferating MMϕ. In line with the scRNAseq findings, proliferation of MMϕ, assessed by intracellular Ki67 expression, was increased at P10 compared to P56 (Figure 3F). While around 30% of MMϕ were undergoing replication at P10, at P56, upon completion of tissue growth, only 5% of MMϕ were proliferating. Also via immunohistochemistry, Ki67^{+} MMϕ could be observed in the myenteric plexus at both P10 and P56 (Figure 3G). The high degree of proliferation coupled with the absence of monocytes in the tissue suggests that the expanding muscularis niche is filled via proliferation of self-maintaining macrophages rather than by infiltration of monocytes that differentiate into macrophages.

In contrast to MMϕ isolated at P10, MMϕ at P56 were characterised by the emergence of differentiating MMϕ and NA-MMϕ. NA-MMϕ were characterised by the upregulation of canonical microglia genes, such as *Tmem119*, *Olfml3* and *Hexb* (Figure 2K, S2J). Of interest, this cluster highly expressed the tight

junction protein F11r (JAM-A), typically expressed by endothelial cells in the gastrointestinal tract[169]. Indeed, F11r was expressed by endothelial cells within the muscularis externa at both P10 and P56 (Figure 3H). However, at P56 but not at P10, a subset of MMϕ expressing F11r^{+} could be observed in close proximity to neuronal cell bodies in the myenteric plexus, and to neuronal fibres within the muscle layer (Figure 3H-I). Of note, NA-MMϕ could not be detected in the serosa where neuronal cell bodies and fibers are absent (Figure 3I). Quantification via flow cytometry revealed that F11r^{hi} NA-MMϕ are present almost exclusively at P56, in line with our scRNAseq findings (Figure 3J).

Of note, the most abundant cluster at P56 was composed of differentiating MMϕ. We did not identify surface marker expression restricted to differentiating macrophages, and these cells were thus identified as Lyve1^{-} F11r^{-} Ki67^{-} MMϕ (Figure S2I). Lyve1^{-} F11r^{-} Ki67^{-} MMϕ were more abundant at P56 compared to P10 mice, in line with our scRNAseq analysis (Figure 3K). To understand whether these cells may ultimately differentiate into one of the identified mature clusters, we performed an RNA Velocity analysis on all non-replicating cells to estimate the direction of transcriptional shifts[170]. This analysis indicated a potential differentiation trajectory from differentiating MMϕ to NA-MMϕ, suggesting that these cells may ultimately differentiate into NA-MMϕ (Figure 3L). In line, regulatory network inference using SCENIC revealed that differentiating MMϕ activated multiple regulons characteristic for NA-MMϕ, including those driven by the *Nrf2* and *Atf3* transcription factor, but at a lower level (Figure 3M, S3E)[171].

Finally, to determine whether the frequency of the identified clusters undergoes further age-related shifts, we compared the cluster distribution in 8 and 20 weeks old mice using flow cytometry. Differentiating Lyve1^{-} F11r^{-} Ki67^{-} MMϕ decreased in frequency, while the abundance of F11r^{hi} NA-MMϕ increased with age (Figure 3K). Interestingly, the frequency of Lyve1^{+} MMϕ also decreased with age, representing less than 5% of all MMϕ at 20 weeks of age compared to 14% at 8 weeks of age (Figure 3N). Taken together, we identified distinct subpopulations of MMϕ that change their abundance during development and age and occupy specific subtissular niches in the muscularis.

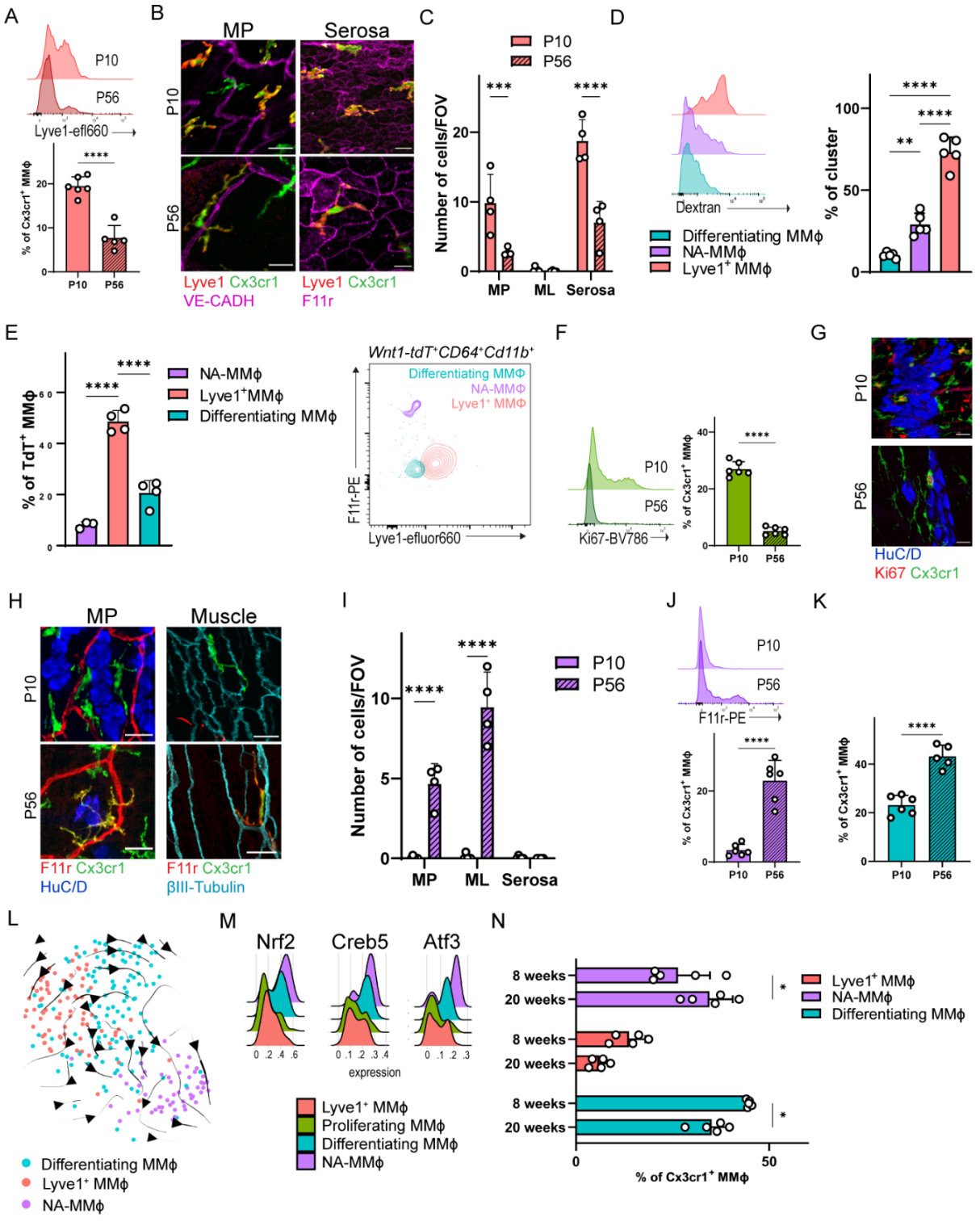
A
P10
P56
Lyve1-efl660
% of Cx3cr1+ MMΦ
B
MP
Serosa
P10
P56
Lyve1 Cx3cr1
VE-CADH
Lyve1 Cx3cr1
F11r
C
P10
P56
Number of cells/FOV
MP
ML
Serosa
D
Dextran
Differentiating MMΦ
NA-MMΦ
Lyve1+ MMΦ
% of cluster
E
% of TdT+ MMΦ
NA-MMΦ
Lyve1+MMΦ
Differentiating MMΦ
Wnt1-tdT+CD64+Cd11b+
Differentiating MMΦ
NA-MMΦ
Lyve1+ MMΦ
F11r-PE
Lyve1-efluor660
F
P10
P56
Ki67-BV786
% of Cx3cr1+ MMΦ
G
P10
P56
HuC/D
Ki67 Cx3cr1
H
MP
Muscle
P10
P56
F11r Cx3cr1
HuC/D
F11r Cx3cr1
βIII-Tubulin
I
Number of cells/FOV
P10
P56
MP
ML
Serosa
J
P10
P56
F11r-PE
% of Cx3cr1+ MMΦ
K
% of Cx3cr1+ MMΦ
L
Differentiating MMΦ
Lyve1+ MMΦ
NA-MMΦ
M
Nrf2
Creb5
Atf3
expression
Lyve1+ MMΦ
Proliferating MMΦ
Differentiating MMΦ
NA-MMΦ
N
8 weeks
20 weeks
8 weeks
20 weeks
8 weeks
20 weeks
Lyve1+ MMΦ
NA-MMΦ
Differentiating MMΦ
% of Cx3cr1+ MMΦ

Figure 3: MMϕ subsets occupy distinct micro-anatomical niches in the muscularis externa. (**A**) Representative histogram depicting Lyve1 expression in all MMϕ, and quantification of Lyve1$^+$ MMϕ in the muscularis externa of P10 and P56 mice via flow cytometry. (**B**) Representative confocal images showing Lyve1$^+$ MMϕ in the myenteric plexus (MP) and serosa at P10 and at P56. (**C**) Relative frequency of Lyve1$^+$ MMϕ quantified via immunohistochemistry, in the different micro-anatomical niches of the *muscularis externa*. (**D**) Quantification of phagocytic index of identified MMϕ populations and representative histograms depicting fluorescent dextran signal within each population. (**E**) Distribution of MMϕ populations within Wnt1-tdTomato+ MMϕ engulfing neuronal debris. Representative contour plot depicting MMϕ subsets within the Wnt1-tdTomato+ MMϕ compartment. (**F**) Representative histogram depicting Ki67 expression in all MMϕ, and quantification of Ki67$^+$ MMϕ in the muscularis externa of P10 and P56 mice via flow cytometry. (**G**) Representative confocal images showing Ki67$^+$ MMϕ in the myenteric plexus (MP) at P10 and at P56. (**H**) Representative confocal images showing F11r$^+$ MMϕ in the myenteric plexus (MP) and the muscle layer at P10 and at P56. (**I**) Relative frequency of NA-MMϕ quantified via immunohistochemistry, in the different micro-anatomical niches of the *muscularis externa*. (**J**) Representative histogram depicting F11r expression in total MMϕ, and quantification of F11r$^+$ MMϕ in the muscularis externa of P10 and P56 mice via flow cytometry. (**K**) Quantification via flow cytometry of Lyve1$^-$F11r$^-$ Ki67$^-$ MMϕ in the muscularis externa at P10 and at P56. (**L**) RNA Velocity analysis (n=253) reveals direction of transcriptional shifts between MMϕ. Proliferating MMϕ were excluded from this analysis. (**M**) Ridge plots SCENIC AUC distributions representing the activation of transcription factors significantly upregulated in NA-MMϕ (**N**) Quantification via flow cytometry of population frequency at 8 weeks (P56) and 20 weeks. In all data shown, MMϕ were obtained by gating on live CD45$^+$Cd11b$^+$Cd64$^+$Cx3cr1$^+$. Data are shown as Mean ± SD and are representative of at least 2 independent experiments. Data are analysed using T-tests or ANOVA followed by Tukey's multiple comparisons. Data are representative from at least 2 independent experiments, apart from experiments shown in D,E, L and M. N=4-7 mice per experiment, apart from data in L-N. Scale bars are 20µm. * $p < 0.05$; ** $p < 0.01$; **** $p < 0.0001$.

3.3.5 *ENS-derived TGFß Instructs MMφ to Adopt a Neuron-Associated Phenotype*

It is well established that the niche in which tissue resident macrophages reside largely determines their phenotype and transcriptome[2]. We next aimed to investigate the niche-driven imprinting of the neuron-associated phenotype in MMϕ after weaning, and which molecular mediators may be involved in shaping this phenotype. Transforming Growth Factor β (TGFβ) is a signalling molecule that is encoded by 3 isoforms in mammals, TGFβ1, 2 and 3. In the brain, TGFβ1 has been shown to be crucial in conferring the mature microglia signature[144]. As NA-MMϕ upregulate numerous microglia signature genes, we sought to investigate a possible role of TGFβ in imprinting the NA-MMϕ phenotype. Thus, the expression of TGFβ1, 2 and 3 was assessed in the muscularis externa at P10 and at P56. Interestingly, TGFβ3 expression increased significantly at P56 compared to P10 (Figure 4A).

We next sought to determine the source of TGFβ in the muscularis externa via flow cytometry using a non-isoform specific antibody. As NA-MMϕ are located in close proximity to the ENS, we hypothesised that enteric neurons or glia may represent the source of TGFβ. To assess TGFβ expression in the ENS, transgenic mice expressing tdTomato in neural crest-derived cells (*Wnt1*$^{cre/wt}$*Rosa26*$^{tdT/wt}$) were used. As this genetic construct labels both enteric neurons and enteric glia, enteric glia were distinguished from enteric neurons by CD49b expression, as previously described[172]. TGFβ expression was detected within the tdTomato^{+} population, with almost all enteric glia expressing TGFβ and around 25% of enteric neurons also expressing TGFβ (Figure 4B, S4A). Of note, TGFβ was also detected in Wnt1^{-} cells, suggesting that there may be other sources of TGFβ within the muscularis externa (Figure S4B). We did not detect TGFβ expression within the immune cell compartment (Figure S4B). To further validate these findings, enteric neurons (Wnt1^{+}CD49b^{-}), enteric glia (Wnt1^{+}CD49b^{+}), immune cells (CD45^{+}) and non-neural CD45^{-} cells were sorted from the muscularis externa and analysed for expression of TGFβ1, 2 and 3 via qRT-PCR. TGFβ1 expression was detected only at very low levels within all sorted populations (Figure 4C). TGFβ2 was expressed by enteric glia and enteric neurons, while TGFβ3 was mainly detected in enteric neurons and non-neural CD45^{-} cells (Figure 4C). Finally, we assessed expression of TGFβ2 and TGFβ3 in the ENS via *in situ* Hybridization Chain Reaction (HCR) combined with immunohistochemistry. Transcripts of TGFβ2 and TGFβ3 were detected within enteric neurons and enteric glia in the myenteric plexus of adult mice (Figure 4D, S4C). These findings confirm the cells of the adult ENS serve as a source of TGFβ within the muscularis externa.

Next, we assessed whether TGFβ may drive the expression of genes expressed by NA-MMϕ, bone marrow-derived macrophages (BMDMs) were cultured in the presence of TGFβ1, 2 or 3. Incubation with TGFβ led to the upregulation of canonical NA-MMϕ marker F11r, as assessed via flow cytometry (figure 4E). We further determined the expression of genes expressed by Lyve1^{+} macrophages, differentiating

macrophages and proliferating macrophages upon stimulation of TGFβ. While low levels of upregulation of genes such as Lyz2 and Apoe were observed, this was not sufficient to induce Lyve1 expression on the surface of BMDMs (figure 4E, S4D).

To investigate the role of ENS-derived TGFβ in determining NA-MMϕ phenotype, we performed ENS ablation in the muscularis externa using benzalkonium chloride (BAC), a cationic surfactant which, when applied directly to the muscularis externa, causes extensive neurodegeneration[173,174]. BAC treatment led to ablation of the ENS in the treated portion of the muscularis externa 5 days after treatment (Figure 4F). Loss of HuC/D^{+} neurons in the myenteric plexus was accompanied by reduced expression of neuronal (*Uchl1*) and glial (*Gfap*) gene expression (Figure S4E). BAC treatment led to a significant reduction of TGFβ3 expression only, whereas TGFβ2 expression remained unchanged (Figure 4G). Loss of enteric neurons and glia resulted in a reduction of the NA-MMϕ population within the MMϕ compartment, while other MMϕ subpopulations and global MMϕ cell counts were not affected (Figure 4H, S4F).

As BAC treatment leads to complete ablation of the ENS, we next sought to directly assess the role of ENS-derived TGFβ. To this end, Tgfb2$^{fl/fl}$-Tgfb3$^{fl/fl}$ (labelled as Tgfb2-3^{fl} hence forth) mice and Tgfb2-3^{wt} controls were infected with an AAV9 viral vector that contained a Cre recombinase and a GFP reporter to label infected cells. AAV9 has been effectively used to transduce neurons in the myenteric plexus in mice, and the construct was placed under the control of the neuronal promoter CamKII to ensure expression in only neuronal cells[175]. As transduction frequency varied between tissue regions, we focused our analyses on ganglia in which at least 15% of neuronal cell bodies were infected (GFP^{+}) (Figure S4G). We observed a significant reduction in the frequency of F11r^{+} MMϕ in Tgfb2-3^{fl} compared to Tgfb2-3^{wt} controls (Figure 4I-J), further supporting the role of enteric neuron-derived TGFβ in the induction of the NA-MMϕ phenotype.

Finally, we assessed the MMϕ compartment in *Cx3cr1^{CreERT2} Tgfbr2$^{fl/fl}$* mice, in which the TGFβ receptor type II, Tgfbr2, is excised from all Cx3cr1-expressing macrophages upon tamoxifen administration. TGFβ-signalling requires binding of TGFβ to Tgfbr2, that may then phosphorylate the TGFβ receptor type I (Tgfbr1), enabling the kinase activity of Tgfbr1[176,177]. Adult *Cx3cr1^{CreERT2} Tgfbr2$^{fl/fl}$* (Cre^{+}) mice and *Cx3cr1^{WT} Tgfbr2$^{fl/fl}$* (Cre^{-}) littermate controls were treated with tamoxifen and MMϕ subsets, whole gut transit time and neuronal density were assessed 4 weeks after tamoxifen administration. Loss of TGFβ receptor signalling led to a significant reduction in NA-MMϕ in Cre+ mice compared to Cre- controls (Figure 4K-L, S4H-I). Notably, loss of NA-MMϕ led to a trend toward an increase in total gut transit time and a significant loss of neurons in the myenteric plexus in Cre^{+} mice compared to Cre^{-} controls (Figure

4M-N). Taken together, these findings suggest that ENS-derived TGFβ imprints the NA-MMϕ phenotype observed in the adult muscularis externa.

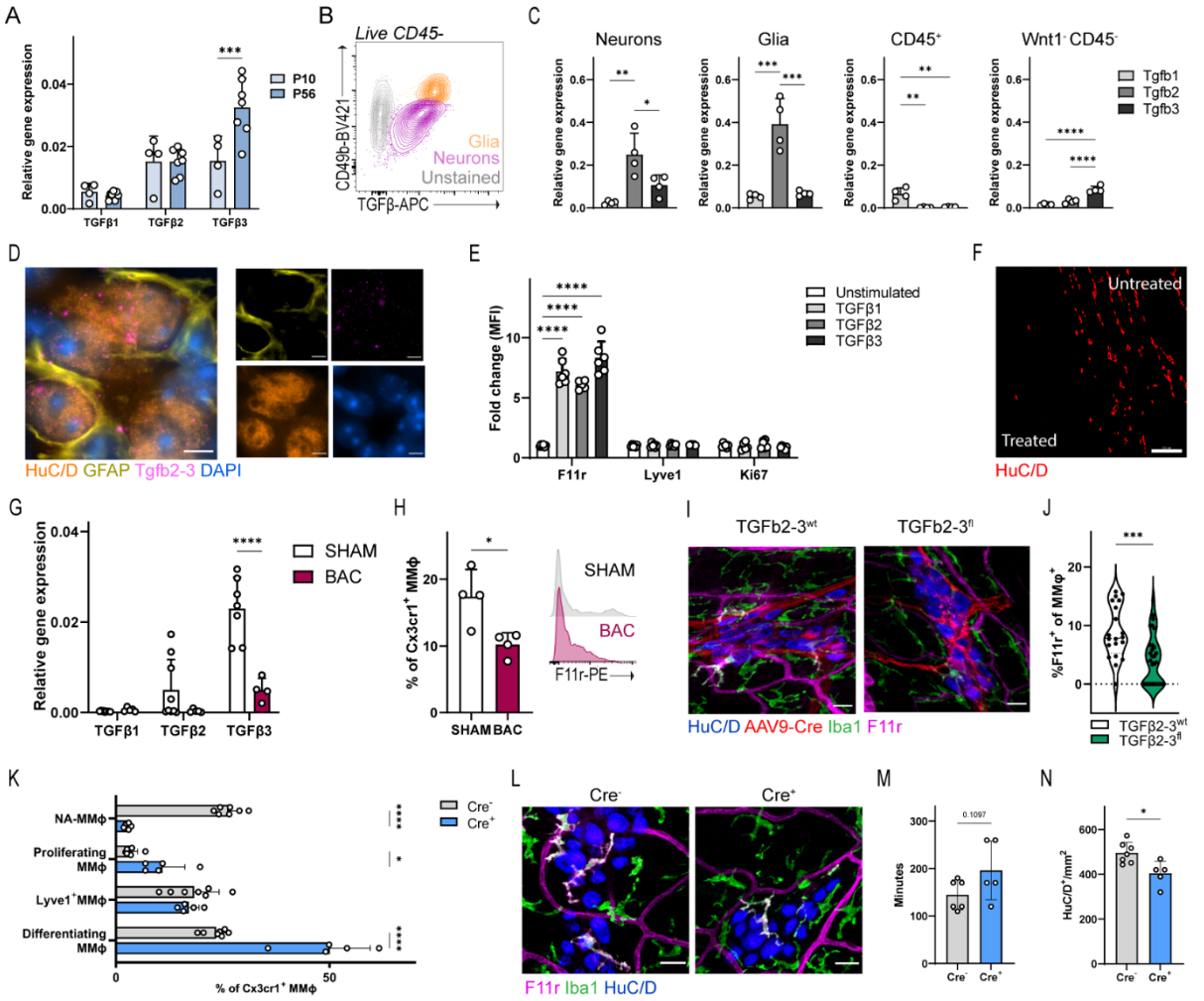

Figure 4: ENS-derived TGFβ instructs the NA-MMϕ phenotype. (**A**) Gene expression of TGFβ orthologues within the muscularis externa at P10 and P56. (**B**) Representative contour plot of TGFβ expression in enteric neurons and enteric glia, as assessed via flow cytometry. Cells were pre-gated on live CD45$^-$ Wnt1$^+$. The graph depicts the percentage of neurons and glia expressing TGFβ. (**C**) Gene expression of TGFβ1, TGFβ2 and TGFβ3 in enteric neurons (Wnt1$^-$Cd49b$^-$), enteric glia (Wnt1$^+$Cd49b$^+$), immune cells (CD45$^+$) and non-immune non neural (Wnt1$^-$ Cd49b$^-$) cells sorted from the muscularis externa of Wnt1$^{cre/wt}$ Rosa26$^{tdT/WT}$ mice. (**D**) Hybridization Chain Reaction (HCR) combined with immunohistochemistry showing transcripts of Tgfb2 and Tgfb3 in the ENS. Scale bar is 5 µm. (**E**) Expression of MMϕ subset marker genes in BMDM following 24h stimulation with TGFβ1, TGFβ2 or TGFβ3. (**F**) Representative confocal image depicting BAC-treated and untreated muscularis externa. Scale bar is 200µm. (**G**) Gene expression of TGFβ1, TGFβ2 and TGFβ3 in the muscularis externa 5 days after enteric denervation with BAC compared to SHAM. (**H**) Percentage of F11r^{hi} Cx3cr1$^+$ macrophages in mice denervated with BAC compared to controls (SHAM). Representative histogram of F11r expression in live CD45$^+$ Cd11b$^+$ CD64$^+$ Cx3cr1$^+$ cells. (**I**) Representative confocal images of the myenteric plexus in TGFb2-3^{wt} and TGFb2-3^{fl} mice infected with a neurotropic AAV9-Cre-GFP viral vector. Scale bar is 20µm. (**J**) Quantification of NA-MMϕ associated to transfected ganglia in TGFb2-3^{wt} and TGFb2-3^{fl} mice infected with a neurotropic AAV9-Cre-GFP viral vector. (**K**) Frequency of MMϕ populations in the muscularis externa of Cx3cr1$^{creERT2/WT}$ TGFbr2$^{fl/fl}$ (Cre$^+$) and Cx3cr1$^{WT/WT}$ TGFbr2$^{fl/fl}$ (Cre$^-$) mice 4 weeks after tamoxifen administration, as assessed via flow cytometry. (**L**) Representative confocal image of the myenteric plexus of Cx3cr1$^{creERT2/WT}$ TGFbr2$^{fl/fl}$ (Cre$^+$) and Cx3cr1$^{WT/WT}$ TGFbr2$^{fl/fl}$(Cre$^-$) mice. Scale bar is 20µm. Whole gut transit time (**M**) and neuronal density (**N**) assessed in Cx3cr1$^{creERT2/WT}$ TGFbr2$^{fl/fl}$ (Cre$^+$) and Cx3cr1$^{WT/WT}$ TGFbr2$^{fl/fl}$ (Cre$^-$) mice 4 weeks after tamoxifen administration. Data are shown as Mean ± SD. Data are analysed using T-tests or ANOVA followed by Holm-Sidak multiple comparisons. N=5-7. * $p < 0.05$; ** $p < 0.01$; *** $p < 0.001$; **** $p < 0.0001$; ns = not significant.

3.4 Discussion

Correct development and maturation of the ENS is critical for survival. Especially early in life the gastro-intestinal tract, and thus also the ENS, has to significantly adapt its function to the type of food ingested, changing from milk to solid food at the time of weaning. In the here presented study, we present a novel role of MMϕ in the postnatal maturation of the ENS. Furthermore, we describe different MMϕ sub-populations which change in their composition with age and serve distinct functions in sub-anatomical niches in the muscularis externa, including a distinct, neuron-associated MMϕ subset which expresses a microglia-like phenotype. Of note, this microglia-like phenotype is instructed by the ENS itself, via production of TGFβ. These findings suggest that MMϕ display a high degree of developmental plasticity, adapting their transcriptome and function to the evolving needs of the tissue. Furthermore, we shed light on the mediators involved in the establishment of the neuron-associated macrophage niche, which may open new opportunities to treat intestinal neurodegenerative disorders by manipulating the ENS-macrophage niche.

3.4.1 *Remodelling of the ENS by MMφ*

Although the intestine is colonized by enteric neurons at birth, the ENS still requires significant remodelling before it acquires its typical organization into ganglia connected by nerve tracks[94,162]. Reorganisation of the ENS in early postnatal life requires refinement of enteric neurons, the number of ganglia and the fibers that connect the ganglia to each other. Here, we show that depletion of MMϕ during a critical refinement period between P10 and P17 led to hyperganglionosis, a disorganised immature ENS structure and increased synaptic density, demonstrating that MMϕ are involved in the reorganisation of the ENS during early postnatal life. Depletion of MMϕ at earlier or later timepoints in the postnatal period did not affect neuronal density, suggesting that refinement is restricted to a specific developmental time window, a finding that mirrors early postnatal neurodevelopment in the brain.

Refinement of the ENS by MMϕ, which requires phagocytosis of neurons, is critical for the correct establishment of peristalsis, as depletion of MMϕ throughout early postnatal life led to increased neuronal density and accelerated intestinal transit in adulthood. Our findings are in line with previous studies using *Csf1*$^{op/op}$ mice, which are devoid of MMϕ, and which display a disorganised ENS and increased neuronal density in adulthood[166]. In line with these findings, when we performed transcriptional profiling of MMϕ at P10, we observed that MMϕ at P10 were predominantly Lyve1^{+} MMϕ. Lyve1^{+} MMϕ upregulated numerous canonical phagocytosis genes, presented superior phagocytic capacity as tested in an *ex-vivo* phagocytosis assay compared to other identified MMϕ subpopulations. Moreover, they were found to be the MMϕ subset mainly responsible for the

engulfment of neuronal debris. Although further investigations are warranted to pinpoint the triggers that cue the developmental refinement of the ENS, one might speculate that the exposure to solid food and food antigens, or the profound shifts in intestinal microbiota that occur during early postnatal life may initiate ENS maturation[178]. Finally, it cannot be excluded that ENS maturation during early postnatal life may be consequence of developmental programming of neurons themselves. Nevertheless, our findings demonstrate that early in life, MMϕ play a crucial role in remodelling the ENS, enabling it to adapt to the evolving needs of the gut.

3.4.2 *ENS-MMφ Relationship in Adulthood*

We previously demonstrated that loss of MMϕ in adulthood leads to significant neurodegeneration and impaired GI function[22]. Here we confirmed these findings; depletion of MMϕ at 8 weeks of age led to a significant reduction in neuronal density, suggesting that in adulthood, MMϕ shift toward a neuro-supportive function. In line, scRNAseq of P56 MMϕ revealed the emergence of a novel, neuron-associated MMϕ (NA-MMϕ) population. This NA-MMϕ population upregulated genes including *Tmem119*, *Hexb*, *Olfml3* and its surface marker *F11r*, and was found to be associated to neuronal cell bodies and fibres in mice in adulthood. As we previously demonstrated that MMϕ preferentially associated to enteric neurons are long-lived, we speculate that this population represents a specialised population of MMϕ that is critical for neuronal support and survival in adulthood[22]. In line, loss of NA-MMϕ led to loss of enteric neurons and delayed intestinal transit time. The identification of a specific MMϕ, associated to enteric neurons and designated with a specific marker (F11r) opens the door to future studies on neurodegenerative disorders of the GI tract, in which NA-MMϕ may play a crucial role.

3.4.3 *The ENS-MMϕ Niche*

Recently, we described a macrophage population associated to neurons in the enteric nervous system, which displayed an upregulation of canonical microglia genes[22]. Since then, several similar 'microglia-like' macrophage populations have been reported to be associated to large peripheral nerve bundles including dorsal root ganglia, vagal nerve, subcutaneous fascial nerves and sciatic nerves[96,97]. The definition of 'microglia-like' largely derives from the transcriptional signature, as these cells have been shown to upregulate canonical microglia genes, including *Hexb*, *Siglech*, *Trem2* and *Olfml3*[179,180]. It should be emphasized though that they fail to upregulate the typical microglial transcription factor Sall1, suggesting that distinct anatomical niches might still vary to a certain amount in the factors released to specify nerve-associated macrophages[96,97,179]. Intriguingly, while neuron-associated macrophage subsets share a microglia-like transcriptional signature, the signals inducing this signature have not been identified. Here, we identify TGFβ, a cytokine critical for microglial instruction in the brain, as a molecular cue employed by the ENS to instruct local macrophages to adopt a neuron-associated profile. *In vitro*

stimulation of BMDM with TGFβ led to the upregulation of genes identified in NA-MMϕ while *in vivo*, chemical ablation of the ENS or genetic inhibition of TGFβR signalling in MMϕ led to the reduction of NA-MMϕ in the muscularis externa. TGFβ-TGFβR signalling is thus crucial for the maintenance of NA-MMϕ in the adult muscularis externa. This is, to our knowledge, the first study which identifies the molecular mediator that defines the neuron-associated macrophage niche. To what extent TGFβ might be a conserved signal used by neuronal niches throughout the body to imprint a specific phenotype to the local macrophage pool requires further study.

3.4.4 *Functional Plasticity of MMϕ*

With the notable exception of microglia, the notion that macrophages within tissues retain the plasticity to adapt their function in order to respond to evolving needs of the tissue has largely been restricted to the context of disease and inflammation. Here, we demonstrate that resident MMϕ undergo profound transcriptional maturation from postnatal development to adulthood, a maturation that is likely cued by the surrounding cells and the evolving needs of the tissue. A similar developmental plasticity has been demonstrated in the brain, where microglia are critical for the refinement of synaptic connectivity during early postnatal development and for neuronal homeostasis and neurogenesis in adulthood[181–183]. Also in the brain, this functional adaptation is mirrored by transcriptional shifts that enable microglia to respond to the evolving requirements of the rapidly developing surrounding cells, which is crucial for the development and maturation of the central nervous system (CNS)[146]. Strikingly, the global transcriptional shifts observed in MMϕ resemble those observed in microglia, with a global upregulation of genes involved in phagocytosis and replication during early postnatal life, and subsequently, in adulthood, upregulation of genes involved in immune surveillance[146]. Similarly, changes in morphology and proliferative rates of MMϕ also paralleled microglial differentiation[184,185].

3.4.5 *Paralleled Role for Macrophages/Microglia in the Central and Enteric Nervous System*

The finding that macrophages participate in the process of neuronal refinement in the ENS opens up new horizons in our understanding of neurodevelopmental disorders of the ENS. In the brain, depletion of microglia during a time window critical for synaptic pruning leads to altered learning and memory, social, mood-related, and locomotor behaviours[186,187]. Of note, hyperganglionosis of the myenteric and submucous plexus is associated to severe constipation in children, and has been associated with gastrointestinal motility disorders[159,160]. Whether these abnormalities in ENS morphology and gut dysfunction can be ascribed to insufficient MMϕ function early in life requires further study. Conversely, based on our findings, MMϕ dysfunction in adulthood should be considered as a potential disease mechanism in neurodegeneration in the ENS, as described during aging and in diseases such as diabetes and obesity[22,188,189]. The resemblance between the neuronal niche in the muscularis externa and the

brain, where TGFβ is critical for the instruction of microglia, is striking, and further supports the notion that the ENS may resemble the CNS more than previously anticipated. Indeed, it is widely reported that neurodegenerative and neurological disorders of the CNS, including Parkinson's disease, Alzheimer's disease and Multiple Sclerosis, present wide-ranging ENS symptomatology[161,190,191]. It is intriguing to speculate that the ENS, as the 'brain of the gut', may mirror the CNS in homeostasis and in disease, and may thus offer an unexploited snapshot of ongoing pathological processes in the brain.

3.5 Acknowledgements

We thank Pier Andrée Penttila and Reena Chinnaraj from the KU Leuven FACS core for their excellent support and cell sorting. We also thank the Cell Imaging Core (Pieter Vanden Berghe and Tobie Martens, KU Leuven) for confocal imaging (supported by AKUL 15/37 and FWO I001918N). We also thank Dr. Escamilla-Ayala of the VIB Leuven BioImaging Core for her support and assistance in this work. We thank Katrin Kierdorf, Marco Prinz and Mohamad Azhar for providing mice. MFV is supported by FWO PhD fellowship 11C2219N. GB is funded by ERC Advanced grant number 833816-NEUMACS.

3.6 Author Contributions

MFV designed experiments, conducted experiments and wrote the manuscript. MCP performed histological analyses. EM and AS performed analysis of scRNAseq data. IA and NF provided excellent technical support throughout all experiments. MD performed FACS-sorting of cells and IV injections. NS performed BAC experiments. JVH prepared the scRNAseq library. TM performed ex-vivo time-lapse imaging. KV performed HCR experiments. SV, SDS, PVB,TV and AS provided intellectual input. KK and MP provided mice and PP performed genotyping and tamoxifen injections. GB led the project and revised the manuscript.

3.7 Declaration of interests

The authors declare no competing interests.

3.8 Data Availability

The scRNAseq dataset generated and analysed during the current study is available in the ArrayExpress repository at https://www.ebi.ac.uk/arrayexpress/experiments/E-MTAB-11453. All other relevant data generated and analysed during the current study are available upon reasonable request to the corresponding author.

3.9 Materials and Methods

3.9.1 *Mice*

All animal experiments were performed in accordance with the European Community Council and approved by the Animal Care and Animal Experiments Committee of the Medical Faculty of the KU Leuven. Mice were maintained under a 14h/10h dark/light cycle, at a temperature of 20-22 °C, provided with food and water ad libitum. Both male and female mice were used for this study. *Cx3cr1*$^{GFP/GFP}$ mice were obtained from Steffen Jung, Weizmann Institute of Science[192]. Wnt1.Cre mice were obtained from Pieter Vanden Berghe[193]. *Rosa26*$^{TdT/TdT}$ mice were obtained from Jackson Laboratory. *Wnt1*$^{Cre/WT}$ *Rosa26*$^{TdT/WT}$ *Cx3cr1*$^{GFP/WT}$ mice were bred in our facility and maintained on a C57Bl/6 background. *Cx3cr1*$^{CreERT2/WT}$ *Tgfbr2*$^{fl/fl}$ mice were kindly provided by Katrin Kierdorf and Marco Prinz, University of Freiburg. Tgfb2$^{fl/fl}$ Tgfb3$^{fl/fl}$ mice were kindly provided by Mohamad Azhar, University of South Carolina School of Medicine.

3.9.2 *Histology and immunofluorescence*

The ileum was dissected, carefully flushed using Hank's Balanced Salt Solution (HBSS) (Gibco) supplemented with fetal calf serum (FCS, 3%, Lonza) and HEPES (1.8%) and pinned on a sylgard plate. The tissue was cleaned of mesenteric fat, opened longitudinally and pinned with the muscle layer facing upwards. The muscle layer was carefully peeled from the submucosa, pinned flat on the sylgard plate and then fixed for 30 minutes in PFA 4%. Fresh whole mount tissue was stained within one week of collection. Tissue was permeabilized in PBS supplemented with Triton X-100 (0.3%; permeabilization buffer) for 2 hours at room temperature, and then blocked with permeabilization buffer supplemented with Donkey serum (5%) and Bovine serum albumin (BSA, 5%; blocking buffer) for 2 hours at room temperature. Tissue was incubated with primary antibodies diluted in blocking buffer overnight at 4°C. Tissue was extensively washed in PBS prior to incubation with secondary antibodies diluted in blocking buffer for 2 hours at room temperature. Samples were washed and mounted using SlowFade Diamond Antifade mounting medium (Thermofischer Scientific) and imaged using a Zeiss LSM880 confocal microscope. Negative controls (incubated with secondary antibody, but no primary antibody) were included for every analysis. All antibodies used are listed in supplementary table 1.

3.9.3 *Ex-vivo live imaging*

The ileum of *Wnt1*$^{Cre/WT}$ *Rosa26*$^{TdT/WT}$ *Cx3cr1*$^{GFP/WT}$ mice was carefully in carbogenated Krebs solution at 4°C. The mucosal, submucosal, and longitudinal muscle layers were carefully removed to obtain a circular muscle with adherent myenteric plexus preparation which was mounted over a small inox ring, immobilized by a matched rubber O-ring[194]. Inox rings with muscularis externa preparations were positioned in FluoroDishes and maintained at 37°C with 5% CO2 in Krebs solution with 1µm nifedipine

for time-lapsed imaging using a LSM880 Airyscan confocal microscope (Zeiss). Stitched videos were analysed and processed using ImageJ software (Fiji).

3.9.4 *Quantification of synaptic volume and synaptic engulfment*

Quantification of synaptic engulfment was carried out using a published protocol adapted to our purpose[167]. Briefly, Z-stacks were imported to Imaris (Bitplane) for analysis, where digital 3D reconstructions were performed to calculate MMϕ volume, and synaptic machinery. Engulfment was determined to be the volume of synaptic machinery engulfed by MMϕ, normalised to the volume of the MMϕ. Synaptic density was determined as the volume of synaptic machinery, normalised to the volume of the region of interest.

3.9.5 *Analysis of MMφ morphology*

Z-stacks of confocal images were imported into Imaris software (Bitplane). The filament tool was used to trace the filopodia of each MMϕ manually. Number, length and branching of filopodia was calculated using the filament tool. MMϕ cell volume was estimated using the volume tool.

3.9.6 *Tissue harvest for single cell suspensions*

The small intestine was removed from mesenteric fat tissue, opened longitudinally and cleaned in Hank's Balanced Salt Solution (HBSS) (Gibco) supplemented with fetal calf serum (FCS, 3%, Lonza) and HEPES (1.8%). The opened tissue was pinned to a sylgard plate and the muscle layer was carefully dissected and collected in RPMI supplemented with FCS (3%) and HEPES (2%). The tissue was cut in small pieces and incubated with Collagenase IV (500U/ml) and DNAse for 30 minutes at 37°C in constant agitation. After digestion, cells were filtered through a 70 µm cell strainer and washed using PBS supplemented with FCS (2%) and EDTA (1.6mM) and counted prior to staining for Flow Cytometry.

3.9.7 *Flow cytometry*

Single cell suspensions were blocked using anti CD16/CD32 (Fc block) and subsequently labelled for flow cytometry analysis using fluorophore-conjugated anti-mouse antibodies for 30 min at 4°C using the antibodies listed in supplementary table 2. For intracellular staining, cells were fixed using the FoxP3 Intracellular Staining kit (eBioscience), and incubated with conjugated intracellular antibodies for 1 hour at 4°C. Samples were acquired using a Symphony A5 (BD Biosciences). Analysis was carried out using FlowJo (v10, Tree Star).

3.9.8 *Sorting of live cells confocal imaging*

Single-cell suspensions were obtained from the ileum of $Wnt1^{Cre/WT}$ $Rosa26^{TdT/WT}$ $Cx3cr1^{GFP/WT}$ mice as previously described, and further processed for staining with cell-surface markers. Cells were sorted

using a Sony MA900 cell sorter into PBS containing 0.1% bovine serum albumin (BSA). Cells were transferred to a glass slide using a cytocentrifuge, then fixed for 15 minutes in 4% PFA. After fixation, cells were processed for immunohistochemistry as detailed above, and imaged using a confocal microscope (LSM880, Zeiss). Orthogonal views of cells were obtained using Imaris (Bitplane).

3.9.9 *Depletion of muscularis macrophages*

Muscularis macrophages were depleted as previously described[45]. Briefly, mice received 2 injections (37.5 µg/g) of either α-CSF1R (Clone AFS98, Bio X Cell) or IgG2a isotype control (Clone 2A3, Bio X Cell) I.P., 3 days apart, and were euthanized via CO2 overdose 4 days after the last injection. For depletion throughout the postnatal period, mice received 2 injections (37.5 µg/g) of either α-CSF1R (Clone AFS98, Bio X Cell) or IgG2a isotype control (Clone 2A3, Bio X Cell) I.P. twice a week, from P10 until P22.

3.9.10 *Whole Gut Transit Time*

Whole gut transit time was assessed using carmine red gavage as previously described[195]. Briefly, two days prior to the assessment, mice were acclimatized by a saline gavage and a period of 3 hours in single-housing. Following an overnight fast, mice were gavaged with a 6% w/v solution of carmine red (Sigma) in sterile methyl cellulose (0.5%) and single-housed. Mice were monitored every 15 minutes until the appearance of the first red pellet. The time elapsed from the gavage of carmine red until the appearance of the first red pellet was recorded as total gut transit time.

3.9.11 *scRNAseq library preparation*

Single-cell suspensions were obtained from the ileum of $Cx3cr1^{GFP/WT}$ mice as previously described. Cells were counterstained with DAPI to exclude dead cells and sorted using an Aria III cell sorter (BD) into skirted 96-well plates for scRNAseq. cDNA libraries from 376 cells were generated based on the Smart-seq2 protocol[196]. Briefly, mRNA was reverse transcribed and cDNA was amplified via PCR. Amplification was carried out using KAPA HIFI Hot Start ReadyMix (Roche, 07958919001) and purification by magnetic beads (CleanNA CPCR). Quantity and quality of cDNA was assessed with the quantifluor RNA system (Promega E3310) and Agilent 2100 BioAnalyzer with a high-sensitivity chip. Library was prepared using the Nextera XT library prep and index kit (Illumina). cDNA was tagmented by transposase Tn5 and amplified with dual-index primers. Reagents were mixed together by the Echo 555 (Labcyte) and pooled-nextera XT libraries were purified. Single-cell libraries were pooled together and sequenced single-end 50 bp on a single lane of a HiSeq4000 (Illumina). All results related to scRNA-seq are based on 4 pooled biological replicates per group.

3.9.12 *scRNAseq analysis*

Raw fastq reads were obtained from the sequencer and underwent a series of steps before being imported to Seurat (v4.1.0) for analysis. The reads were trimmed with cutadapt 3.0 to remove adapters. Reads were then mapped to the mouse genome (GRCm38.p6) with STAR 2.7.6a and reads that mapped to a gene were counted with htse-count 0.12.4. Metrics were then collected and optical duplicates were marked using Picard 2.23.8. Finally, multiqc 1.9 was used to collect all the analyses log files into a single report and countmatrix files were generated (genes per cell counts). After pre-processing of the reads, each library was matched with a sample using the predetermined Nextera barcodes. Following a quality check and filtering of these samples (features: 2000-7500; mitochondrial gene content < 5%), cells were normalized, scaled and batch-corrected (5000 anchors and using 35 neighbors to filter the anchors) using Seurat. Highly variable genes (i.e. 1742) were then used for PCA dimensionality reduction and visualized using 2-D Uniform Manifold Approximation and Projection (UMAP) in Seurat. Cells were grouped by unsupervised clustering at different clustering resolutions and the clustering resolution 1.1 was chosen to reflect clear biologically-driven transcriptional differences between clusters. The smallest cluster of the dataset, comprising of 34 cells, was excluded from further analysis due to cargo contamination (Figure S2D-G). All further analyses, including identification of marker genes, single-cell regulatory network inference and clustering (SCENIC) and RNA Velocity were performed after removal of this cluster.

Gene regulatory network analysis was performed using pySCENIC (v.0.9.3) using default parameters. SCENIC is a tool to infer gene regulatory networks from single-cell RNA-seq data[171]. Differentially activated regulons were determined by performing a two-sided Kolmogorov–Smirnov non-parametric rank sum test on the regulon AUC values of cells in the various clusters, P values were false discovery rate (FDR)-adjusted using the Benjamini–Hochberg method and regulons with an adjusted P value less than 0.01 were considered differentially activated.

To perform lineage trajectory analysis, we employed RNA Velocity. RNA Velocity is a high-dimensional vector that predicts the future state of individual cells on a timescale of hours. As proliferating cells tend to create circular trajectories which can confound data interpretation, we excluded these cells from RNA Velocity analysis. Splicing information of reads (spliced/unspliced) was extracted from the binary file containing the sequence aligned data (.bam) from a Smartseq2 run of each separate sample using the velocyto (01.17.17) pipeline (http://velocyto.org). It was then stored in a loom file and then read into an AnnData with python (v 2.7.5) object for downstream analysis with scVelo (0.2.4) and numpy (1.19.4). For the estimation of velocities and the RNA force field the recommended steps of scVelo were followed, namely: Filtering, normalisation and log transformation of the data, computing first- and second-order moments, estimating velocities, and constructing a velocity graph. First- and second-order moments were calculated for each cell across its nearest neighbors of a single-cell neighbourhood-graph

in PC space (number of neighbors=30, number of PCs=35). Then estimates for velocities were obtained by fitting a dynamic model of transcription for each gene. Finally, a velocity graph was computed from the correlations between potential cell transitions in the neighbourhood graph and the predicted cell state change given by the velocity vector. This graph was then used to project the estimated velocities into the original low dimensional UMAP space.

3.9.13 *Ex-vivo phagocytosis assay*

Cells were isolated to obtain single-cell suspensions. To assess ex-vivo phagocytosis, cells were incubated for 45 minutes at 37°C in the presence of Texas Red-conjugated Dextran (MW 70 000, Invitrogen) prior to extracellular surface marker staining, while controls were maintained at 4° in the presence of Texas Red-conjugated Dextran. Cells were further processed as described for flow cytometry. Phagocytic index is defined as percentage of cells engulfing dextran, multiplied by the MFI (mean fluorescence intensity) of the fluorescently labelled dextran engulfed by the cells.

3.9.14 *RNA Isolation and qRT-PCR*

RNA from tissue or cells was extracted using the innuPREP RNA Mini Kit 2.0 (AnalytikJena), according to manufacturers' guidelines. RNA was retrotranscribed using the qScript cDNA Synthesis Kit (Quantabio) according to manufacturers' instructions using a GeneAmp PCR System 2700 (Applied Biosystems). qRT-PCR was performed using LightCycler® 480 SYBR Green I master mix (Lifescience, Roche) on a Lightcycler 480 (Roche) using the primers detailed in supplementary table 3. All data were normalized to Rpl32 quantified in parallel amplification reactions.

3.9.15 *Sorting of live cells for gene expression analysis*

Single-cell suspensions were obtained from the ileum of $Wnt1^{Cre/WT}$ $Rosa26^{TdT/WT}$ $Cx3cr1^{GFP/WT}$ mice as previously described, and further processed for staining with cell-surface markers. Cells were sorted using a Sony MA900 cell sorter directly into RLT buffer additioned with β-mercaptoethanol. After sorting, samples were vortexed as per manufacturer's instructions and stored at -80°C until further analysis.

3.9.16 *Hybridization Chain Reaction (HCR)*

Probes for Tgfb2 and Tgfb3 were purchased from Molecular Instruments (Los Angeles, California). To avoid losing efficiency due to the targeting of transcripts with a high degree of homology, Tgfb2 and Tgfb3 probes were designed conjugated to the same amplifier After two consecutive washes in PBS and then 2XSSCT, pre-hybridization was carried out by incubating tissue at 37°C in probe hybridization buffer (Molecular Instruments) for 30 minutes. V3.0 Tgfb2 and Tgfb3 HCR-FISH probes (2 pmol of each probes set, Molecular Instruments) were hybridised overnight at 37°C in probe hybridization buffer. Excess

probes were removed by washing tissue 4 times for 5 minutes each at 37°C in probe wash buffer, then for 5 minutes in 5XSSCT. HCR hairpins were prepared by snap cooling separately (95°C for 90 seconds, cool to room temperature in the dark for 30min), followed by adding to probe amplification buffer. Tissue was incubated with 30 pmol HCR hairpins in probe amplification buffer for 4 hours. Tissue was washed for 5 minutes and 30 minutes in 5XSSCT, then incubated for 10 minutes with 5XSSCT and DAPI (300nm). Tissue was then washed 3 times for 10 minutes with 5XSSCT. Tissue was mounted using Slowfade Diamond Antifade Mountant and imaged using structured illumination microscopy (SIM).

3.9.17 *Structured illumination microscopy (SIM)*

Structured illumination microscopy (SIM) was done with a Plan Apo Lambda Sil 100x/1.35 NA objective lens coupled to a Ti2 N-SIM-S (Nikon Instruments) microscope with a sCMOS camera (Orca Flash 4.0, Hamamatsu) and a Nano-drive piezo Z-stage (Mad City Labs, Inc.). The device was controlled by Nikon NIS-Elements (Version 5.21.03) software. Multi-color images were acquired in 3D-SIM mode (3 angles, 5 phases) with a Z-stack (step size 0.12um). Reconstruction was done using NIS slice reconstruction optimized for each channel.

3.9.18 *BMDM experiments*

Femura bones from 8 week old C57/Bl6J mice were isolated and collected in RPMI. The extremities of the bones were cut, and a 24G gauge needle was used to flush out the bone marrow into complete RPMI (10% FCS, 1% P/S, 1% L-glutamine, 1% Sodium Pyruvate and 1% Hepes). The cells were then centrifuged, resuspended in red cell lysis buffer for 1 minute, then washed with PBS and centrifuged. The pelleted cells were then resuspended and plated in complete RPMI supplemented with 7.5% L929 medium. Cells were grown for 7 days prior to stimulation with either 2ng/ml of TGFb1, 2 or 3. 24 hours after stimulation, cells were collected for RNA extraction and qRT-PCR analysis, or analysis via flow cytometry.

3.9.19 *Enteric denervation using Benzalkonium Chloride (BAC)*

Animals were anesthetized by i.p. injection of ketamine (Ketalar; 100 mg/kg; Pfizer) and xylazine (Rompun; 10 mg/kg; Bayer). A laparotomy with a midline incision was performed, and a portion of the ileum was exposed. Sterile cellulose filter paper disks (5-mm diameter; Whatman) soaked in 0.1% BAC (Sigma-Aldrich) in NaCl solution were placed on the exteriorized intestine, 2 cm from the ileocecal valve. Sham mice received the same procedure, however cellulose filter disks were soaked in NaCl solution online. The tissue was incubated for 15 min with BAC or NaCl, after which the paper disk was removed and the treated area thoroughly rinsed with sterile saline solution. Mice were killed with CO2 overdose 14 days after treatment. The treated segments of bowel were harvested from each animal, and the muscularis layer was isolated for flow cytometry analysis as previously described.

3.9.20 *AAV9 Transfection Experiments*

AAV9 serotype viral vector with CamKII(0.4) promoter driven EGFP-T2A-iCre was purchased from Vector Biolabs (Malvern, PA, USA). 8 week-old $Tgfb2^{fl/fl}$ $Tgfb3^{fl/fl}$ and $Tgfb2^{wt/wt}$ $Tgfb3^{wt/wt}$ mice received 10^{12} GC of vector via IV injection. 2 weeks after injections, mice were euthanised for tissue collection and histological analysis.

3.9.21 *Tamoxifen treatment*

For activation of Cre recombinase, tamoxifen (TAM, Sigma-Aldrich, Taufkirchen, Germany), was dissolved in sterile corn oil (Sigma-Aldrich, Taufkirchen, Germany) prior to injection at a concentration of 20mg/ml. Cre recombination was induced by injecting 4 mg TAM/200µl corn oil subcutaneously twice 48 h apart.

3.9.22 *Statistics*

Statistical analysis was performed using Prism 9 (GraphPad Software). Data are represented as Mean ± SD and analysed using T-tests, ANOVA (followed by Tukey's multiple comparisons) or Kruskal-Wallis (followed by Dunn's multiple comparisons). Statistical outliers were removed using Grubbs outlier test. A p value < 0.05 was considered statistically significant.

3.10 Supplementary Information

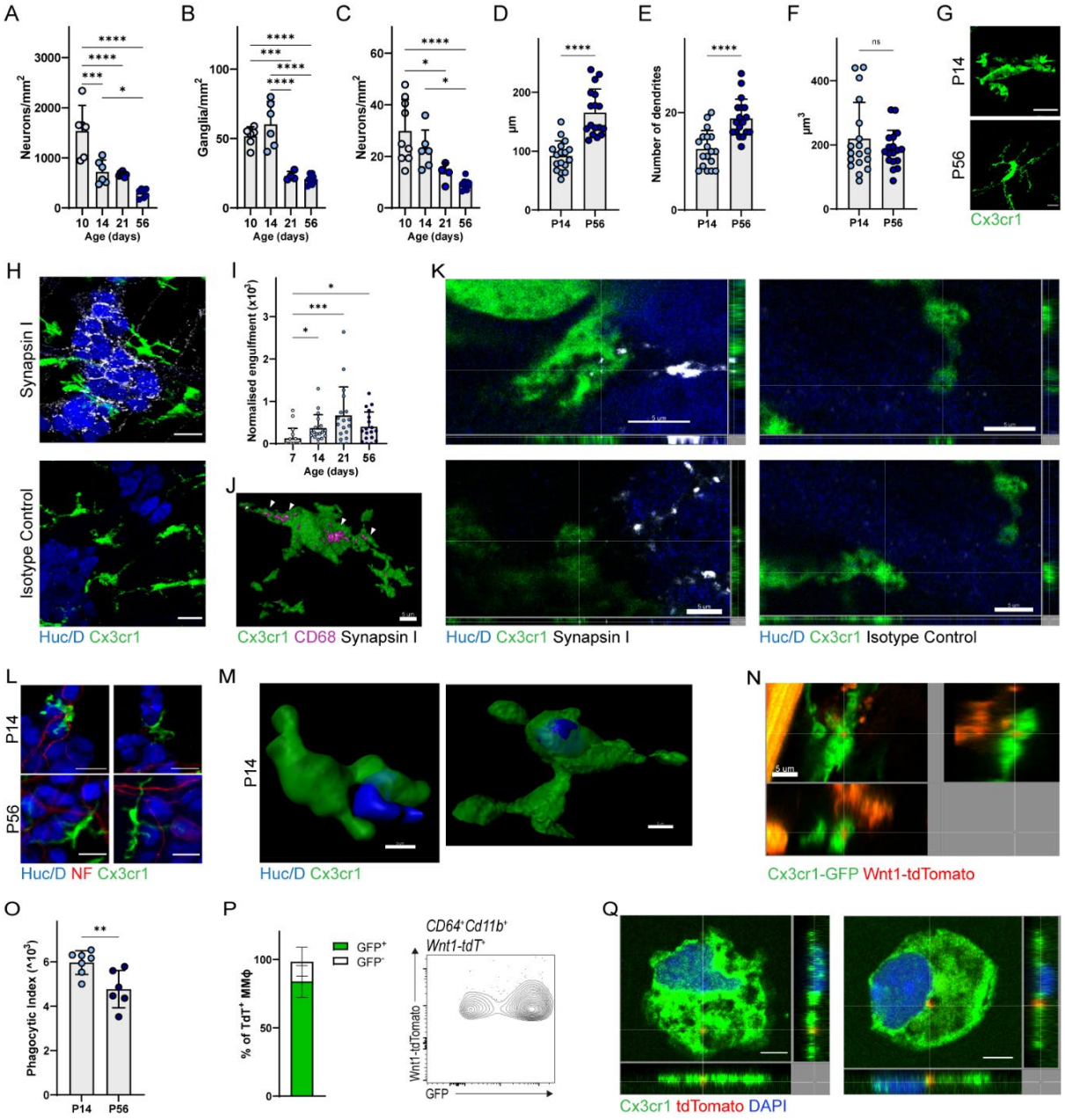

Figure S1: Quantification of neuronal density (**A**), the number of ganglia (defined as containing 5 or more neurons) per mm^2 (**B**), and the number of single extra-ganglionic neurons per mm^2 (**C**), in the myenteric plexus at 10, 14, 21, and 56 days of age, corrected for tissue growth. Total length of MMϕ filopodia (**D**), number of dendrites (**E**) and MMϕ cell volume (**F**) as assessed via 3D reconstruction using Imaris. (**G**) Representative confocal images displaying MMϕ morphology at P14 and at P56. Scale bar is 10µm. (**H**) Representative confocal image of the myenteric plexus at P14 using either Synapsin-I or isotype control. Scale bar is 20µm. (**I**) Percentage of synaptic engulfment per cell, determined as volume of $Synapsin^+$ volume/MMϕ volume, normalised to synaptic density in the ROI analysed. (**J**) Digital reconstruction using Imaris depicting synapses engulfed by MMϕ located within CD68+ lysosomes. White arrowheads indicate engulfed synapses Scale bar is 5 µm. (**K**) Representative orthogonal view depicting MMϕ engulfing synaptic machinery at P14, compared to tissue stained with appropriate isotype control. Scale bar is 5 µm. (**L**) Representative confocal images displaying MMϕ engulfing neuronal cell bodies and extending filopodia towards neuronal cell bodies and filaments. Scale bar is 20µm. (**M**) Digital reconstructions of MMϕ engulfing enteric neurons, performed using Imaris. Scale bar is 5µm. (**N**) Representative orthogonal view depicting MMϕ engulfing tdTomato+ neural debris. Scale bar is 5µm. (**O**) Mean fluorescence intensity of MMϕ engulfing neural cells at 14 days (P14) and 56 days (P56) of age. (**P**) Graph and representative contour plot depicting contribution of engulfment of neuronal debris ($tdTomato^+$) by MMϕ that occurs in vivo (GFP^+) and ex vivo during enzymatic digestion (GFP^-). (**Q**) Representative orthogonal view depicting MMϕ engulfing $tdTomato^+$ neuronal debris, obtained via confocal imaging of FACS-sorted $tdTomato^+$ MMϕ. Scale bar is 5 µm. Unpaired t-tests or Ordinary One-Way ANOVAs with Tukey's multiple comparisons. Data are shown as Mean ± SD. N=4-7 per experiment. Single data points indicate biological replicates, apart from D-F where single data points indicate images analysed. * $p < 0.05$; ** $p < 0.01$; *** $p < 0.001$; **** $p < 0.0001$; ns = non significant.

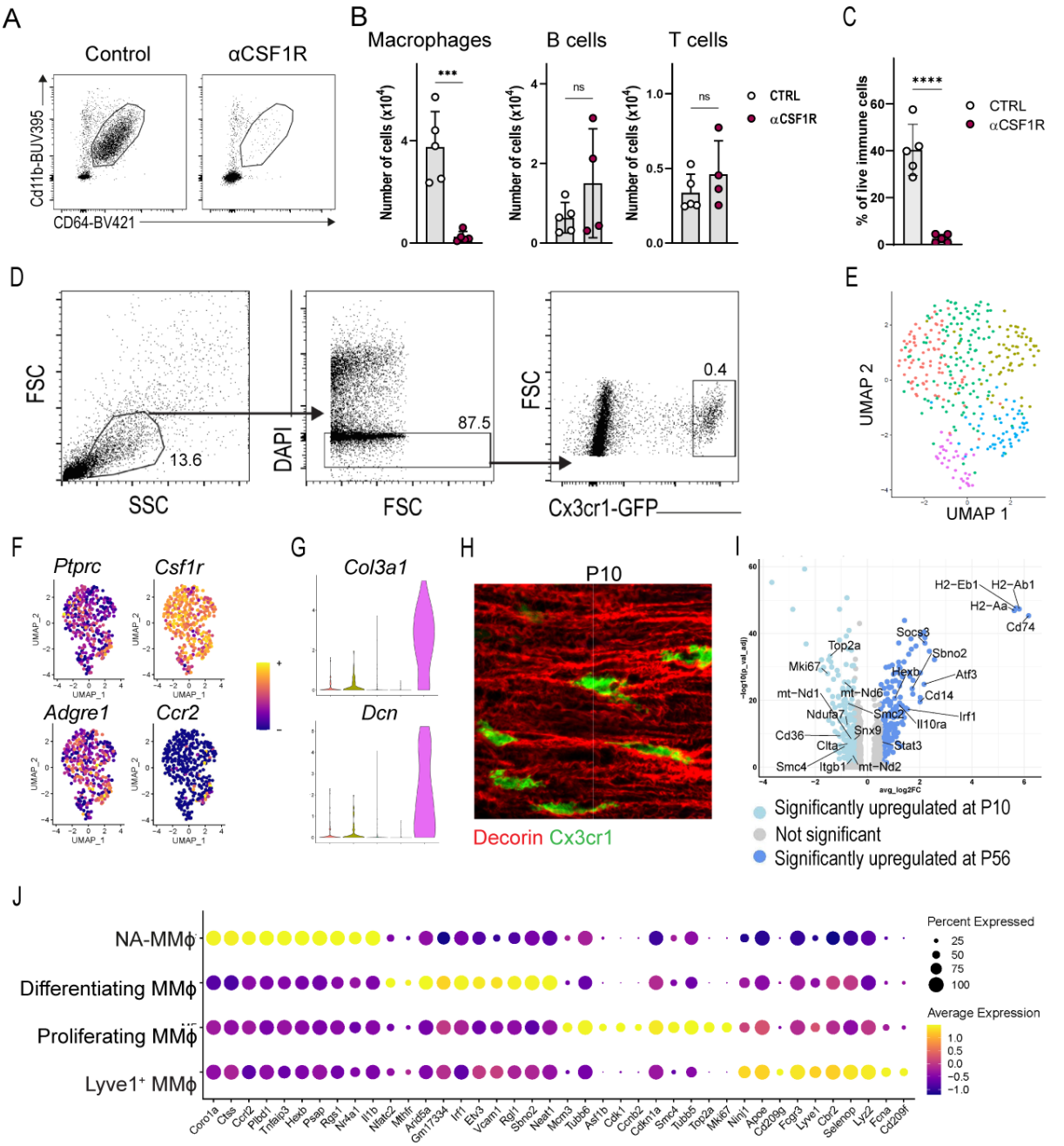

Figure S2: (**A**) Representative dot plot in αCSF1R-treated mice and controls to show efficient depletion of MMϕ. Cells shown are pre-gated on fsc/ssc, single cells, live and CD45$^+$. (**B**) Quantification of immune cells in αCSF1R-treated mice and controls. Macrophages are defined as CD45$^+$CD11b$^+$CD64$^+$, B cells as CD45$^+$CD3e$^-$CD64$^-$CD11b$^-$CD19$^+$ and T cells as CD45$^+$CD3e$^+$. All populations were pre-gated on fsc/ssc and live cells. (**C**) Quantification mature macrophages (CD45$^+$CD11b$^+$CD64$^+$Cx3cr1$^+$) in the lamina propria of P56 αCSF1R-treated mice and controls. (**D**) Gating strategy used to isolate Cx3cr1$^+$ MMϕ from the muscularis externa for scRNAseq. (**E**) UMAP of data prior to exclusion of contaminating cluster (pink). (**F**) UMAP with heatmap colour-coding to show expression for canonical macrophage markers and CCR2 within the scRNAseq dataset. (**G**) Violin plots showing the upregulation of extracellular matrix genes in the contaminating cluster (pink). (**H**) Representative confocal image of the muscularis externa at P10, showing Cx3cr1$^+$ MMϕ embedded within the extracellular matrix (Dcn, Decorin). (**I**) Volcano plot depicting globally differentially expressed genes at P10 and P56. Coloured dots represent significantly (p<0.05) upregulated genes over Log_2FC>0.5. (**J**) Dot plot to depict expression of top 10 upregulated genes within each cluster. Colour of dots represents expression level, while size of dots represents percentage of cells expressing the gene identified. Only genes significantly ($p \leq 0.05$) upregulated (logFC ≥ 0.2) are shown. Unpaired t-tests. Data are shown as Mean ± SD. Each data point indicates a separate biological replicate. N=4-7. *** $p <$ 0.001; ns = not significant.

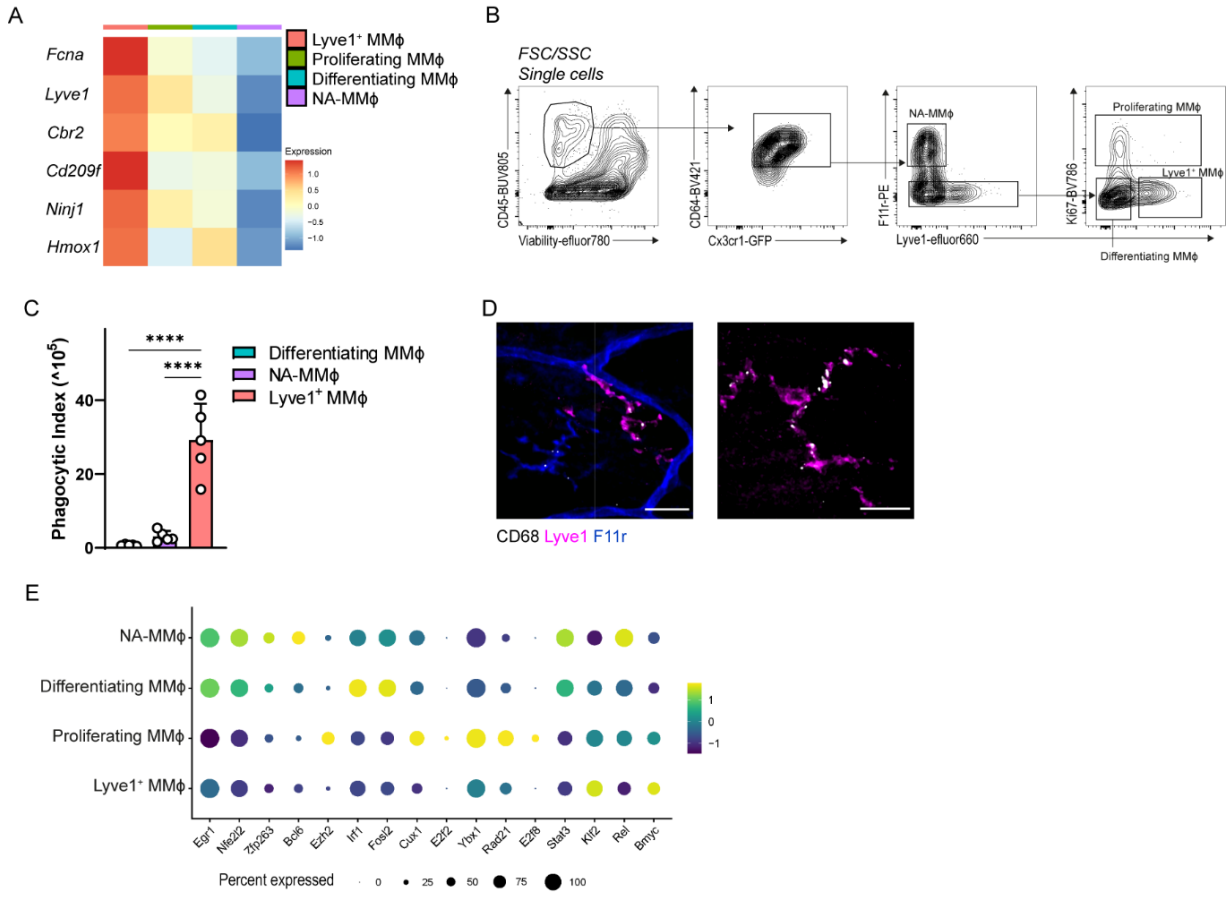

Figure S3: (**A**) Heatmap depicting expression of genes identified by Chakarov et al., within each cluster, cells pooled. (**B**) Representative gating strategy used to identified MMϕ subsets via flow cytometry. (**C**) Phagocytic index of each MMϕ subset phagocytosing fluorescently labelled dextran. Data are shown as Mean ± SD, analysed ANOVA followed by Tukey's multiple comparisons. Each data point indicates a separate biological replicate. ** $p < 0.01$; **** $p < 0.0001$. (**D**) Representative confocal images showing CD68+ lysosomes in NA-MMϕ and Lyve1⁺ MMϕ. Scale bar is 20µm. (**E**) Dot plot depicting expression of top 5 transcription factors identified via SCENIC within each cluster. Colour of dots represents expression level, while size of dots represents percentage of cells expressing the transcription factor identified. Only genes significantly ($p \leq 0.05$) upregulated (logFC ≥ 0.2) are shown.

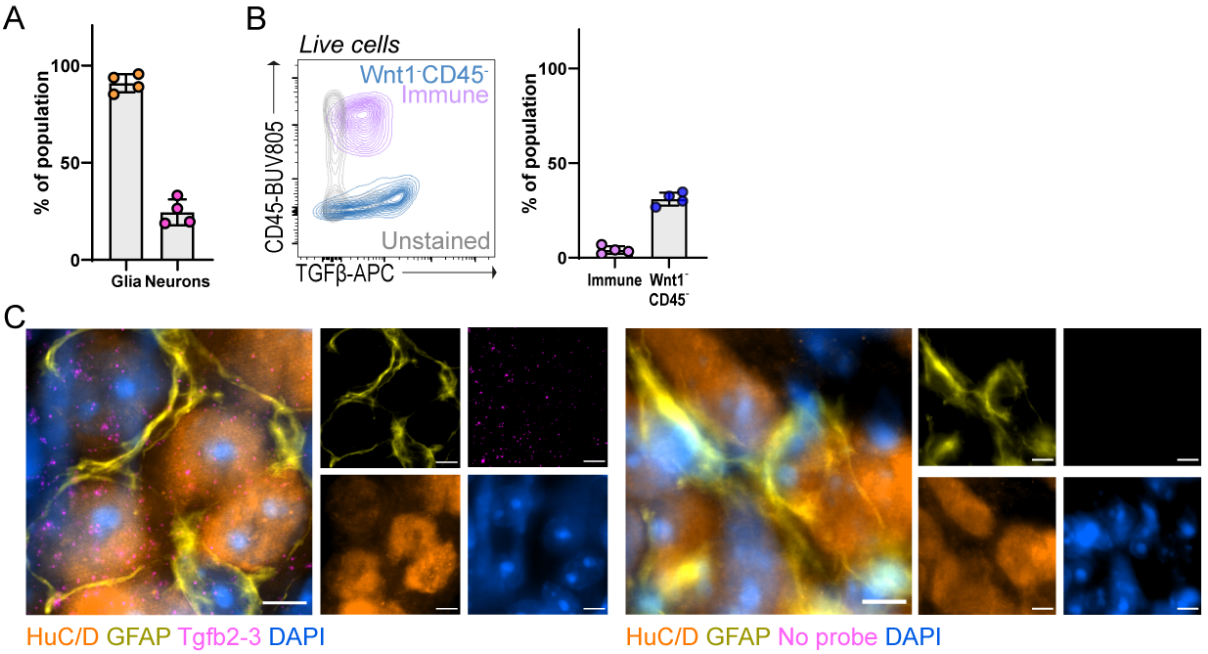
A
% of population
100
50
0
Glia Neurons
B
Live cells
Wnt1-CD45-
Immune
Unstained
CD45-BUV805
TGFβ-APC
% of population
Immune
Wnt1-CD45-
C
HuC/D GFAP Tgfb2-3 DAPI
HuC/D GFAP No probe DAPI

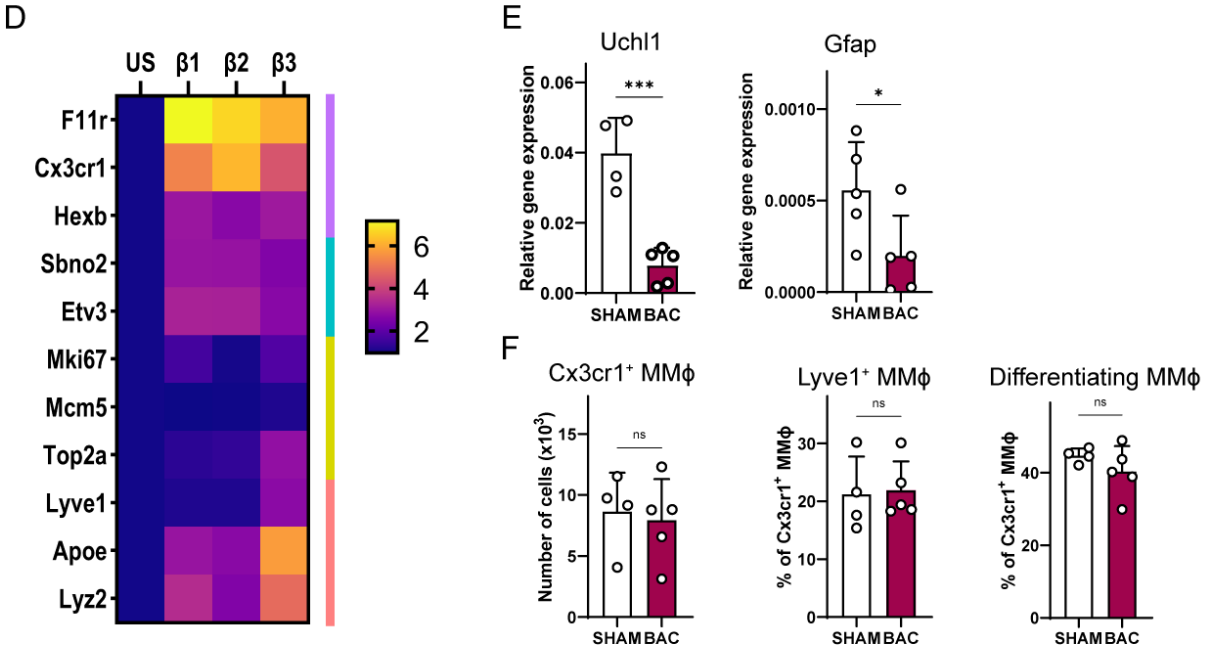
D
US
β1
β2
β3
F11r
Cx3cr1
Hexb
Sbno2
Etv3
Mki67
Mcm5
Top2a
Lyve1
Apoe
Lyz2
6
4
2
E
Uchl1
***
Relative gene expression
SHAM
BAC
Gfap
*
F
Cx3cr1+ MMϕ
ns
Number of cells (x10³)
Lyve1+ MMϕ
% of Cx3cr1+ MMϕ
Differentiating MMϕ

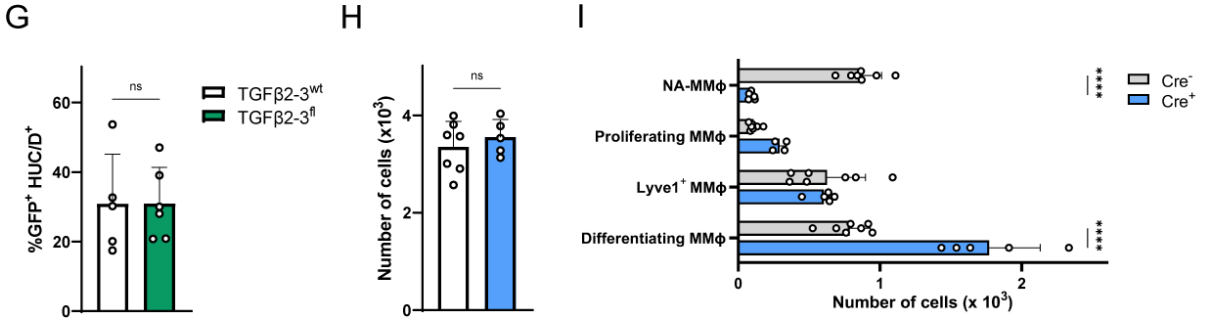
G
%GFP+ HUC/D+
TGFβ2-3wt
TGFβ2-3fl
H
Number of cells (x10³)
I
NA-MMϕ
Proliferating MMϕ
Lyve1+ MMϕ
Differentiating MMϕ
Cre-
Cre+
****
Number of cells (x 10³)

Figure S4: (**A**) Quantification of TGFβ-expressing enteric neurons and glia, as detected via flow cytometry. (**B**) Representative contour plot showing TGFβ expression in immune cells ($CD45^+$) and $Wnt1^-CD45^-$ cells. Only live cells are shown. The graph depicts the percentage of cells of each population expressing TGFβ. (**C**) Hybridization Chain Reaction (HCR) combined with immunohistochemistry to detect transcripts of Tgfb2 and Tgfb3 in the ENS, compared to samples in which no probes were included as control. Scale bar is 5 µm. (**D**) Gene expression of neuron-specific Uchl1 and glia-specific Gfap in the muscularis externa 5 days after enteric denervation with BAC compared to SHAM. (**D**) Gene expression of NA-MMϕ marker genes in BMDM following 24h stimulation with TGFβ1, TGFβ2 or TGFβ3. (**E**) Gene expression of Uchl1 and Gfap in the muscularis externa 5 days after enteric denervation with BAC. (**F**) Number of live $CD45^+$ $CD64^+$ $CD11b^+$ $Cx3cr1^+$ MMϕ< normalised to cell count, and relative percentages of $Lyve1^+$ MMϕ and differentiating MMϕ detected in the muscularis externa in SHAM and BAC-treated mice. (**G**) Transfection efficiency, expressed as percentage of GFP^+ HUC/D^+ cells of HUC/D^+ cells, in ganglia analysed for quantification of NA-MMϕ TGFb2-3^{wt} and TGFb2-3^{fl} mice that were infected with a neurotropic AAV9-Cre-GFP viral vector. (**H**) Number of live $Cx3cr1^+$ $Cd64^+$ $Cd11b^+$ $Cd45^+$ macrophages in the muscularis externa of $Cx3cr1^{creERT2/WT}$ $TGFbr2^{fl/fl}$ (Cre^+) and $Cx3cr1^{WT/WT}$ $TGFbr2^{fl/fl}$ (Cre^-) mice as assessed via flow cytometry. (**I**) Cell counts of MMϕ subsets in the muscularis externa of $Cx3cr1^{creERT2/WT}$ $TGFbr2^{fl/fl}$ (Cre^+) and $Cx3cr1^{WT/WT}$ $TGFbr2^{fl/fl}$ (Cre^-) mice as assessed via flow cytometry. Data are shown as Mean ± SD, analysed using T-test or ANOVA followed by Holm-Sidak multiple comparisons. Each data point indicates a separate biological replicate. N=4-7. * $p < 0.05$; *** $p < 0.001$; **** $p < 0.0001$; ns = not significant.

Supplementary table 1: Antibodies used for immunofluorescence

Antibody	Source	Cat. Number
Anti-GFP	Nacalai Tesque	04404-26
Anti-HuC/D	Supplied by V. Lennon (Mayo Clinic)	
Anti-Neurofilament	Abcam	ab72996
Anti-Synapsin I	Abcam	ab64581
Anti-Decorin	R&D Systems	AF1060-S
Anti-Lyve1	Abcam	ab14917
Anti-VE-Cadherin	R&D Systems	AF-1002
Anti-F11r (JAM-A)	R&D Systems	AF-1077
Anti-Ki67	Abcam	ab15580
Anti-βIII-Tubulin	Abcam	ab78078
Anti-Iba1	FUJIFILM Wako Pure Chemical Corporation	019-19741
Anti-GFAP	DAKO	Z0334
Polyclonal Rabbit IgG	R&D Systems	AB-105-C
Donkey Anti-Rat AF488	Thermofischer Scientific	A-21208
Donkey Anti-Human Cy5	Jackson ImmunoResearch	709-175-149
Donkey Anti-Human Cy3	Jackson ImmunoResearch	709-165-149
Donkey Anti-Chicken Cy5	Jackson ImmunoResearch	703-175-155
Donkey Anti-Rabbit Cy3	Jackson ImmunoResearch	711-165-152
Donkey Anti-Rabbit AF488	Thermofischer Scientific	A-21206
Donkey Anti-Goat AF647	Thermofischer Scientific	A-21447

Supplementary table 2: Antibodies used for flow cytometry

Name	Clone	Company	Catalogue Number
BUV805 CD45	30-F11	BD	748370
APC-efl780 CD45	30-F11	eBioscience	47-0451-82
BUV395 Cd11b	M1/70	BD	563553
BV421 CD64	X54-5/7.1	Biolegend	139309
BV711 CD64	X54-5/7.1	Biolegend	139311
Efl660 Lyve1	ALY7	eBioscience	50-0443-82
PE CD321 (Jam-A/F11r)	H202-106	BD	564908
BV421 CD321 (Jam-A/F11r)	H202-106	BD	744772
BV786 Ki67	B56	BD	563756
AF488 Cx3cr1	SA011F11	Biolegend	149022
BV605 Cx3cr1	SA011F11	Biolegend	149027
Efl450 CD3	17A2	eBioscience	48-0032-82
APC-CY7 CD8a	53-6.7	Biolegend	100714
BV605 CD4	RM4-5	Biolegend	100548
PE-CY5 CD19	eBio1D3	eBioscience	15-0193-82
BV421 Cd49b	DX5	BD	563063
APC TGFβ	1D11	R&D	IC1835A

Chapter 4

Loss of Neuron-Associated Macrophages Promotes Neurodegeneration and Constipation in Aging Female Mice

Maria Francesca Viola[1], Elodie Modave[1], Marta Chavero Pieres[1], Javier Aguilera-Lizarraga[1*], Naomi Fabre[1], Iris Appeltans[1], Nathalie Stakenborg[1], Alejandro Sifrim[2,3], Thierry Voet[3,4] and Guy Boeckxstaens[1].

Affiliations

[1] Laboratory for Intestinal Neuro-Immune Interaction, Translational Research Center for Gastrointestinal Disorders (TARGID), Department of Chronic Diseases and Metabolism (ChroMeta), KU Leuven, Leuven, Belgium

[2] Laboratory of Multi-Omic Integrative Bioinformatics (LMIB), Department of Genetics, KU Leuven, Leuven, Belgium.

Leuven AI Institute, KU Leuven, Leuven, Belgium

[3] Leuven Institute of Single Cell Omics (LISCO), KU Leuven, Leuven, Belgium

[4] Laboratory of Reproductive Genomics, Department of Genetics, KU Leuven, Leuven, Belgium.

[*]Current affiliation: Department of Pharmacology, University of Cambridge, Cambridge, United Kingdom

Under preparation

4.1 Introduction

Thanks to the increasing quality of medical care, life expectancy of the Western population has increased exponentially, resulting in an aging society. The downside of this evolution however is that aging results in a significant increase in patient morbidity and economic costs. Of note, 35-40% of geriatric patients and up to 80% of long-term care residents are affected by gastrointestinal (GI) complaints every year, most commonly constipation[155]. The urgent need to treat this growing body of patients has fuelled the recent interest in the age-related changes intrinsic to the gut, with particular focus on understanding the 'normal' aged gut, as distinct from disordered bowel function that is the result of comorbid conditions and/or GI side effects of medications used to treat those conditions. Increasing evidence suggests that functional changes observed with advanced age can be attributed to age-related neurodegenerative changes in the enteric nervous system (ENS). In fact, numerous morphological studies have demonstrated the loss of enteric neurons in both submucosal and myenteric plexuses in humans and in rodents, affecting mainly the cholinergic population that modulates ascending contractions during peristalsis[156,157]. Aging in general is associated to chronic low-grade inflammation and an increase in oxidative stress, which disrupts homeostasis and affects cell survival. In the ENS, neuronal loss appears to be caused by both increased neuronal apoptosis and reduction of precursor proliferation, leading to a steady decline in neuronal numbers[195,197].

In humans, constipation in aging is more prevalent in females compared to males, however no studies to date have addressed age-related changes in the GI tract in females compared to males[155]. While high estrogen levels, which accompany the follicular phase in the female menstrual cycle, or estradiol administration in rats, are associated to decreased GI motility and delayed gastric emptying, it is unclear how long-term exposure to female gonadal hormones may affect intrinsic GI motility and enteric neurons themselves[198].

Tissue-resident macrophages can be found throughout the layers of the GI tract, and in particular a specific population of macrophages is located in close proximity to enteric neurons in the submucous and myenteric plexus. We previously showed that these neuron-associated macrophages (NA-MMΦ) are long-lived, self-maintaining, and are characterised by a distinct transcriptome[22]. Strikingly, depletion of these cells led to extensive neurodegeneration, delayed intestinal transit and colonic dilation, a classic hallmark of constipation[22]. Furthermore, enteric neurons appear to maintain this dedicated population of macrophages via production of colony-stimulating factor 1 (CSF-1), a growth factor critical for macrophage survival, and shape their phenotype via production of Transforming Growth Factor β (TGFβ)[104](pruning). Given the critical role of NA-MMΦ in supporting and maintaining the population of enteric neurons in the GI tract, we hypothesised that age-related neurodegeneration and constipation may be a consequence of NA-MMΦ dysfunction or loss. Here, we investigate changes in GI function in

male and female mice with age, and study the potential contribution of altered function of NA-MMΦ in this process.

4.2 Results

4.2.1 *Female mice develop constipation with age*

To assess the onset of age-related constipation in mice, we assessed whole-gut transit time, faecal output and faecal water content in male and female C57Bl/6J mice at 3, 12 and 20 months of age. Female mice developed a delay in whole gut transit time at 12 months, which persisted at 20 months of age. In line, faecal output was reduced in female mice with age, accompanied by a significant reduction in faecal water content (Figure 1A-C). Whole gut transit time, faecal output and faecal water content did not change with age in male mice (Figure 1A-C). Delayed intestinal transit time may result as a consequence of multiple factors, including neurodegeneration in the myenteric plexus, loss of smooth muscle contractility or degeneration in the submucous plexus leading to altered fluid absorption. To assess smooth muscle contractility in aging mice, we measured smooth muscle contractions of isolated colonic muscle strips evoked by carbachol from male and female mice of 3 and 20 months. No differences in response to carbachol were observed when comparing 3 month old to 20 month old male and female mice, suggesting that the constipation observed in female mice with age is not due to loss of smooth muscle contractility (Figure S1A-B). Delay in gastro-intestinal transit may also be consequence of neurodegeneration in the myenteric plexus, which is critical for the regulation of peristalsis. We therefore quantified enteric neurons in the myenteric plexus of the small intestine and the colon 3- and 20- month old male and female mice. Aging was accompanied by a significant reduction in myenteric neurons in the proximal and distal colon in female mice, but not in male mice (Figure 1D-F). We did not observe differences in neuronal densities in the small intestine (Figure S1C-D). These findings suggest that neurodegeneration in the colonic myenteric plexus may contribute to the delay in transit observed in female mice with age.

As intestinal transit is also affected by anion secretion, regulated by submucosal neurons, we assessed neuron-evoked anion secretion in the colon of 3-, 12- and 20- month old male and female mice. We observed no significant changes in neuron-evoked anion secretion in female or mice with age (Figure S1E). Furthermore, baseline current was unchanged in male and female mice at all ages analysed (Figure S1F). We therefore assessed neuronal density in the colonic submucous plexus in male and female mice at 3, 12 and 20 months and observed no changes in neuronal density (Figure S1G).

Previous reports have suggested that insoluble protein aggregates may accumulate in the aging muscularis externa, however the role of such aggregates remains to be elucidated[199]. In line, we observed the presence of insoluble protein aggregates in the myenteric plexus in 20 month old, but not

3 month old mice (Figure 1G). Insoluble protein aggregates were associated to enteric ganglia or nerve fibres, suggesting that they may represent a form of neuronal debris. Of interest, Cx3cr1^{+} macrophages could be observed in close proximity to these aggregates (Figure 1H). These findings suggest that aging is associated to increased accumulation of insoluble protein aggregates that fail to be cleared by the local resident macrophage population.

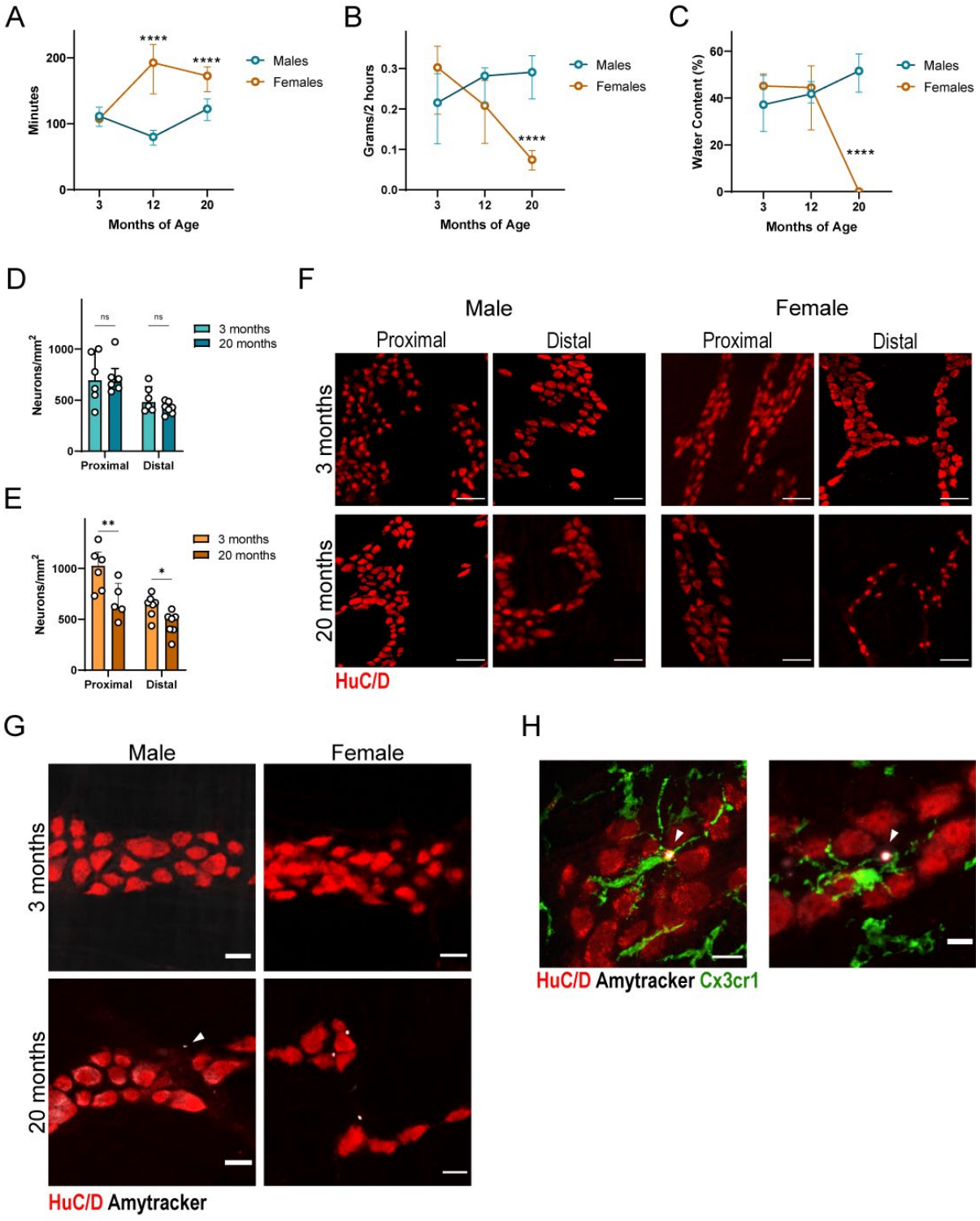

Figure 1: Aging is accompanied by constipation and neurodegeneration in female, but not male mice. (**A**) Whole gut transit time measured in 3-, 12- and 20-month old male and female mice. (**B**) Faecal output measured in 3-, 12- and 20-month old male and female mice. (**C**) Faecal water content measured in 3-, 12- and 20-month old male and female mice. (**D**) Neuronal density assessed via immunohistochemistry in the colon of male mice of 3 and 20 months. (**E**) Neuronal density in the myenteric plexus assessed via immunohistochemistry in the colon of female mice of 3 and 20 months. (**F**) Representative confocal images of the myenteric plexus in the proximal and distal colon of male and female mice at 3 and at 20 months of age. Scale bar is 50µm. (**G**) Representative confocal images of the myenteric plexus in 3- and 20- month male and female mice. Arrows indicate Amytracker+ insoluble protein aggregates. Scale bars are 20µm. (**H**) Representative confocal images showing MMΦ interacting with insoluble protein aggregates in the myenteric plexus. Arrows indicate Amytracker+ insoluble protein aggregates. Scale bars are 10µm. Data were analysed using 2-way ANOVA with Sidak correction for multiple comparisons in A-C; Student's t-test in D-E, J; Data are shown as Mean ± SD. N=6-10. * $p < 0.05$; ** $p < 0.01$;**** $p < 0.0001$.

4.2.2 *Characterisation of MMΦ in the aging muscularis externa*

As macrophages in the *muscularis externa* are critical for the function and the survival of myenteric neurons, we next evaluated the potential role of these macrophages in the aging-related neuronal loss and accumulation of insoluble protein aggregates in the myenteric plexus. We therefore isolated Cx3cr1^{+} macrophages from the colonic *muscularis externa* of 3- and 20-month old male and female mice for single-cell RNA sequencing using the 10x Genomics platform. For each sample, 4 biological replicates were pooled to obtain one technical replicate per condition, yielding a total of 15.899 cells after quality control and filtering. Unbiased hierarchical clustering revealed 14 clusters, 8 of which could be identified as macrophages, with 5 minor contaminating clusters containing T cells, epithelial cells, natural killer (NK) cells, dendritic cells (DCs) and fibroblasts that were removed prior to further analysis (Figure S2A). Final reclustering revealed 7 mature macrophage clusters, which were characterised by the expression of canonical macrophage markers including *Csf1r*, *Mafb* and *Adgre1* (Figure 2A, S2B).

We previously demonstrated that macrophages in the muscularis externa are able to self-maintain, and in line we identified MMΦ undergoing replication in a cluster that upregulated cell cycle genes including *Mki67, Top2a, Birc5c* (Figure 2B). We also observed a cluster of cells expressing genes typical of monocytes, including *Ly6c2*, *Msrb1*, *Plac8* and *Napsa* (Figure 2B). When we assessed expression of mature macrophage markers such as *Fcgr1*, *Adgre1* and *Cx3cr1*, we found that these cells also express mature macrophage markers, suggesting that these cells represent a newly differentiated cluster of monocyte-derived macrophages. These findings are in line with our previous studies that upon loss of self-maintaining macrophages, MMΦ may be replaced by incoming monocytes[22].

Further in line with our previous findings, we identified a cluster that upregulated *Lyve1* (Lyve1^{+} MMΦ), in addition to other genes implicated with phagocytosis including *CD163*, *CD209f* and *Mrc1* (Figure 2B). In addition to the Lyve1^{+} MMΦ population, we identified a second population that upregulates the scavenger receptor *CD163,* but does not express *Lyve1*. This cluster, which we named CD163+ Lyve1- MMΦ, upregulated numerous chemokines including *Ccl3, Ccl4* and *Cxcl16* (Figure 2B).

Next, we identified one cluster of MMΦ that was characterised by genes involved in lipid metabolism, such as *Lpl*, *Lyz1*, *Lgals3* and cell motility, including *Capg* and *Anxa2*. Macrophages expressing such genes have been described to be expressed by microglia rich in lipid droplets in murine models of multiple sclerosis, and in lipid-loaded macrophages in models of atherosclerosis, however a similar population has not yet been described in the gut[200–203]. We also observed one small cluster that upregulated genes known to be involved in interferon response (IFN-responding MMΦ). This cluster upregulated genes including *Isg15, Ifit3, Irf7* and *Ifit2* (Figure 2B).

Finally, in line with our previous findings, we identified one cluster of neuron-associated macrophages (NA-MMΦ), that upregulated canonical microglia genes such as *Tmem119*, *Hexb* and *Olfml3*, and could be identified via expression of *F11r* (Figure 2B).

As our scRNAseq experiment revealed minor age- and gender-dependent shifts in cluster proportions (Figure 2C), we further investigated our findings by analysing MMΦ via flow cytometry using the candidate marker genes identified via scRNAseq. We observed an increase in Ly6C^{+} MMΦ infiltrating the *muscularis externa*, suggesting an increase in replenishment of macrophages by monocytes in male mice with age (Figure 2C, S2C). However, in female mice we observed no differences in Ly6C^{+} MMΦ (Figure 2C, S2C). These findings may reflect previous reports that macrophage replenishment by self-maintenance or replacement by macrophages is differently regulated in male and female mice[204]. Furthermore, we observed no changes in Lyve1^{-}CD163^{+} and LPL^{+} MMΦ in both male and female mice with age (Figure 2D, S2D). We detected gender-associated differences when assessing the Lyve1^{+}CD163^{+} MMΦ, which were significantly decreased in female mice with age, but not in male mice (Figure 2E, S2E).

Finally, evaluation of NA-MMΦ at 20 months compared to 3 months in male and female mice revealed that while cell numbers appeared unchanged in male mice, there was a significant decline in NA-MMΦ in female mice with age (Figure 2F, S2F). As we previously demonstrated that NA-MMΦ play a critical role in supporting neuronal survival and gastro-intestinal motility, loss of NA-MMΦ may underlie age-related constipation and neuronal loss in female mice[205].

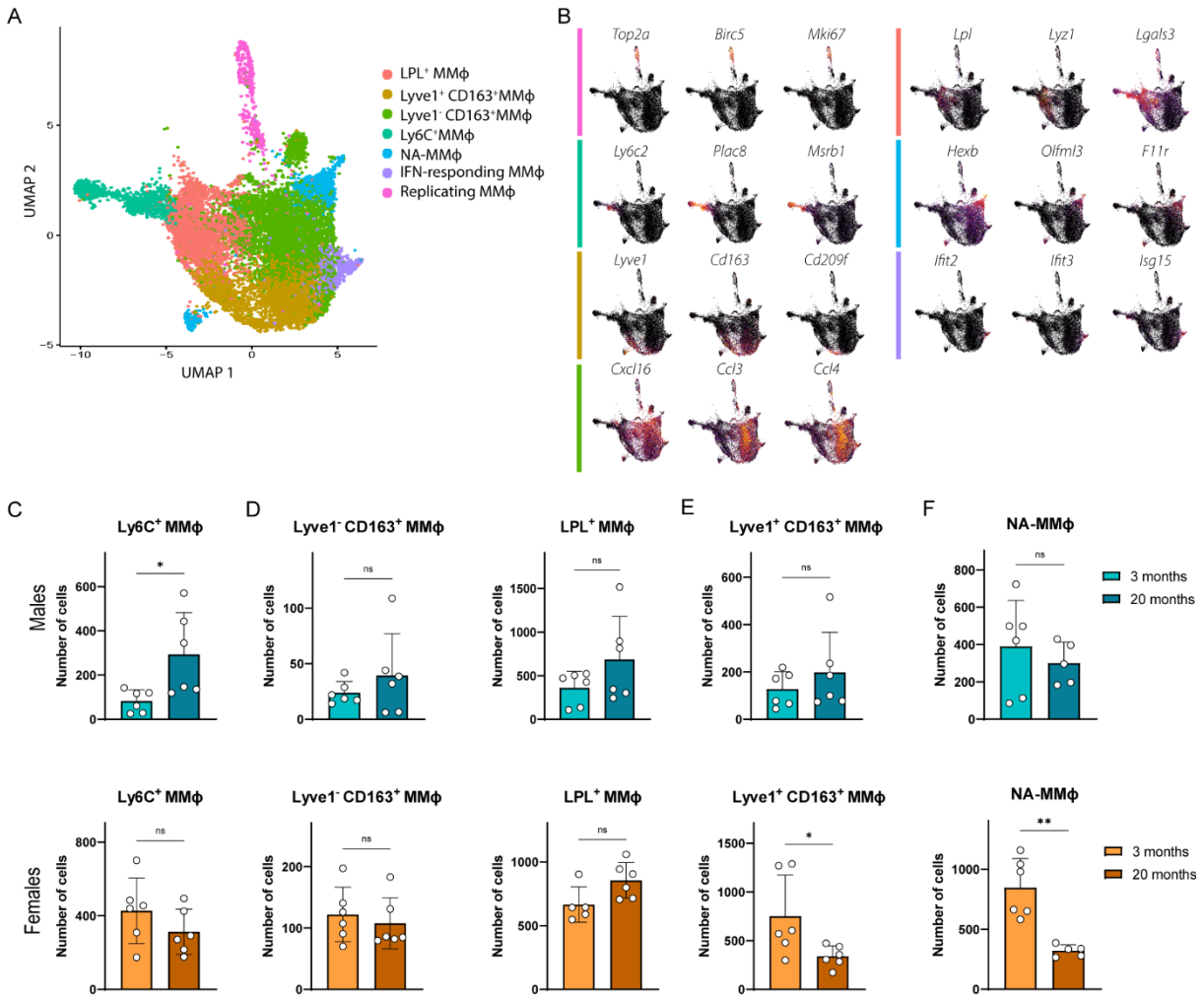

Figure 2: Single-cell RNA sequencing reveals MMΦ subtypes in the *muscularis externa* of young and aged male and female mice. (**A**) UMAP dimensionality reduction and clustering analysis of 10X scRNAseq data reveals 7 subpopulations of MMϕ, colour coded on the UMAP plot. (**B**) Feature plots displaying expression distributions of individual genes. (**C**) Quantification via flow cytometry of Ly6C$^+$ MMΦ in the *muscularis externa* of 3- and 20- month male and female mice. (**D**) Quantification via flow cytometry of Lyve1$^-$CD163$^+$ MMΦ in the *muscularis externa* of 3- and 20- month male and female mice. (**E**) Quantification via flow cytometry of LPL$^+$ MMΦ and Lyve1$^+$CD163$^+$ MMΦ in the *muscularis externa* of 3- and 20- month male and female mice. (**F**) Quantification via flow cytometry of NA-MMΦ in the muscularis externa of 3- and 20- month male and female mice. Data were analysed using T-test. N=10. * $p < 0.05$; ** $p < 0.01$. ns = not significant.

4.2.3 *Gender-specific changes in MMΦ in the aging muscularis externa*

To further investigate the loss of NA-MMΦ that we observed specifically in the female aging *muscularis externa*, we performed more in-depth analyses on this cluster. Interestingly, further sub-clustering of the NA-MMΦ cluster revealed 3 subclusters (Figure 3A). The main cluster was characterised by high expression of MHCII chains and *Il1b* (MHCII^{hi} NA-MMΦ; Figure 3B). The second cluster upregulated *S100a6, S100a10*, which are genes known to mediate stress and inflammation response, and *Crip1* (S100a^{+} NA-MMΦ; Figure 3B)[206]. Finally, one small cluster was characterised by the upregulation of homeostatic microglia genes, including *Hexb, P2ry12* and *Siglech* (P2ry12^{+} NA-MMΦ; Figure 3B). Of note, this last cluster was present almost exclusively in the aging *muscularis externa* of 20 month-old male mice (Figure 3C). While the low number of cells prevent further analysis, future studies should focus on elucidating the role of these P2ry12^{+} NA-MMΦ in preserving neuronal function in the aging *muscularis externa* in male mice.

Moreover, the extensive changes in MMΦ subsets in the aging females *muscularis externa* suggests that these cells undergo profound shifts from young age to old in females, but not in males. To further investigate these changes, we performed differential gene expression analysis within the NA-MMΦ and compared cells from 3 month old and 20 month old mice in males and females separately. We observed more differentially expressed genes in female mice with age than in male mice (89 differentially expressed genes in females; 9 differentially expressed genes in males; Figure 3D). When we performed the same analysis in the other identified clusters, we observed similar findings (Figure S3A-C). These findings suggest that profound transcriptional changes occur in MMΦ in female mice with age, while MMΦ appear to retain a comparable transcriptional signature in advanced age in males.

To further identify transcriptional changes that occur in female mice with age, but not in males, we compared gene expression within each cluster between aged male and female MMΦ. Interestingly, when comparing transcriptional signatures of aged female and aged male mice, differentially expressed genes were conserved throughout different clusters (Figure 3E, S3). In particular, aged male MMΦ upregulated *Pfn1, Cebpb, Fau* and *Itgb5*. While *Cebpb* and *Pfn1* have been implicated in aging in the nervous system, their role in macrophages are unknown[207,208]. However, *Itgb5* is of particular interest as loss of this gene has been linked to retinal degeneration due reduced phagocytosis and accumulation of autofluorescent storage bodies[209,210]. The upregulation of *Itgb5* by males compared to females was therefore of particular interest, as we observed the accumulation of insoluble protein aggregates in the aging *muscularis externa*, which may reflect reduced clearance by MMΦ. To investigate phagocytic capacity of aging female MMΦ, we assessed neuronal engulfment by MMΦ using Wnt1$^{Cre/+}$ Rosa26$^{tdTomato/+}$ Cx3cr1$^{GFP/wt}$ mice, which express tdTomato in all neural cells.

Of interest, we observed a significant reduction of neuronal phagocytosis in aged female mice compared to young (Figure 3F). These findings suggest that in female mice, aging is accompanied by reduced clearance of neurons and neuronal debris, leading to the accumulation of insoluble protein aggregates.

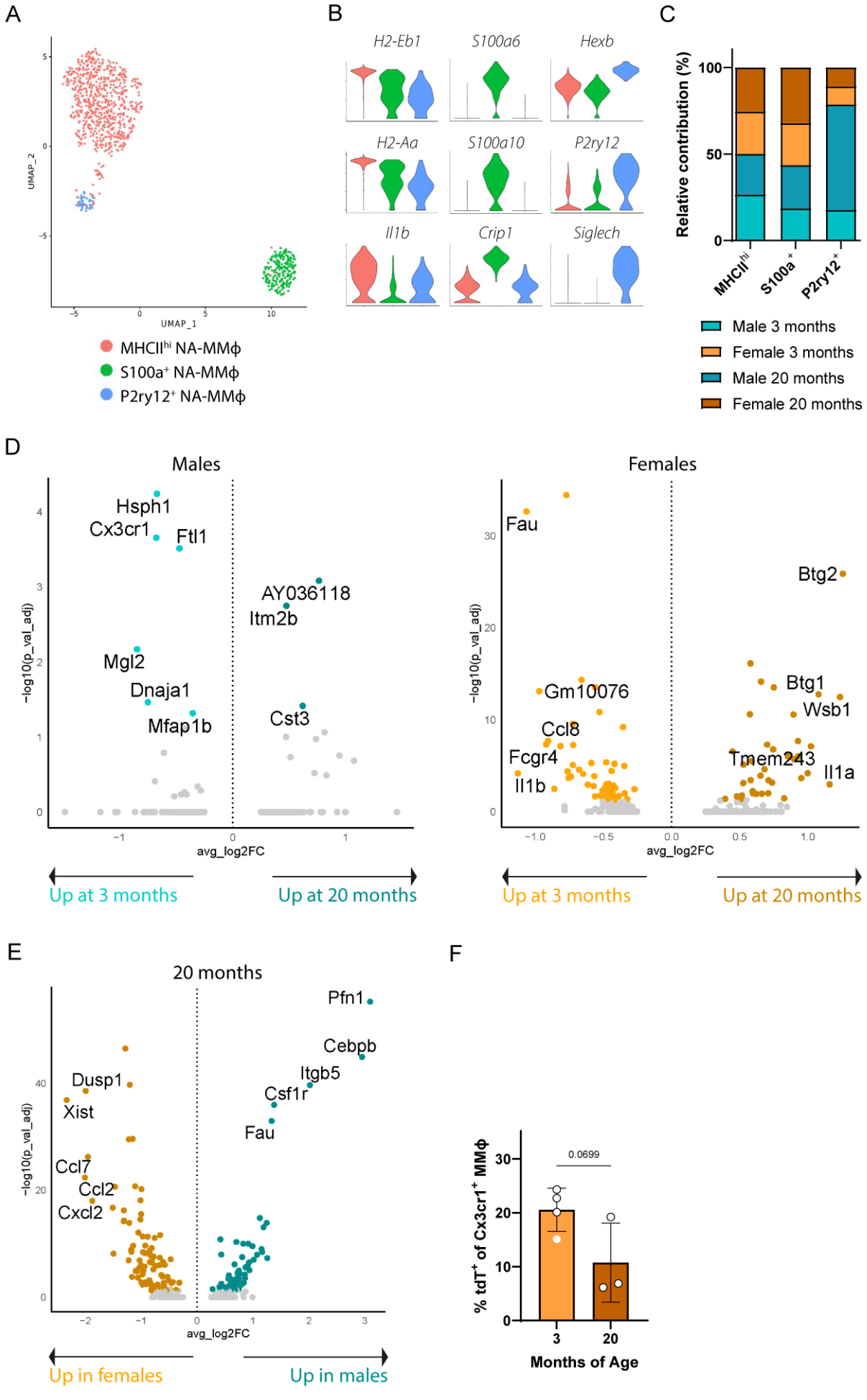
A
UMAP_2
UMAP_1
MHCIIhi NA-MMϕ
S100a+ NA-MMϕ
P2ry12+ NA-MMϕ
B
H2-Eb1
S100a6
Hexb
H2-Aa
S100a10
P2ry12
Il1b
Crip1
Siglech
C
Relative contribution (%)
MHCIIhi
S100a+
P2ry12+
Male 3 months
Female 3 months
Male 20 months
Female 20 months
D
Males
Hsph1
Cx3cr1
Ftl1
AY036118
Itm2b
Mgl2
Dnaja1
Mfap1b
Cst3
−log10(p_val_adj)
avg_log2FC
Up at 3 months
Up at 20 months
Females
Fau
Btg2
Gm10076
Btg1
Wsb1
Ccl8
Fcgr4
Tmem243
Il1a
Il1b
E
20 months
Pfn1
Cebpb
Itgb5
Csf1r
Fau
Dusp1
Xist
Ccl7
Ccl2
Cxcl2
Up in females
Up in males
F
0.0699
% tdT+ of Cx3cr1+ MMϕ
3
20
Months of Age

Figure 3: Age- and gender-associated shifts in MMΦ subsets in the *muscularis externa*. (**A**) UMAP dimensionality reduction and clustering analysis of sub-clustered NA-MMϕ reveals 3 subclusters, indicated by different colours on the umap. (**B**) Violin plots displaying expression distributions of individual genes within NA-MMϕ subsets, subclustered as indicated in C. (**C**) Relative distribution of identified NA-MMϕ subclusters in 3 month and 20 month male and female mice. N=1. (**D**) Volcano plots showing differentially expressed genes in NA-MMϕ obtained from 3 month old or 20 month old male and female mice, separated by gender. (**E**) Volcano plot showing differentially expressed genes in NA-MMϕ obtained from 20 month old male and female mice. Coloured dots indicate genes upregulated logFC >0.25 with $p < 0.05$. (**F**) Quantification via flow cytometry of percentage of MMϕ engulfing neural cells (Wnt1-tdTomato$^+$) in the *muscularis externa* of 3- and 20- month female mice. T-test.

4.2.4 *Insoluble protein aggregates do not cause neurodegeneration in the muscularis externa*

While our data suggest that the accumulation of insoluble protein aggregates may be the consequence of disordered MMΦ function in age, it cannot be excluded that protein aggregates themselves may be promoting a change in MMΦ phenotype and neuronal death. Indeed, studies have shown that insoluble protein aggregates lead to an increase in oxidative stress and inflammation, which may trigger a change in MMΦ phenotype[211]. Therefore, we sought to directly investigate the role of insoluble protein aggregates in the *muscularis externa* by injecting pre-formed fibrils (PFFs) of α-Synuclein into the *muscularis externa* of young mice, and performing assessment of gastro-intestinal function over time. Mice that received injections of PFF did not develop changes in whole-gut transit time compared to controls treated with either α-Synuclein or saline (Figure 4A). Furthermore, no changes in faecal output or faecal water content were detected in PFF-treated mice compared to controls (Figure 4B, S4A). These findings suggest that the presence of insoluble protein aggregates in the aging GI tract does not cause age-related constipation and neuronal dysfunction.

To investigate whether insoluble protein aggregates could introduce phenotypic shifts in MMΦ similar as to those that we observed in aging, we investigated MMΦ subtypes in mice treated with PFFs, or monomeric α-Synuclein and saline as controls. We observed no changes in overall immune cells and number of MMΦ in the muscularis externa after PFF injections (Figure S4B). While we observed an increase in Ly6C$^+$ MMΦ in PFF-treated mice compared to controls, we observed no further changes in identified MMΦ subsets in PFF-treated mice (Figure 4C, S4C).

These findings suggest that accumulation of insoluble protein aggregates is likely not the leading cause of neuronal death and changes in MM subsets observed in aging, but rather that age-related increase of insoluble protein aggregates may reflect reduced clearance by aged MMΦ. While the role of *Itgb5* is currently under investigation, the downregulation of this integrin in aging female MMΦ may underlie their decreased phagocytic capacity in aging, and further studies will focus on the role of *Itgb5* in the reduced clearance of MMΦ in the aging female *muscularis externa.*

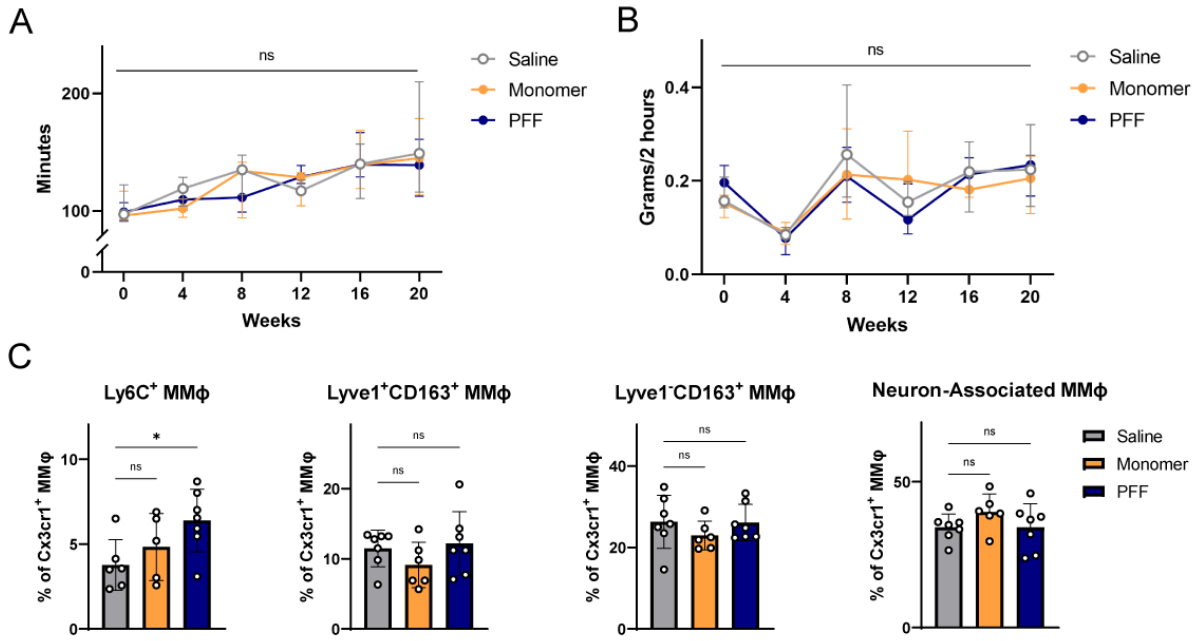

Figure 4: The role of insoluble protein aggregates in the aging *muscularis externa* (A) Whole gut transit time measured in mice treated with α-Synuclein PFFs, α-Synuclein monomer or saline. (B) Faecal output measured in mice treated with α-Synuclein PFFs, α-Synuclein monomer or saline. (D) Quantification of MMΦ subsets via flow cytometry in mice treated with α-Synuclein PFFs, α-Synuclein monomer or saline, expressed as percentage of Cx3cr1^{+} MMΦ. Data were analysed using 2-way ANOVA with Sidak correction for multiple comparisons. N=10. * $p < 0.05$. ns = not significant.

4.3 Discussion

With an increasingly aging society, there has been a rise in age-related disorders and diseases, which represents a significant socio-economic burden. In particular, there is a high incidence of gastro-intestinal dysfunction in the elderly, most commonly constipation, that can severely impact quality of life. While age-related gastro-intestinal dysfunction may arise as a consequence of other neurological diseases, such as stroke or parkinsonism, or as a side-effect of medication, the process of aging may directly affect the function of the gastro-intestinal tract itself. Here, we report that aging C57bl6/J female mice develop delayed gastro-intestinal transit and reduced faecal output with age, while male mice are protected from an aging-associated decline in gastro-intestinal function. Constipation observed in female mice was associated with significant neurodegeneration in the colonic myenteric plexus and accumulation of protein aggregates. Strikingly, we observed transcriptional shifts in aging female MMΦ, with a reduction in neuroprotective NA-MMΦ while we observed only few changes in the aging male MMΦ population, with maintenance of the transcriptional signature displayed by young MMΦ. Compared to aged females, macrophages in males upregulated homeostatic genes, but also genes which have shown to play a critical role in clearance of debris, such as *Itgb5.* Taken together, our findings highlight a critical role of MMΦ in age-related neurodegeneration and constipation, but also highlight the profound effect of gender on MMΦ function in aging.

4.3.1 *Single-Cell RNA sequencing reveals gender-specific transcriptional shifts in aging MMΦ*

To investigate changes in MMΦ transcriptome that may underlie neurodegeneration and constipation in aging female mice, we performed single-cell RNA sequencing on 3- and 20- month old male and female mice. Our scRNAseq experiment revealed 7 MMΦ clusters characterised by a distinct transcriptional signature, which enabled further validation by flow cytometry. Strikingly, while we mainly observed an increase in monocyte-derived MMΦ in male mice with aging, female mice showed a significant reduction in phagocytic Lyve1+ CD163+ MMΦ, but also in NA-MMΦ, which we previously demonstrated to be critical for the function and the survival of enteric neurons. Strikingly, in female mice NA-MMΦ were not only significantly depleted, but also displayed a profound change in transcriptional signature, while in males, the transcriptional signature of NA-MMΦ was largely unaffected by aging. These findings highlight the critical role of NA-MMΦ in supporting enteric neurons, and suggest that neurodegeneration in the female aging myenteric plexus may be driven by loss or dysfunction of NA-MMΦ.

In addition, while NA-MMΦ appeared largely unaffected in male mice with age, we observed the presence of a specific NA-MMΦ cluster in aging male mice which was absent in young male and female

mice, but also absent in aged female mice. This cluster, which we named P2ry12^{+} NA-MMΦ upregulated homeostatic microglia genes, including *P2ry12, Hexb* and *Siglech*. In the brain, P2ry12 expressed by microglia acts as a sensor for neuronal health at somatic junctions, and is critical for regeneration following injury via recruitment of microglial processes to the site of neuronal injury[212]. It is intriguing to speculate that such a population may be involved in neuronal repair and regeneration in aging male mice, however further investigation is warranted to confirm these findings. Furthermore, the absence of such a cluster in the aging female *muscularis externa* may further contribute to aging-associated neurodegeneration.

Finally, assessment of differential gene expression within single MMΦ subsets revealed that while few genes were differentially expressed from young to old male MMΦ, female MMΦ undergo profound transcriptional shifts in aging. While the driving force underlying such transcriptional changes remain to be elucidated, these findings suggest that aging impacts female MMΦ more than male MMΦ.

4.3.2 *The role of insoluble protein aggregates in neurodegeneration*

In line with previous reports, we observed an accumulation of insoluble protein aggregates in the aging myenteric plexus[199,213]. The role of insoluble protein aggregates has long been debated, however it is widely accepted that aggregates form to reduce toxicity of more toxic precursors, such as α-Synuclein fibrils[214]. In this view, the presence of insoluble protein aggregates in the aging myenteric plexus may represent an accumulation of debris as a result of reduced clearance by aging MMΦ, rather than drive neurodegeneration itself. In line, when we injected preformed fibrils (PFFs) into the *muscularis externa* of young mice, we observed no changes in gastro-intestinal function or MMΦ populations.

The accumulation of insoluble protein aggregates in the aging *muscularis externa* may thus rather reflect reduced clearance by aged MMΦ. In support of this hypothesis, we observed reduced neuronal engulfment by MMΦ in females mice with age. Furthermore, we observed significant differences when comparing the transcriptome of aged female MMΦ to aged male MMΦ: aging female MMΦ upregulated genes involved in inflammatory response, in the production of cytokines and in the regulation of cell death. Of interest, aged male MMΦ upregulated a number of genes that were conserved throughout clusters, including *Cebpb, Pfn1, Fau* and *Itgb5.* Of note, the upregulation of *Itgb5* is of particular interest, as loss of this gene leads to the accumulation of autofluorescent storage bodies in the retina, causing accelerated degeneration and blindness[210]. While the link between insoluble protein aggregates and *Itgb5* downregulation remains to be explored, it is intriguing to speculate that age- and gender-specific transcriptional shifts may underlie MMΦ dysfunction and accumulation of debris in the aging *muscularis externa.*

4.3.3 *The role of gender in age-related neurodegeneration*

Our findings largely support the hypothesis that changes in MMΦ transcriptome and function may underlie neurodegeneration and constipation in aging female mice. However, it remains unclear why age-associated loss of NA-MMΦ and associated neurodegeneration occurs in female mice, while male mice appear to be protected.

Differences in gastro-intestinal function, including permeability, absorption and motility, have been described to exist between males and females, and have largely been attributed to the presence of female gonadal hormones[215,216]. The significant shifts in gene expression observed in female MMΦ with age, while male MMΦ remained largely unchanged from young to old mice, suggest that profound changes occur in female gut tissue with age, which might then drive transcriptional reprogramming. Alternatively, female gonadal hormones may reprogram MMΦ via direct signalling, as has been reported for macrophages in the cardiovascular system and in the lung[217,218]. Tissue-resident macrophages in various organs indeed express estrogen receptors, and direct signalling via these receptors may mediate macrophage function[219]. For example, signalling via estrogen receptors mediates macrophage polarization, inflammatory cytokine production and gene expression[217,220]. Interestingly, expression of *Itgb5* regulates estrogen and TGFβ signalling, suggesting that downregulation of *Itgb5* in aging female MMΦ may be caused by declining estrogen levels[221]. Further experiments will elucidate the role of estrogen in mediating transcriptional shifts in MMΦ.

Finally, it cannot be excluded that post-menopausal drops of circulating hormone levels may drive transcriptional shifts, rather than the presence of female gonadal hormones themselves. Several studies have demonstrated increased expression of pro-inflammatory cytokines by macrophages obtained from post-menopausal humans and ovariectomized mice, which could be rescued by estradiol treatment[222,223]. The precise mechanism through which estrogen signalling may influence MMΦ function is currently under further investigation.

4.3.4 *Conclusions and future prospects*

Our findings here highlight the critical role MMΦ in supporting neuronal homeostasis and survival, and suggest that age-associated neurodegeneration and constipation observed in female mice may be caused by dysfunction of MMΦ. While these findings open the door to potential therapeutic modulation of the neuron-MMΦ axis in neurodegeneration and aging, future research should focus on dissecting the role of estrogen and female gonadal hormones on macrophage function in the gut, in addition to evaluating the long-term effects macrophage dysfunction may have in the gastro-intestinal tract in females with aging.

4.3.5 *Acknowledgements*

We thank Pier Andrée Penttila and Reena Chinnaraj from the KU Leuven FACS core for their excellent support and cell sorting. We also thank the Cell Imaging Core (Pieter Vanden Berghe and Tobie Martens, KU Leuven) for confocal imaging (supported by AKUL 15/37 and FWO I001918N). MFV is supported by FWO PhD fellowship 11C2219N. GB is funded by ERC Advanced grant number 833816-NEUMACS.

4.3.6 *Author Contributions*

MFV designed experiments, conducted experiments and wrote the manuscript. EM and AS performed analysis of scRNAseq data. MCP performed histological analyses. JAL performed Ussing chamber experiments. IA and NF provided excellent technical support throughout all experiments. NS assisted with scRNAseq experiments. TV provided intellectual input. GB led the project and revised the manuscript.

4.3.7 *Declaration of interests*

The authors declare no competing interests.

4.4 Materials and Methods

4.4.1 *Mice*

All animal experiments were performed in accordance with the European Community Council and approved by the Animal Care and Animal Experiments Committee of the Medical Faculty of the KU Leuven. Mice were maintained under a 14h/10h dark/light cycle, at a temperature of 20-22 °C, provided with food and water ad libitum. 3 month old and 20 month old C57Bl/6 mice were obtained from Envigo. *Cx3cr1*$^{GFP/GFP}$ mice were obtained from Steffen Jung, Weizmann Institute of Science[192]. Wnt1.Cre mice were obtained from Pieter Vanden Berghe[193]. *Rosa26*$^{TdT/TdT}$ mice were obtained from Jackson Laboratory. *Wnt1*$^{Cre/WT}$ *Rosa26*$^{TdT/WT}$ *Cx3cr1*$^{GFP/WT}$ mice were bred in our facility and maintained on a C57Bl/6 background.

4.4.2 *Whole Gut Transit Time*

Whole gut transit time was assessed using carmine red gavage as previously described[195]. Briefly, two days prior to the assessment, mice were acclimatized by a saline gavage and a period of 3 hours in single-housing. Following an overnight fast, mice were gavaged with a 6% w/v solution of carmine red (Sigma) in sterile methyl cellulose (0.5%) and single-housed. Mice were monitored every 15 minutes until the appearance of the first red pellet. The time elapsed from the gavage of carmine red until the appearance of the first red pellet was recorded as total gut transit time.

4.4.3 *Faecal Output and Faecal Water Content*

To measure faecal output, mice were housed for 2 hours on a metal grid with regular access to food and water. Faecal pellets produced during 2 hours were collected and weighed, and the total weight was deemed faecal output/2h. Faecal pellets were then dried for 24 hours at 56°C and then weighed once more. Faecal Water Content was calculated as (wet weight-dry weight)/wet weight and expressed as a percentage.

4.4.4 *Muscle Strip Organ Bath Experiments*

Mice were sacrificed by cervical dislocation and freshly obtained intestinal samples were placed in Sylgard plates and maintained in bubbled Krebs solution (95% O2- 5% CO2). Intestinal segments were then opened along the mesenteric border and pinned flat in a Sylgard-lined dish. Next, the mucosal layer was removed and strips (5 mm x 15 mm) were cut. Strips were suspended along their longitudinal axis in organ bath chambers filled with Krebs buffer at 37°C. After equilibration at optimal stretch (60 mN), carbachol was added in increasing concentrations (10^{-8}M to 10^{-5}M) to measure smooth muscle contractility. Contractions were measured using an isometric force transducer/amplifier (Harvard

Apparatus). Data was sampled using the Windaq data acquisition system and a DI-720 box (Dataq Instruments). All contractile responses were normalized for the cross-weight of the strip.

4.4.5 *Histology and immunofluorescence*

The intestine was dissected, carefully flushed using Hank's Balanced Salt Solution (HBSS) (Gibco) supplemented with fetal calf serum (FCS, 3%, Lonza) and HEPES (1.8%) and pinned on a sylgard plate. The tissue was cleaned of mesenteric fat, opened longitudinally and pinned with the muscle layer facing upwards. The muscle layer was carefully peeled from the submucosa, pinned flat on the sylgard plate and then fixed for 30 minutes in PFA 4%. Fresh whole mount tissue was stained within one week of collection. Tissue was permeabilized in PBS supplemented with Triton X-100 (0.3%; permeabilization buffer) for 2 hours at room temperature, and then blocked with permeabilization buffer supplemented with Donkey serum (5%) and Bovine serum albumin (BSA, 5%; blocking buffer) for 2 hours at room temperature. Tissue was incubated with primary antibodies diluted in blocking buffer overnight at 4°C. Tissue was extensively washed in PBS prior to incubation with secondary antibodies diluted in blocking buffer for 2 hours at room temperature. Insoluble protein aggregates were visualised by incubating with Amytracker-680 (Ebba biotech) according to the manufacturer's instructions. Samples were washed and mounted using SlowFade Diamond Antifade mounting medium (Thermofischer Scientific) and imaged using a Zeiss LSM880 confocal microscope. Negative controls (incubated with secondary antibody, but no primary antibody) were included for every analysis. All antibodies used are listed in supplementary table 1.

4.4.6 *Ussing Chambers*

Mice were sacrificed by cervical dislocation and the colon was carefully removed to avoid tissue damage and maintained in bubbled Krebs solution (95% O2-5% CO2). The intestinal samples were then pinned in Sylgard plates with LP surface down and ME was gently peeled off with forceps to prepare a LP-submucosal plexus intestinal strip, termed intestinal preparations throughout[224]. Then, intestinal preparations were mounted in Ussing chambers (exposed area 0.0096 cm2) with Krebs solution, glucose-supplemented at the basolateral side and mannitol-supplemented at the apical side (95% O2-5%; CO2, 37°C). Tissues were voltage clamped at 0 mV using an automatic voltage clamp and the short-circuit current (Isc) to keep the 0-mV potential was monitored over time. The transepithelial resistance (TEER) was calculated by Ohm's law. Veratridine was added (30 µM) to the basolateral reservoir to stimulate voltage-sensitive Na+ intrinsic submucosal neurons[225]. Veratridine-induced changes in Isc were recorded for 60 min, before TTX was added (100nM) to inhibit neurogenic Isc responses. Chambers were connected to a PC with Clamp Software Version 9 (KMSCI) to record Isc.

4.4.7 *Tissue harvest for single cell suspensions*

The colon was removed from mesenteric fat tissue, opened longitudinally and cleaned in Hank's Balanced Salt Solution (HBSS) (Gibco) supplemented with fetal calf serum (FCS, 3%, Lonza) and HEPES (1.8%). The opened tissue was pinned to a sylgard plate and the muscle layer was carefully dissected and collected in RPMI supplemented with FCS (3%) and HEPES (2%). The tissue was cut in small pieces and incubated with Collagenase IV (500U/ml) and DNAse for 30 minutes at 37°C in constant agitation. After digestion, cells were filtered through a 70 µm cell strainer and washed using PBS supplemented with FCS (2%) and EDTA (1.6mM) and counted prior to staining for Flow Cytometry or FACS-sorting.

4.4.8 *scRNAseq library preparation*

Single-cell suspensions were obtained from the colon of Cx3cr1GFP/WT mice as previously described. Cells were counterstained with DAPI to exclude dead cells and sorted using an Aria III cell sorter (BD) into sterile PBS supplemented with 0.3% BSA. Cells were immediately counted and viability assessed using a Luna-FL Dual Fluorescence Cell Counter (Logos Biosystems). Single cell libraries were prepared with the Chromium Single Cell 3′ V2 Chemistry Library Kit, Gel Bead & Multiplex Kit and Chip Kit from 10X Genomics. The barcoded library was sequenced on an Illumina HiSeq4000 in 25-8-98 paired-end configuration.

4.4.9 *scRNAseq analysis*

Raw data obtained from the sequencer were demultiplexed to generate fastq files, which were aligned to the mouse refence genome build mm10 (release M23), using STAR, with the CellRanger count function (10x Genomics – version 6.1.2). A single-cell expression matrix (i.e. counts by cells) was then generated by CellRanger and the generated data for each sample was uploaded to Seurat. Following a quality check and filtering of these samples (features: 400-6000; mitochondrial gene content < 20%: UMIs > 1000), cells were normalized, scaled and integrated using Harmony[226]. The highly variable genes of the integrated dataset (i.e. standard 2000 genes) were then used as a tool for a dimensional reduction to plot each single cell on a 2-D Uniform Manifold Approximation and Projection (umap). Depending on their similar gene expressions, cells clustered in different groups (i.e. cell populations) after creation of a vector of resolutions. The differential gene expression within each cluster was calculated using the FindMarker function of Seurat with the Wilcoxon rank sum test to measure the level of expression of genes between different age groups. At least 10% of the cells in one cluster needed to express a gene at a minimum of 0.25 log2FC.

4.4.10 *Flow cytometry*

Single cell suspensions were blocked using anti CD16/CD32 (Fc block) and subsequently labelled for flow cytometry analysis using fluorophore-conjugated anti-mouse antibodies for 30 min at 4°C using the

antibodies listed in supplementary table 2. Samples were acquired using a Symphony A5 (BD Biosciences). Analysis was carried out using FlowJo (v10, Tree Star).

4.4.11 *Injection of Preformed Fibrils (PFFs)*

8 week old mice were anesthetised using a cocktail of xylazine and ketamine, and placed on a heated pad (32°C) for the duration of the experiment. A 1-cm midline abdominal incision was made and the peritoneal cavity accessed via another incision along the linea alba. The cecum and proximal colon was carefully externalized onto the gauze using two saline-moistened cotton swabs. Using a Hamilton needle, 5 injections of 2µg of either PFFs or monomers, or 2µl saline were performed in the colonic muscle wall. PFFs were subject to sonication prior to injection as per manufacturer's instructions. After this treatment, the colon was carefully repositioned in the abdomen with two moist cotton swabs. The abdomen was closed by single sutures (Mersilene 6-0 silk). Mice were allowed to recover for 2 weeks prior to any further assessments.

4.4.12 *Statistics*

Statistical analysis was performed using Prism 9 (GraphPad Software). Data are represented as Mean ± SD and analysed using T-tests, ANOVA (followed by Tukey's multiple comparisons) or Kruskal-Wallis (followed by Dunn's multiple comparisons). Statistical outliers were removed using Grubbs outlier test. A p value < 0.05 was considered statistically significant.

4.5 Supplementary Information

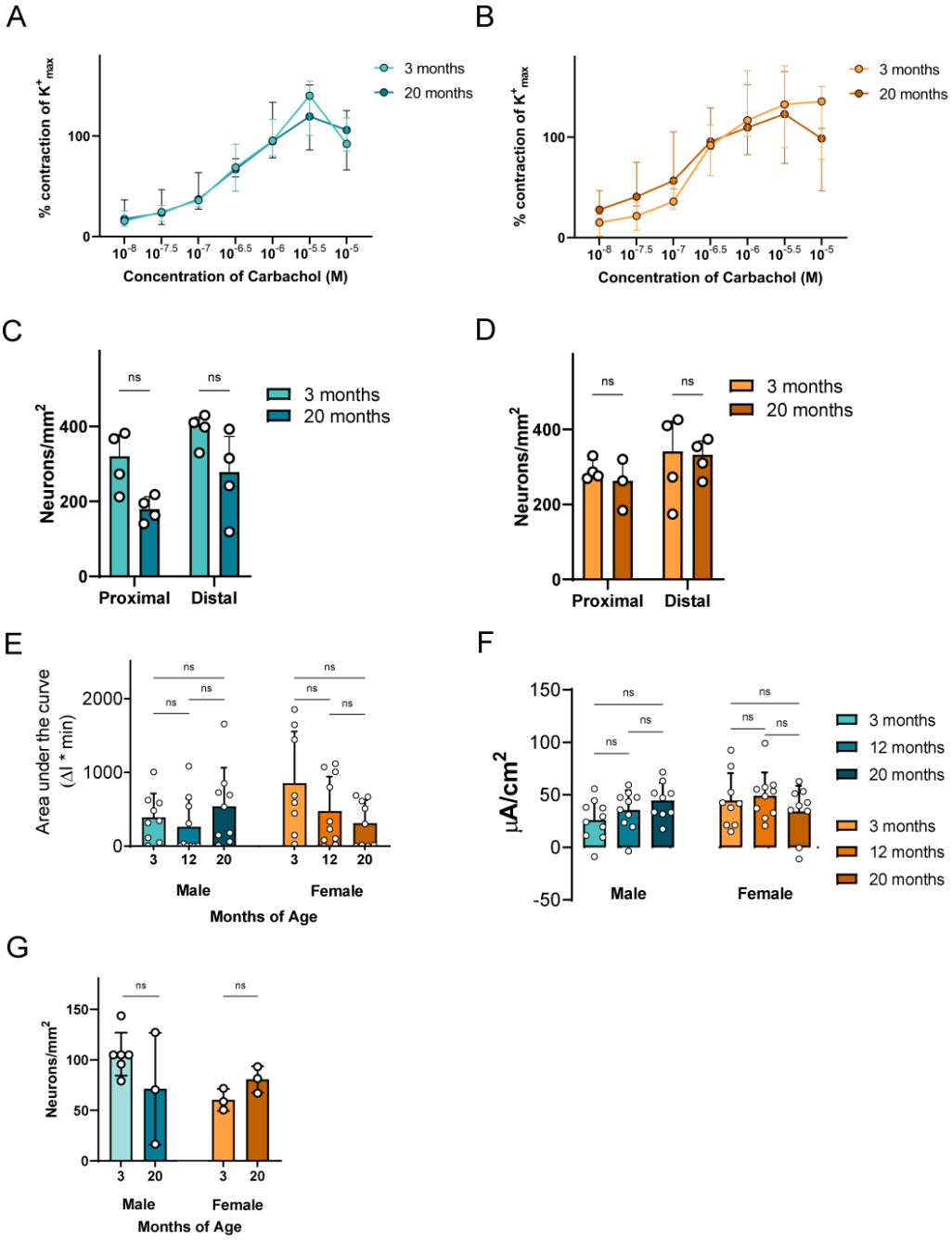

Figure S1: Functional characterisation of aging-associated gastro-intestinal dysfunction in female mice. (**A**) Smooth muscle contractility assessed using increasing carbachol concentrations in muscle strip organ bath experiments with isolated colonic strips from male mice of 3 and 20 months and (**B**) female mice of 3 and 20 months. (**C**) Neuronal density in the myenteric plexus assessed via immunohistochemistry in the small intestine of male mice of 3 and 20 months and (**D**) female mice of 3 and 20 months. (**E**) Area under the curve shows short-circuit current (Isc) responses to 30 µM veratridine over a period of 40 minutes (n =10 mice from 2 independent experiments). (**F**) Baseline current recorded in isolated colonic lamina propria from male and female mice of 3, 12 and 20 months. (**G**) Neuronal density in the submucous plexus assessed via immunohistochemistry in the colon of female and male mice of 3 and 20 months. Data were analysed using 2-way ANOVA in A-B, T-tests in C-D, Kruskal Wallis in E-F. ns: not significant.

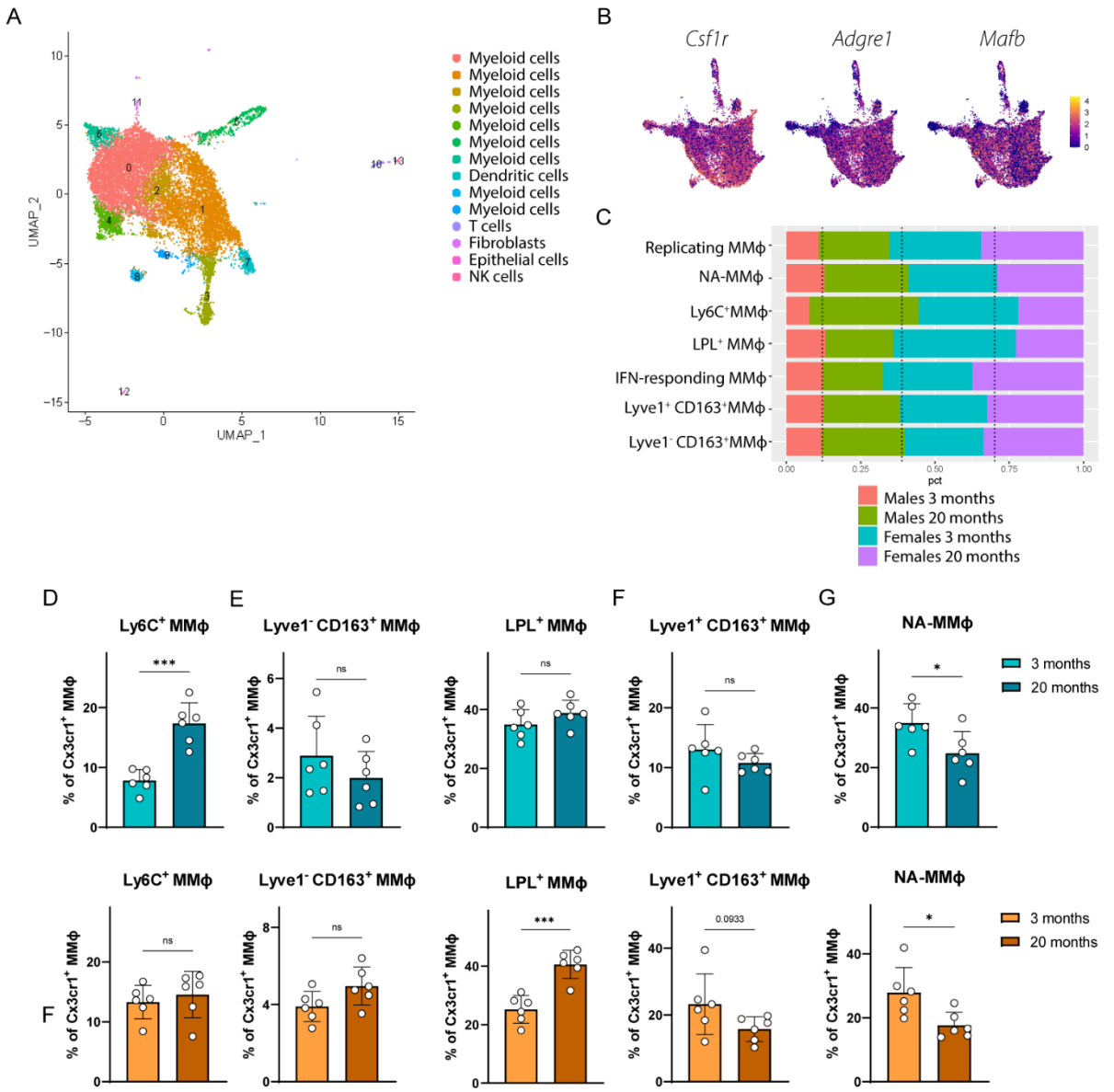

Figure S2: (**A**) UMAP dimensionality reduction and clustering analysis of 10X scRNAseq data at resolution 1.1 reveals 9 subpopulations of myeloid cells and contaminating clusters, colour coded on the UMAP plot. (**B**) Feature plots displaying expression distributions of canonical macrophage marker genes. (**C**) Relative cluster proportions in 3- and 20- month old male and female mice. Dashed line represents predicted value. (**D**) Quantification via flow cytometry of Ly6C$^+$ MMΦ in the *muscularis externa* of 3- and 20- month male and female mice, expressed as percentage of Cx3cr1$^+$ MMΦ. (**E**) Quantification via flow cytometry of Lyve1$^-$CD163$^+$ MMΦ in the *muscularis externa* of 3- and 20- month male and female mice, expressed as percentage of Cx3cr1$^+$ MMΦ. (**F**) Quantification via flow cytometry of LPL$^+$ MMΦ and Lyve1$^+$CD163$^+$ MMΦ in the *muscularis externa* of 3- and 20- month male and female mice, expressed as percentage of Cx3cr1$^+$ MMΦ. (**G**) Quantification via flow cytometry of NA-MMΦ in the muscularis externa of 3- and 20- month male and female mice, expressed as percentage of Cx3cr1$^+$ MMΦ. Data were analysed using T-test. N=10. * $p < 0.05$; *** $p < 0.001$. ns = not significant.

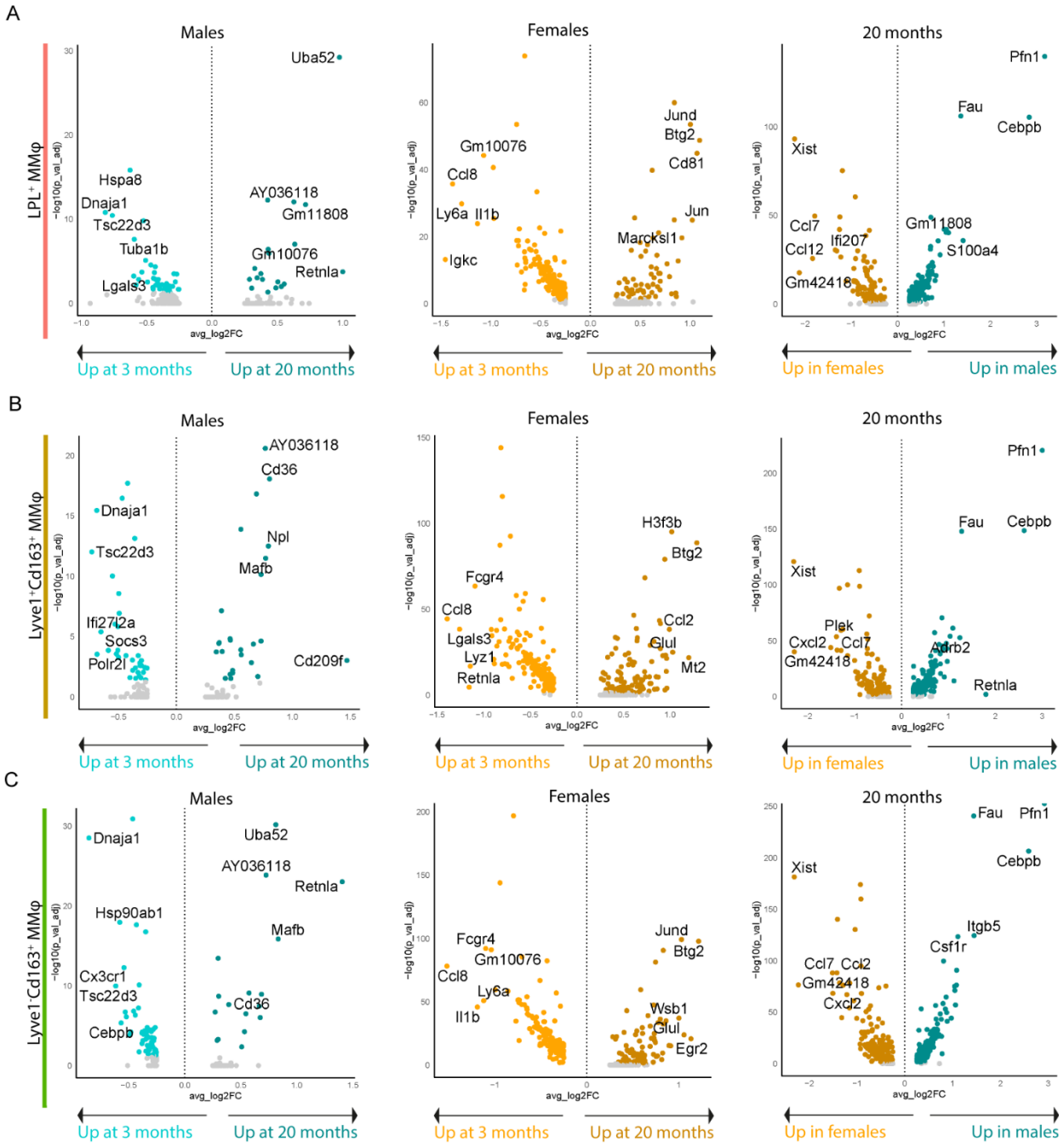

Figure S3: Age- and gender-associated shifts in MMΦ subsets in the *muscularis externa*. (**A**) Volcano plot depicting differential gene expression within LPL$^+$ MMΦ between young and old, separated by gender, and in the third panel, differentially expressed genes in LPL$^+$ MMφ obtained from 20 month old male and female mice. (**B**) Volcano plot depicting differential gene expression within Lyve1$^-$CD163$^+$ MMΦ between young and old, separated by gender, and in the third panel, differentially expressed genes in Lyve1$^-$CD163$^+$ MMφ obtained from 20 month old male and female mice. (**C**) Volcano plot depicting differential gene expression within Lyve1$^+$CD163$^+$ MMΦ between young and old, separated by gender, and in the third panel, differentially expressed genes in Lyve1$^+$CD163$^+$ MMφ obtained from 20 month old male and female mice. Coloured dots indicate genes upregulated logFC >0.25 with $p < 0.05$.

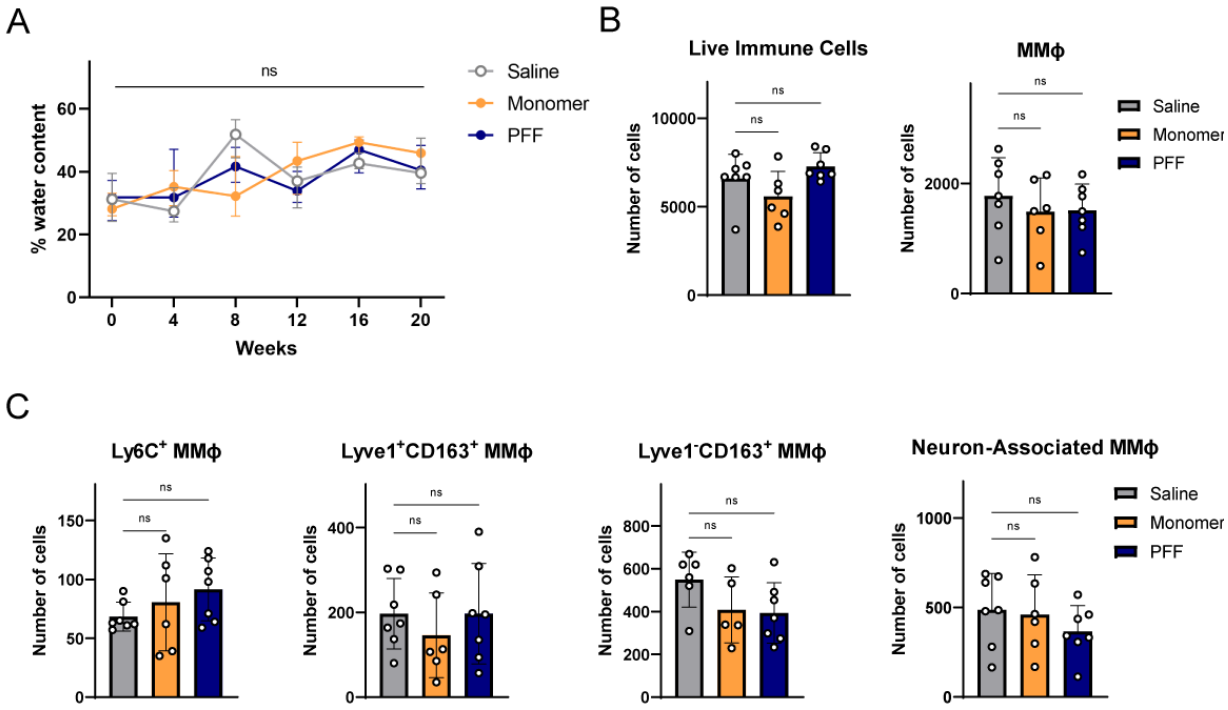

Figure S4: The role of insoluble protein aggregates in the aging *muscularis externa.* (**A**) Faecal water content measured in mice treated with α-Synuclein PFFs, α-Synuclein monomer or saline. (**B**) Quantification of live immune cells and Cx3cr1^{+} MMΦ via flow cytometry in mice treated with α-Synuclein PFFs, α-Synuclein monomer or saline. (**C**) Quantification of MMΦ subsets via flow cytometry in mice treated with α-Synuclein PFFs, α-Synuclein monomer or saline. Data were analysed using 2-way ANOVA with Sidak correction for multiple comparisons. N=10. ns = not significant.

Supplementary Table 1: Antibodies used for immunofluorescence

Antibody	**Source**	**Cat. Number**
Anti-GFP	Nacalai Tesque	04404-26
Anti-HuC/D	Supplied by V. Lennon (Mayo Clinic)	
Anti-Iba1	FUJIFILM Wako Pure Chemical Corporation	019-19741
Donkey Anti-Rat AF488	Thermofischer Scientific	A-21208
Donkey Anti-Human Cy5	Jackson ImmunoResearch	709-175-149
Donkey Anti-Human Cy3	Jackson ImmunoResearch	709-165-149
Donkey Anti-Rabbit Cy3	Jackson ImmunoResearch	711-165-152
Donkey Anti-Rabbit AF488	Thermofischer Scientific	A-21206

Supplementary Table 2: Antibodies used for flow cytometry

Name	Clone	Company	Catalogue Number
BUV805 CD45	30-F11	BD	748370
APC-efl780 CD45	30-F11	eBioscience	47-0451-82
BUV395 Cd11b	M1/70	BD	563553
BV421 CD64	X54-5/7.1	Biolegend	139309
BV711 CD64	X54-5/7.1	Biolegend	139311
Efl660 Lyve1	ALY7	eBioscience	50-0443-82
PE CD321 (Jam-A/F11r)	H202-106	BD	564908
PE-efluor610 CD163	TNKUPJ	eBioscience	61-1631-82
AF488 Cx3cr1	SA011F11	Biolegend	149022
BV711 Ly6C	HK1.4	Biolegend	128037
AF647 CD64	558539	BD Pharmingen	X54.5/7.1
Pe-Cy7 Cd11b	552850	BD Pharmingen	M1/70

Chapter 5

Conclusions

5.1 Muscularis Macrophages From Development to Aging: Common Mechanisms of Neuro-Immune Interaction in the Gut and in the Brain?

Tissue resident macrophages have been studied since the end of the 19th century, when they were discovered by Nobel Prize winner Ilya Metchnikoff. It was rapidly established that macrophages play a crucial role in organ homeostasis via host defence and clearance of pathogens; in fact, their function is so vital that it has been conserved throughout evolution[227]. However, only in recent years the scientific community has come to appreciate that macrophages carry out functions far more elaborate than mere host defence. Indeed, tissue-resident macrophages have been shown to carry out functions specific to the tissue in which they reside: in the heart, macrophages regulate electric conduction; in the lung, macrophages recycle surfactant; and in the brain, macrophages participate the wiring of neuronal circuitry[39,228]. This functional specialisation, which is characterised by a specific transcriptional signature, is imprinted on the tissue resident macrophage via the surrounding cells, a concept known as the *macrophage niche*[2]. The niche imprints a specific function and phenotype on resident macrophages via the production of mediators, cell-cell contact or other signalling molecules that drive transcriptional programming in the resident macrophage, which is then able to carry out functions specific to the niche in which it resides. However, despite the fact that some advances have been made in defining the molecular mediators involved in shaping macrophage phenotype, such as TGFβ in the brain, or BMP9 in the liver, little is known about how the macrophage niche is established[55,144].

In the gastro-intestinal tract, macrophages are present throughout the distinct layers of tissue, where they carry out functions specific to the niche they occupy[165]. In this thesis, I focused on a specific subset of macrophages that lies in close proximity to enteric neurons of the myenteric plexus, which are located between the two muscle layers of the *muscularis externa.* Neurons of the myenteric plexus are critical for intestinal motility, and their loss can lead to delayed gastro-intestinal transit and constipation, which can severely impact quality of life[229]. However, it remains unclear how the ENS develops, and matures, to adapt to the constantly evolving needs of the gut. Macrophages located in close proximity to these neurons provide support and protection, and their loss leads to neurodegeneration and delayed gastro-intestinal transit[22]. However, while we have established that these macrophages are critical for the survival of myenteric plexus in adulthood, little is known about the role of these cells during early postnatal development, and whether these cells participate in postnatal rewiring of the ENS. Furthermore, while it is known that myenteric neurons produce colony-stimulating factor 1 (CSF1), a growth factor critical for macrophage survival, it remains unclear which specific molecular signals are involved in instructing the phenotype of a neuron-associated macrophage in the *muscularis externa.* Finally, it is unclear whether loss of neuron-associated macrophages may underlie neurodegeneration

and constipation in disease, such as aging. As such, the major findings of this thesis can be summarised as follows (Figure 1):

1. Macrophages prune synapses and refine myenteric neurons during early postnatal development, thereby contributing to the functional maturation of the ENS (*Chapter 3*).
2. At weaning, a developmental switch occurs which leads to a shift of muscularis macrophage (MMΦ) transcriptome and function (*Chapter 3*).
3. Developmental maturation of MMΦ is orchestrated by myenteric neurons, that via production of TGFβ imprint a neuron-associated MMΦ (NA-MMΦ) phenotype; loss of these NA-MMΦ in adulthood leads to neurodegeneration and delayed intestinal transit (*Chapter 3*).
4. In female mice, aging is characterised by neurodegeneration and constipation, which is accompanied by the loss of NA-MMΦ (*Chapter 4*).

The implications of these findings, and their impact on our current understanding of macrophage biology, will be detailed point-by-point below.

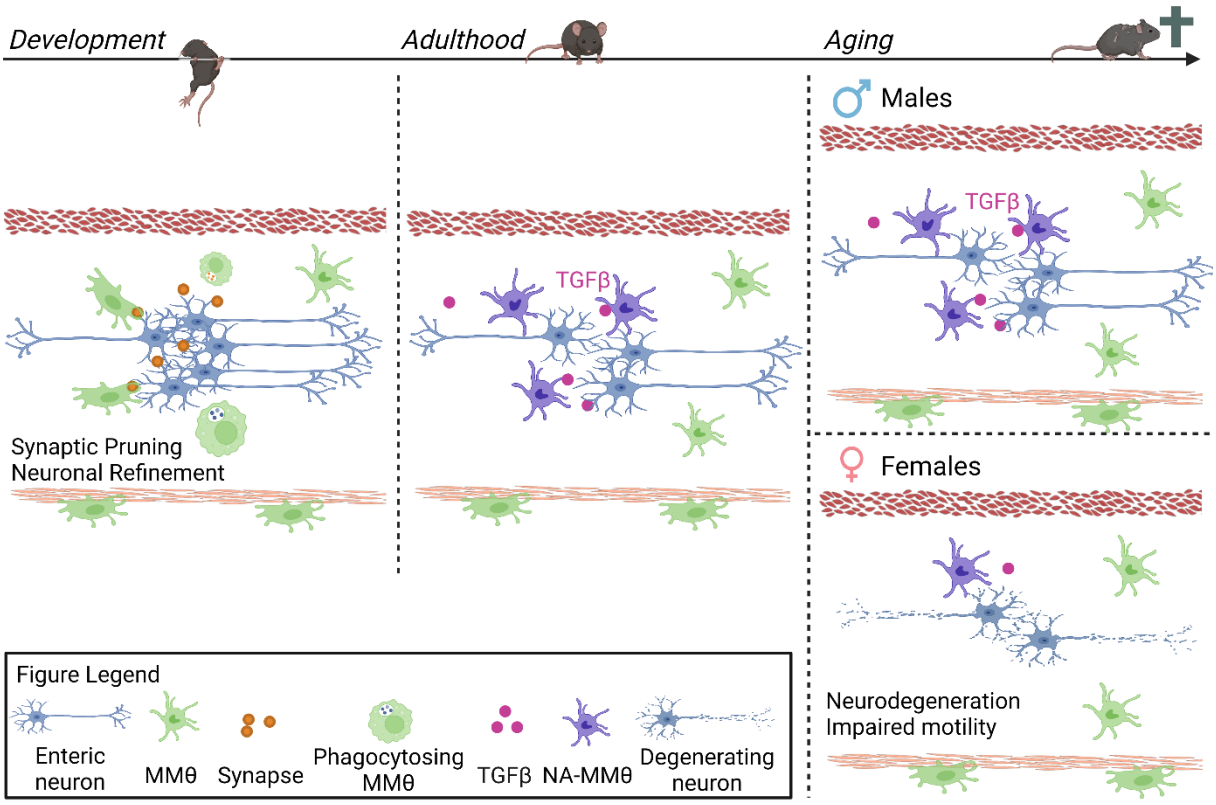

Figure 1: Graphical abstract of the functions of MMΦ throughout life, from early postnatal development to aging. Figure created with BioRender.

5.1.1 *Macrophages prune synapses and refine myenteric neurons during early postnatal development, thereby contributing to the functional maturation of the ENS (Chapter 3).*

The intestine is colonised by neural precursors prior to birth, and requires intricate signalling to ensure complete innervation of the entire gastro-intestinal tract. However, while the innervation of the gut occurs prior to birth, it has been reported that the ENS, similarly to the CNS, undergoes further refinement during early postnatal life, and only reaches full functional maturity after weaning[162,163]. The postnatal maturation enables the intestine to deal with the transition from a liquid to a solid diet, however the mechanisms underlying ENS maturation remain unclear. Here we show that, similar to the CNS, tissue resident macrophages are responsible for the engulfment of synapses and excess neurons, and thus participate in shaping the ENS circuitry during postnatal development (Figure 1). Furthermore, loss of MMΦ during the developmental time window in which refinement occurs leads to hyperganglionosis and accelerated intestinal transit.

Intriguingly, the postnatal refinement of the ENS somewhat mirrors that of the CNS, where dedicated resident macrophages, microglia, orchestrate the pruning of excess synapses and the engulfment of dying neurons[184]. This refinement, like in the ENS, is restricted to a specific time window, and loss of microglial function during this critical time window has been shown to promote symptoms of neurodevelopmental disorders, affecting learning and memory, social, mood-related, and locomotor behaviours[186,187]. Whether similar long-term consequences of early life macrophage dysfunction exist in the ENS remain to be explored, however there have been reports of children affected by ENS hyperganglionosis which develop gastrointestinal motility disorders[159,160].

5.1.2 *At weaning, a developmental switch occurs which leads to a shift of muscularis macrophage (MMΦ) transcriptome and function (Chapter 3).*

While MMΦ are critical for ENS refinement early in life, we previously demonstrated that long-lived, neuron associated MMΦ are critical for neuronal survival in adulthood[22]. Intriguingly, MMΦ undergo a functional and transcriptional shift between early in life, that enables them to adapt to the requirements of the tissue during specific developmental timepoints. Using single-cell RNA sequencing, we demonstrated that prior to weaning, MMΦ are rapidly proliferating to fill the expanding niche, and are predominantly phagocytic, and characterised by the expression of *Lyve1*. Interestingly, after weaning the Lyve1^{+} MMΦ population shrinks, and another subset of MMΦ, characterised by the expression of canonical microglia genes, expands to fill the growing niche. These MMΦ lie in close proximity to enteric neurons, and are responsible for the survival of enteric neurons in adulthood. This switch in function appears to occur around the time of weaning, and it is intriguing to speculate that it may be triggered by the shift from a liquid diet to a solid diet, the exposure to food antigens, or changes in the microbiota.

The exact mechanism which underlies developmental maturation of MMΦ however remains to be clarified.

While developmental reprogramming of macrophage function has been explored little in other organs, the extensive study of microglia during early postnatal development may offer the opportunity for comparisons. Indeed, microglia undergo a similar stepwise developmental program, which has been characterised from the embryo until adulthood. During early postnatal development, microglia upregulate phagocytic genes, while adulthood is characterised by the upregulation of genes involved in immune surveillance, mirroring the functional shift microglia undergo from postnatal synaptic pruning to homeostatic and neuro-supportive functions in adulthood[146]. However, whether this transcriptional and functional shift is dictated by local environmental cues, or is dictated by developmental programming remains to be explored.

5.1.3 *Developmental maturation of MMΦ is orchestrated by myenteric neurons, that via production of TGFβ imprint a neuron-associated MMΦ (NA-MMΦ) phenotype; loss of these NA-MMΦ in adulthood leads to neurodegeneration and delayed intestinal transit (Chapter 3).*

After weaning, a specialised subset of MMΦ, neuron-associated MMΦ (NA-MMΦ) expands and positions itself in close proximity to neuronal cell bodies in the myenteric plexus, and nerve fibres located in the muscle layer. The emergence of this subset in adulthood suggests that cues from the local niche may be imprinting this specific transcriptional signature on resident, or newly recruited cells. We identified TGFβ as a critical molecular mediator in driving the transcriptional signature of NA-MMΦ, and ablation of TGFβR signalling on MMΦ led to a loss of NA-MMΦ (Figure 1). While TGFβ signalling has been known to be critical for monocyte accumulation and macrophage homeostasis in the intestine, we here demonstrate that TGFβ signalling is also employed by the ENS to imprint the specialised phenotype of MMΦ that lie in their close proximity[51,230]. Indeed, enteric denervation using benzalkonium chloride, or neuron-specific ablation of TGFβ2-3 expression led to a loss of the NA-MMΦ population. Once again, these findings mirror the CNS, where TGFβ is critical for the establishment of microglia function and phenotype, suggesting that TGFβ may act as a common mediator for the instruction of macrophages in close proximity to neurons in both the CNS and the periphery[144,176]. In line, multiple reports have characterised 'nerve-associated' macrophage populations that share some transcriptional features with microglia, which have been identified in tissues including the skin, adipose tissues and peripheral nerves including the sciatic nerve and dorsal root ganglia[97,124,231–233]. It should be noted, however, that microglia are ontogenetically distinct from other tissue-resident macrophages, and while the full implications of ontogeny on phenotype and function remain to be clarified, the transcription factor *Sall1* is exclusively expressed by microglia, suggesting that environmental cues can not completely override ontogenetical programming[97].

In adulthood NA-MMΦ are critical for neuronal survival, as ablation of TGFβ signalling led to neurodegeneration and delayed intestinal transit. Although the exact mechanisms through which NA-MMΦ promote neuronal survival remain to be elucidated, these findings suggest that the ENS itself instructs the local macrophage pool to support its own survival. These findings are in line with previous studies showing the ENS to be a source of CSF1, a growth factor critical for macrophage survival[104]. However, in our hands, ablation of the ENS did not itself affect macrophage numbers, suggesting that other sources of CSF1 are present in the *muscularis externa.* Nevertheless, the concept that the ENS itself produces the mediators required to maintain and instruct a local, specialised macrophage population further highlights the importance of macrophages in maintaining tissue homeostasis beyond host defence and pathogen clearance, and highlights the extreme plasticity of these cells in adapting to the tissue and the cues in different contexts, ranging from development, to homeostasis, to disease.

5.1.4 *In female mice, aging is characterised by neurodegeneration and constipation, which is accompanied by the loss of NA-MMΦ (Chapter 4).*

The critical importance of NA-MMΦ in maintaining neuronal health and function led us to hypothesise that loss or dysfunction of these cells may underlie neurodegenerative diseases of the gastro-intestinal tract. While aging may itself not be considered a disease, it has been shown that an aging-associated decline in gastro-intestinal function is mirrored by neurodegeneration in the myenteric plexus[234]. This represents a significant socio-economic burden, as up to 40% of geriatric patients are affected by gastro-intestinal complaints, most commonly constipation[155]. Here, we showed that in female mice, aging is accompanied by a delay in gastro-intestinal transit and neurodegeneration, while both gastro-intestinal function and neurons are preserved in aged male mice(Figure 1). Interestingly, we observed a loss of NA-MMΦ in aging female mice, which may underlie neurodegeneration and constipation(Figure 1). In addition to the loss of NA-MMΦ in aging female mice, we observed profound transcriptional differences that were age- and gender-specific, which may shed further light on the mechanisms underlying neurodegeneration. While in female mice aging was accompanied by significant transcriptional shifts in all macrophage subsets, in male mice aging was not accompanied by significant changes in gene expression. Moreover, aging in male mice was accompanied by the emergence of a subset of NA-MMΦ which expressed homeostatic microglia genes, including *P2ry12*, a sensor of neuronal health that has been shown to play a critical role in protecting from neurodegeneration[212]. While further studies are warranted to elucidate the role of this P2ry12^{+} NA-MMΦ subset, these findings suggest that tissue homeostasis is largely preserved in the aging male gut.

On the contrary, neurodegeneration and constipation in female mice was accompanied by significant shifts in MMΦ populations in both abundance and gene expression. Of particular interest, we observed the down regulation of *Itgb5* in aging female MMΦ, which may be implicated in the accumulation of

debris and insoluble protein aggregates in the aging *muscularis externa*[210]. While the inoculation of protein aggregates did not itself trigger neurodegeneration or changes in MMΦ function, the accumulation of insoluble protein aggregates in the aging *muscularis externa* may rather reflect reduced clearance by MMΦ in aging. In line, we observed a significant reduction of neuronal phagocytosis by MMΦ in aging females compared to young. Taken together, these findings suggest that loss of NA-MMΦ and reduced clearance by MMΦ may underlie progressive accumulation of debris and neurodegeneration in the aging female myenteric plexus.

5.1.5 *Conclusions and Future Prospects*

Our findings here further underscore the crucial role macrophages play in in the health and function of the enteric nervous system, however many questions still remain unanswered. Indeed, while we uncovered a role of macrophages in shaping the ENS early in life, future studies should elucidate the mechanisms that underlie postnatal ENS refinement, in addition to uncovering long-term consequences of impaired macrophage function early in life. Furthermore, while it is clear that macrophages undergo a significant functional maturation from early in life to adulthood, it is still unclear whether this shift is triggered by developmental programming or environmental cues, such as the adoption of a solid diet. Finally, while we demonstrated that loss of neuron-associated macrophages may underlie neurodegeneration and constipation in aging female mice, it remains unclear why only females, and not males, are affected. The studies presented here were greatly hampered by the fundamental lack of knowledge of the role female gonadal hormones play not only in the most crucial gastro-intestinal functions, but also their role in shaping macrophage function, phenotype and identity. Future studies should thus focus on filling the gap present in the current literature, and elucidate whether female gonadal hormones indeed underlie the profound changes observed in the aging female *muscularis externa.*

While we have shown that neuron-macrophage in the enteric nervous system is of crucial importance throughout life in mice, it will be of great interest to further investigate whether these findings can be translated to humans, and aging-associated constipation in geriatric patients. Of note, constipation is more prevalent in females than in males, also in advanced age, suggesting that gender-specific mechanisms may be conserved from mice to humans[155]. Furthermore, while neuronal loss has been observed in humans with aging, studies have failed to differentiate between male and female patients, so the link between gender and neurodegeneration remains to be clarified. Further studies are required to define the transcriptome and function of muscularis macrophages in humans, and whether their dysfunction may be linked to aging-associated neurodegeneration and constipation.

Our findings here highlight the crucial role of macrophages in shaping, supporting and protecting the ENS from early in life to aging. These data further highlight the parallels between the CNS and the ENS. Indeed, the common mechanisms of neuro-immune interaction shared by CNS and ENS suggest that the ENS, as 'brain of the gut' may offer insight into ongoing pathological processes in the brain. This concept is of particular interest in the context of aging, but also in the context of neurodegenerative disorders of the CNS, which are frequently foreshadowed by ENS symptomatology, and neurodegenerative disorders of the ENS itself, including diabetes and obesity. Taken together, I hope the findings presented in this thesis have convinced the reader of the importance of furthering our understanding of macrophage function and plasticity in the GI tract, with the ultimate goal of harnessing their vast therapeutic potential in neurodegenerative disease and beyond.

Chapter 6

Scientific Summary

Tissue resident macrophages have long been known for their role in host defense and pathogen clearance, but only in recent years have we come to appreciate that these cells can develop a surprising degree of functional specialisation, thereby fulfilling tissue-specific functions in the organ in which they reside. The instruction of such specific functions is largely imprinted via signalling from surrounding cells, the so-called macrophages *niche*. Thanks to the signals derived from the surrounding niche, macrophages can adopt specific transcriptomes and functions, and fulfil tissue-specific functions including the recycling of surfactant in the lung, the regulation of electric conduction in the heart, and regulation of arterial stiffness in the aorta.

In the gut, tissue resident macrophages can be found throughout the distinct layers from the lumen to the serosa, where they perform functions specific to their niche. Beneath the epithelial cells and in close proximity to luminal content, lamina propria macrophages participate in host defense by the clearance of invading pathogens; deeper within the tissue and located close to blood vessels, blood vessel-associated macrophages maintain vascular integrity; finally, muscularis macrophages located close to the neurons of the myenteric plexus maintain neuronal health and regulate peristalsis. Neuron-associated macrophages are thus critical for the correct functioning of the GI tract, and for the support and survival of enteric neurons.

The enteric nervous system (ENS) derives from precursors that colonise the GI tract prior to birth, and continues to undergo maturation during early postnatal life. Indeed, the spontaneous contractions that occur throughout the length of the intestine, and that are required to propel intestinal content, only mature after the time of weaning. This maturation reflects the needs of the intestine, as it needs to adapt to the transition from a liquid diet to a solid diet after the time of weaning. In Chapter 3, we demonstrate that early in life, macrophages located in the *muscularis externa* participate in the refinement of enteric nervous system, and that the absence of such refinement leads to accelerated intestinal transit and hyperganglionosis. At the time of weaning, these macrophages undergo a transcriptional and functional transition, with a reduction of phagocytic Lyve1+ macrophages, and the expansion of a neuron-associated macrophage subset. The phenotype of neuron-associated macrophages was shown to be imprinted by transforming growth factor beta (TGFβ), that is produced by the enteric nervous system itself. Loss of TGFβ signalling led to a reduction in neuron-associated macrophages, loss of enteric neurons and delay in intestinal transit. Taken together, these findings highlight the developmental plasticity of muscularis macrophages, and shed light on how neurons can imprint a local, neurosupportive macrophage population.

Once the neuron-associated macrophage population has been established after weaning, these macrophages provide support and protection to enteric neurons throughout life. Considering their vital

role in sustaining neuronal survival, it is of key importance to investigate the role these cells may play in neurodegenerative diseases of the GI tract. It has been shown that during aging, there is a progressive loss of enteric neurons which may underlie age-associated gastro-intestinal complaints, including constipation. In Chapter 4, we demonstrate that in mice, females develop a delay in gastro-intestinal transit and neurodegeneration with aging, while male mice are protected from age-related gastro-intestinal dysfunction.

To investigate whether loss or dysfunction of muscularis macrophages may underlie aging-associated neurodegeneration, we performed single-cell RNA sequencing on muscularis macrophages on young and old, male and female mice. Single-cell RNA sequencing revealed that significant transcriptional shifts occur between young and old female macrophages, while the transcriptome of old male macrophages remains relatively similar to that of young macrophages. Furthermore, we detected a significant loss of neuron-associated macrophages in aging females mice, that may underlie neurodegeneration in aging female mice. Of interest, neuron-associated macrophages were preserved in aging male mice, an observation that was associated with the expansion of a subset of neuron-associated macrophages upregulating homeostatic genes, which may provide support to neuronal regeneration in aging male mice. Finally, we detected a reduction of phagocytosis by aging female macrophages, coupled with downregulation of key genes including *Itgb5*. To what extent this may be implicated in the clearance of neuronal debris and insoluble protein aggregates remains to be studied. In line, we observed accumulation of such aggregates in the aging *muscularis externa*. While further studies are warranted to validate these findings, our results suggest that dysfunction of loss of muscularis macrophages may play a critical role in neurodegeneration and constipation in the aging female *muscularis externa.*

Taken together, the findings presented in this thesis highlight the exceptional plasticity of muscularis macrophages, that adapt throughout life to the evolving needs of the tissue. Furthermore, we uncover a hitherto unknown role for muscularis macrophages in shaping the enteric nervous system during development, and shed light on the instruction of neuro—supportive macrophages in adulthood. These findings pave the way towards harnessing the therapeutic potential of muscularis macrophages, and may, in the future, enable the scientific community to tackle neurodegenerative diseases that affect the GI tract, which currently lack effective therapeutic strategies.

Bibliography

1. Bain, C. C. *et al.* Constant replenishment from circulating monocytes maintains the macrophage pool in the intestine of adult mice. *Nat. Immunol.* **15**, 929–937 (2014).

2. Guilliams, M., Thierry, G. R., Bonnardel, J. & Bajenoff, M. Establishment and Maintenance of the Macrophage Niche. *Immunity* **52**, 434–451 (2020).

3. van Furth, R. Origin and Kinetics of Mononuclear Phagocytes. *Ann. N. Y. Acad. Sci.* **278**, 161–175 (1976).

4. van Furth, R. *et al.* The mononuclear phagocyte system: a new classification of macrophages, monocytes, and their precursor cells. *Bull. World Health Organ.* **46**, 845–852 (1972).

5. Yona, S. *et al.* Fate mapping reveals origins and dynamics of monocytes and tissue macrophages under homeostasis [Immunity 38 (2013) 79-91]. *Immunity* **38**, 79–91 (2013).

6. Hashimoto, D. *et al.* Tissue-resident macrophages self-maintain locally throughout adult life with minimal contribution from circulating monocytes. *Immunity* **38**, 792–804 (2013).

7. Ginhoux, F. & Jung, S. Monocytes and macrophages: developmental pathways and tissue homeostasis. *Nat. Rev. Immunol.* **14**, 392–404 (2014).

8. Goldmann, T. *et al.* Origin, fate and dynamics of macrophages at central nervous system interfaces. *Nat. Immunol.* **17**, 797 (2016).

9. Hoeffel, G. *et al.* Adult Langerhans cells derive predominantly from embryonic fetal liver monocytes with a minor contribution of yolk sac–derived macrophages. *J. Exp. Med.* **209**, 1167–1181 (2012).

10. Epelman, S. *et al.* Embryonic and adult-derived resident cardiac macrophages are maintained through distinct mechanisms at steady state and during inflammation. *Immunity* **40**, 91–104 (2014).

11. Furness, J. B. The enteric nervous system and neurogastroenterology. *Nat. Rev. Gastroenterol. Hepatol.* **9**, 286–294 (2012).

12. Calderon, B. *et al.* The pancreas anatomy conditions the origin and properties of resident macrophages. *J. Exp. Med.* (2015) doi:10.1084/jem.20150496.

13. Scott, C. L. *et al.* Bone marrow-derived monocytes give rise to self-renewing and fully differentiated Kupffer cells. *Nat. Commun.* **7**, 1–10 (2016).

14. Ginhoux, F. & Guilliams, M. Tissue-Resident Macrophage Ontogeny and Homeostasis. *Immunity* vol. 44 439–449 (2016).

15. Mass, E. *et al.* Specification of tissue-resident macrophages during organogenesis. *Science* **353**, (2016).

16. Tober, J. *et al.* The megakaryocyte lineage originates from hemangioblast precursors and is an integral component both of primitive and of definitive hematopoiesis. *Blood* **109**, 1433–1441 (2007).

17. Palis, J., Robertson, S., Kennedy, M., Wall, C. & Keller, G. Development of erythroid and myeloid progenitors in the yolk sac and embryo proper of the mouse. *Development* **126**, 5073–5084 (1999).

18. Ginhoux, F. *et al.* Fate mapping analysis reveals that adult microglia derive from primitive

macrophages. *Science* **330**, 841–845 (2010).

19. Hoeffel, G. & Ginhoux, F. Ontogeny of Tissue-Resident Macrophages. *Front. Immunol.* **6**, 486 (2015).

20. Palis, J. & Yoder, M. C. Yolk-sac hematopoiesis: the first blood cells of mouse and man. *Exp. Hematol.* **29**, 927–936 (2001).

21. Hoeffel, G. *et al.* C-Myb(+) erythro-myeloid progenitor-derived fetal monocytes give rise to adult tissue-resident macrophages. *Immunity* **42**, 665–678 (2015).

22. De Schepper, S. *et al.* Self-Maintaining Gut Macrophages Are Essential for Intestinal Homeostasis. *Cell* **175**, 400-415.e13 (2018).

23. Shaw, T. N. *et al.* Tissue-resident macrophages in the intestine are long lived and defined by Tim-4 and CD4 expression. *J. Exp. Med.* 1–12 (2018) doi:10.1084/jem.20180019.

24. McGovern, N. *et al.* Human Dermal CD14^{+} Cells Are a Transient Population of Monocyte-Derived Macrophages. *Immunity* **41**, 465–477 (2014).

25. Bajpai, G. *et al.* The human heart contains distinct macrophage subsets with divergent origins and functions. *Nat. Med.* **24**, 1234–1245 (2018).

26. Nayak, D. K. *et al.* Long-Term Persistence of Donor Alveolar Macrophages in Human Lung Transplant Recipients That Influences Donor-Specific Immune Responses. *Am. J. Transplant.* **16**, 2300–2311 (2016).

27. Bujko, A. *et al.* Transcriptional and functional profiling defines human small intestinal macrophage subsets. *J. Exp. Med.* jem.20170057 (2017) doi:10.1084/jem.20170057.

28. Emile, J. F. *et al.* Langerhans cell deficiency in reticular dysgenesis. *Blood* **96**, 58–62 (2000).

29. Vinh, D. C. *et al.* Autosomal dominant and sporadic monocytopenia with susceptibility to mycobacteria, fungi, papillomaviruses, and myelodysplasia. *Blood* **115**, 1519–1529 (2010).

30. Ural, B. B. *et al.* Identification of a nerve-associated, lung-resident interstitial macrophage subset with distinct localization and immunoregulatory properties. *Sci. Immunol.* **5**, eaax8756 (2020).

31. Lim, H. Y. *et al.* Hyaluronan Receptor LYVE-1-Expressing Macrophages Maintain Arterial Tone through Hyaluronan-Mediated Regulation of Smooth Muscle Cell Collagen. *Immunity* **49**, 326-341.e7 (2018).

32. Jaitin, D. A. *et al.* Lipid-Associated Macrophages Control Metabolic Homeostasis in a Trem2-Dependent Manner. *Cell* **178**, 686-698.e14 (2019).

33. van de Laar, L. *et al.* Yolk Sac Macrophages, Fetal Liver, and Adult Monocytes Can Colonize an Empty Niche and Develop into Functional Tissue-Resident Macrophages. *Immunity* **44**, 755–768 (2016).

34. Huffman, J. A., Hull, W. M., Dranoff, G., Mulligan, R. C. & Whitsett, J. A. Pulmonary epithelial cell expression of GM-CSF corrects the alveolar proteinosis in GM-CSF-deficient mice. *J. Clin. Invest.* **97**, 649–655 (1996).

35. Lavin, Y., Mortha, A., Rahman, A. & Merad, M. Regulation of macrophage development and function in peripheral tissues. *Nat. Rev. Immunol.* **15**, 731–744 (2015).

36. Wang, Y. *et al.* IL-34 is a tissue-restricted ligand of CSF1R required for the development of Langerhans cells and microglia. *Nat. Immunol.* **13**, 753–760 (2012).

37. Wiktor-Jedrzejczak, W. *et al.* Total absence of colony-stimulating factor 1 in the macrophage-deficient osteopetrotic (op/op) mouse. *Proc. Natl. Acad. Sci. U. S. A.* (1990) doi:10.1073/pnas.88.13.5937b.

38. Shibata, Y. *et al.* GM-CSF regulates alveolar macrophage differentiation and innate immunity in the lung through PU.1. *Immunity* (2001) doi:10.1016/S1074-7613(01)00218-7.

39. Yoshida, M., Ikegami, M., Reed, J. A., Chroneos, Z. C. & Whitsett, J. A. GM-CSF regulates protein and lipid catabolism by alveolar macrophages. *Am. J. Physiol. Lung Cell. Mol. Physiol.* **280**, L379-86 (2001).

40. Pridans, C. *et al.* Pleiotropic Impacts of Macrophage and Microglial Deficiency on Development in Rats with Targeted Mutation of the Csf1r Locus. *J. Immunol.* **201**, 2683–2699 (2018).

41. Dai, X.-M. *et al.* Targeted disruption of the mouse colony-stimulating factor 1 receptor gene results in osteopetrosis, mononuclear phagocyte deficiency, increased primitive progenitor cell frequencies, and reproductive defects. *Blood* **99**, 111–120 (2002).

42. Guilliams, M. *et al.* Alveolar macrophages develop from fetal monocytes that differentiate into long-lived cells in the first week of life via GM-CSF. *J. Exp. Med.* **210**, 1977–1992 (2013).

43. Nishinakamura, R. *et al.* The pulmonary alveolar proteinosis in granulocyte macrophage colony-stimulating factor/interleukins 3/5 beta c receptor-deficient mice is reversed by bone marrow transplantation. *J. Exp. Med.* **183**, 2657–2662 (1996).

44. Mikkelsen, H. B. & Thuneberg, L. Op/op mice defective in production of functional colony-stimulating factor-1 lack macrophages in muscularis externa of the small intestine. *Cell Tissue Res.* **295**, 485–493 (1999).

45. Muller, P. A. *et al.* Crosstalk between Muscularis Macrophages and Enteric Neurons Regulates Gastrointestinal Motility. *Cell* **158**, 300–313 (2014).

46. Sehgal, A. *et al.* The role of CSF1R-dependent macrophages in control of the intestinal stem-cell niche. *Nat. Commun.* **9**, 1–17 (2018).

47. Avetisyan, M. *et al.* Muscularis macrophage development in the absence of an enteric nervous system. *Proc. Natl. Acad. Sci. U. S. A.* 201802490 (2018) doi:10.1073/pnas.1802490115.

48. Ryan, G. R. *et al.* Rescue of the colony-stimulating factor 1 (CSF-1)-nullizygous mouse (Csf1(op)/Csf1(op)) phenotype with a CSF-1 transgene and identification of sites of local CSF-1 synthesis. *Blood* **98**, 74–84 (2001).

49. Abboud, S. L., Bunegin, M., Ghosh-Choudhury, N. & Woodruff, K. Analysis of the mouse CSF-1 gene promoter in a transgenic mouse model. *J. Histochem. Cytochem. Off. J. Histochem. Soc.* **51**, 941–949 (2003).

50. Huynh, D. *et al.* Colony stimulating factor-1 dependence of paneth cell development in the mouse small intestine. *Gastroenterology* **137**, 136–44, 144.e1–3 (2009).

51. Schridde, A. *et al.* Tissue-specific differentiation of colonic macrophages requires TGFβ receptor-mediated signaling. *Mucosal Immunol.* **10**, 1387–1399 (2017).

52. Yasmin, N. *et al.* Identification of bone morphogenetic protein 7 (BMP7) as an instructive factor for human epidermal Langerhans cell differentiation. *J. Exp. Med.* **210**, 2597–2610 (2013).

53. Capucha, T. *et al.* Sequential BMP7/TGF-β1 signaling and microbiota instruct mucosal Langerhans cell differentiation. *J. Exp. Med.* **215**, 481–500 (2018).

54. Sakai, M. *et al.* Liver-Derived Signals Sequentially Reprogram Myeloid Enhancers to Initiate and

Maintain Kupffer Cell Identity. *Immunity* **51**, 655-670.e8 (2019).

55. Bonnardel, J. *et al.* Stellate Cells, Hepatocytes, and Endothelial Cells Imprint the Kupffer Cell Identity on Monocytes Colonizing the Liver Macrophage Niche. *Immunity* **51**, 638-654.e9 (2019).

56. Haldar, M. *et al.* Heme-mediated SPI-C induction promotes monocyte differentiation into iron-recycling macrophages. *Cell* (2014) doi:10.1016/j.cell.2014.01.069.

57. Guilliams, M. & Scott, C. L. Does niche competition determine the origin of tissue-resident macrophages? *Nat. Rev. Immunol.* **17**, 451–460 (2017).

58. Sawai, C. M. *et al.* Hematopoietic Stem Cells Are the Major Source of Multilineage Hematopoiesis in Adult Animals. *Immunity* **45**, 597–609 (2016).

59. Collins, S. M. & Bercik, P. The relationship between intestinal microbiota and the central nervous system in normal gastrointestinal function and disease. *Gastroenterology* **136**, 2003–2014 (2009).

60. Berry, M. R. *et al.* Renal Sodium Gradient Orchestrates a Dynamic Antibacterial Defense Zone. *Cell* **170**, 860-874.e19 (2017).

61. Lambrecht, B. & Guilliams, M. Monocytes find a new place to dwell in the niche of heartbreak hotel. *J. Exp. Med.* **211**, 2136 (2014).

62. Honda, M. *et al.* Perivascular localization of macrophages in the intestinal mucosa is regulated by Nr4a1 and the microbiome. *Nat. Commun.* **11**, (2020).

63. Mikkelsen, H. B., Garbarsch, C., Tranum-Jensen, J. J. & Thuneberg, L. Macrophages in the small intestinal muscularis externa of embryos, newborn and adult germ-free mice. *J. Mol. Histol.* **35**, 377–387 (2004).

64. Tagliani, E. *et al.* Coordinate regulation of tissue macrophage and dendritic cell population dynamics by CSF-1. *J. Exp. Med.* **208**, 1901–1916 (2011).

65. Tushinski, R. J. *et al.* Survival of mononuclear phagocytes depends on a lineage-specific growth factor that the differentiated cells selectively destroy. *Cell* **28**, 71–81 (1982).

66. Jenkins, S. J. *et al.* IL-4 directly signals tissue-resident macrophages to proliferate beyond homeostatic levels controlled by CSF-1. *J. Exp. Med.* **210**, 2477–2491 (2013).

67. Ulich, T. R., del Castillo, J., Watson, L. R., Yin, S. M. & Garnick, M. B. In vivo hematologic effects of recombinant human macrophage colony-stimulating factor. *Blood* **75**, 846–850 (1990).

68. Asano, K. *et al.* Intestinal CD169 + macrophages initiate mucosal inflammation by secreting CCL8 that recruits inflammatory monocytes. *Nat. Commun.* **6**, 1–7 (2015).

69. Bonnardel, J. *et al.* Innate and Adaptive Immune Functions of Peyer's Patch Monocyte-Derived Cells. *Cell Rep.* **11**, 770–784 (2015).

70. Kang, B. *et al.* Commensal microbiota drive the functional diversification of colon macrophages. *Mucosal Immunol.* **13**, 216–229 (2020).

71. Bain, C. C. *et al.* Resident and pro-inflammatory macrophages in the colon represent alternative context-dependent fates of the same Ly6Chi monocyte precursors. *Mucosal Immunol.* **6**, 498–510 (2013).

72. Smythies, L. E. *et al.* Human intestinal macrophages display profound inflammatory anergy despite avid phagocytic and bacteriocidal activity. *J. Clin. Invest.* **115**, 66–75 (2005).

73. Roberts, P. J. *et al.* The physiological expression of inducible nitric oxide synthase (iNOS) in the human colon. *J. Clin. Pathol.* (2001) doi:10.1136/jcp.54.4.293.

74. Mazzini, E., Massimiliano, L., Penna, G. & Rescigno, M. Oral Tolerance Can Be Established via Gap Junction Transfer of Fed Antigens from CX3CR1+ Macrophages to CD103+ Dendritic Cells. *Immunity* **40**, 248–261 (2014).

75. Worbs, T. *et al.* Oral tolerance originates in the intestinal immune system and relies on antigen carriage by dendritic cells. *J. Exp. Med.* **203**, 519–527 (2006).

76. Schulz, O. *et al.* Intestinal CD103 $^{+}$, but not CX3CR1 $^{+}$, antigen sampling cells migrate in lymph and serve classical dendritic cell functions. *J. Exp. Med.* **206**, 3101–3114 (2009).

77. Hadis, U. *et al.* Intestinal Tolerance Requires Gut Homing and Expansion of FoxP3+ Regulatory T Cells in the Lamina Propria. *Immunity* **34**, 237–246 (2011).

78. Kim, M. *et al.* Critical Role for the Microbiota in CX3CR1+Intestinal Mononuclear Phagocyte Regulation of Intestinal T Cell Responses. *Immunity* **49**, 151-163.e5 (2018).

79. Cassani, B. *et al.* Gut-Tropic T Cells That Express Integrin α4β7 and CCR9 Are Required for Induction of Oral Immune Tolerance in Mice. *Gastroenterology* **141**, 2109–2118 (2011).

80. Niess, J. H. *et al.* CX3CR1-mediated dendritic cell access to the intestinal lumen and bacterial clearance. *Science (80-.).* **307**, 254–258 (2005).

81. Chieppa, M., Rescigno, M., Huang, A. Y. C. & Germain, R. N. Dynamic imaging of dendritic cell extension into the small bowel lumen in response to epithelial cell TLR engagement. *J. Exp. Med.* **203**, 2841 LP – 2852 (2006).

82. Morita, N. *et al.* GPR31-dependent dendrite protrusion of intestinal CX3CR1(+) cells by bacterial metabolites. *Nature* **566**, 110–114 (2019).

83. Huynh, D. *et al.* CSF-1 Receptor-Dependent Colon Development, Homeostasis and Inflammatory Stress Response. *PLoS One* (2013) doi:10.1371/journal.pone.0056951.

84. Sauter, K. A. *et al.* Pleiotropic effects of extended blockade of CSF1R signaling in adult mice. *J. Leukoc. Biol.* (2014) doi:10.1189/jlb.2A0114-006R.

85. Tamoutounour, S. *et al.* CD64 distinguishes macrophages from dendritic cells in the gut and reveals the Th1-inducing role of mesenteric lymph node macrophages during colitis. *Eur. J. Immunol.* **42**, 3150–3166 (2012).

86. Gross-Vered, M. *et al.* Defining murine monocyte differentiation into colonic and ileal macrophages. *Elife* **9**, (2020).

87. Bernardo, D. *et al.* Human intestinal pro-inflammatory CD11c(high)CCR2(+)CX3CR1(+) macrophages, but not their tolerogenic CD11c(-)CCR2(-)CX3CR1(-) counterparts, are expanded in inflammatory bowel disease. *Mucosal Immunol.* **11**, 1114–1126 (2018).

88. Niess, J. H. & Adler, G. Enteric Flora Expands Gut Lamina Propria CX 3 CR1 + Dendritic Cells Supporting Inflammatory Immune Responses under Normal and Inflammatory Conditions . *J. Immunol.* **184**, 2026–2037 (2010).

89. Panea, C. *et al.* Intestinal Monocyte-Derived Macrophages Control Commensal-Specific Th17 Responses. *Cell Rep.* (2015) doi:10.1016/j.celrep.2015.07.040.

90. Kinnebrew, M. A. *et al.* Interleukin 23 production by intestinal CD103(+)CD11b(+) dendritic cells in response to bacterial flagellin enhances mucosal innate immune defense. *Immunity* **36**, 276–287 (2012).

91. Varol, C. *et al.* Intestinal lamina propria dendritic cell subsets have different origin and functions. *Immunity* **31**, 502–512 (2009).

92. Steadman, R. H., Braunfeld, M. & Park, H. Liver and Gastrointestinal Physiology. in *Pharmacology and Physiology for Anesthesia: Foundations and Clinical Application* 475–486 (Elsevier Inc., 2013). doi:10.1016/B978-1-4377-1679-5.00027-2.

93. Kang, Y.-N., Fung, C. & Vanden Berghe, P. Gut innervation and enteric nervous system development: a spatial, temporal and molecular tour de force. *Development* **148**, (2021).

94. Bergner, A. J. *et al.* Birthdating of myenteric neuron subtypes in the small intestine of the mouse. *J. Comp. Neurol.* **522**, 514–527 (2014).

95. Stakenborg, N., Viola, M. F. & Boeckxstaens, G. E. Intestinal neuro-immune interactions: focus on macrophages, mast cells and innate lymphoid cells. *Curr. Opin. Neurobiol.* **62**, 68–75 (2020).

96. Wang, P. L. *et al.* Peripheral nerve resident macrophages share tissue-specific programming and features of activated microglia. *Nat. Commun.* **11**, 2552 (2020).

97. Ydens, E. *et al.* Profiling peripheral nerve macrophages reveals two macrophage subsets with distinct localization, transcriptome and response to injury. *Nat. Neurosci.* **23**, 676–689 (2020).

98. Buttgereit, A. *et al.* Sall1 is a transcriptional regulator defining microglia identity and function. *Nat. Immunol.* **17**, 1397–1406 (2016).

99. Utz, S. G. *et al.* Early Fate Defines Microglia and Non-parenchymal Brain Macrophage Development. *Cell* **181**, 557-573.e18 (2020).

100. Bassotti, G. *et al.* Colonic neuropathological aspects in patients with intractable constipation due to obstructed defecation. *Mod. Pathol.* **20**, 367–374 (2007).

101. Wedel, T. *et al.* Oligoneuronal hypoganglionosis in patients with idiopathic slow-transit constipation. *Dis. Colon Rectum* **45**, 54–62 (2002).

102. Hori, M., Nobe, H., Horiguchi, K. & Ozaki, H. MCP-1 targeting inhibits muscularis macrophage recruitment and intestinal smooth muscle dysfunction in colonic inflammation. *Am. J. Physiol. Cell Physiol.* **294**, C391-401 (2008).

103. Pohl, J.-M. *et al.* Irf4-dependent CD103(+)CD11b(+) dendritic cells and the intestinal microbiome regulate monocyte and macrophage activation and intestinal peristalsis in postoperative ileus. *Gut* **66**, 2110–2120 (2017).

104. Gabanyi, I. *et al.* Neuro-immune Interactions Drive Tissue Programming in Intestinal Macrophages. *Cell* **164**, 378–391 (2016).

105. Stakenborg, N. *et al.* Preoperative administration of the 5-HT4 receptor agonist prucalopride reduces intestinal inflammation and shortens postoperative ileus via cholinergic enteric neurons. *Gut* **68**, 1406–1416 (2019).

106. Matteoli, G. *et al.* A distinct vagal anti-inflammatory pathway modulates intestinal muscularis resident macrophages independent of the spleen. *Gut* **63**, 938–48 (2013).

107. Matheis, F. *et al.* Adrenergic Signaling in Muscularis Macrophages Limits Infection-Induced Neuronal Loss. *Cell* **180**, 64-78.e16 (2020).

108. KASSANDER, P. Asymptomatic gastric retention in diabetics (gastroparesis diabeticorum). *Ann. Intern. Med.* **48**, 797–812 (1958).

109. Bagyánszki, M. & Bódi, N. Diabetes-related alterations in the enteric nervous system and its

microenvironment. *World J. Diabetes* **3**, 80–93 (2012).

110. Zandecki, M. *et al.* Characterization of myenteric neuropathy in the jejunum of spontaneously diabetic BB-rats. *Neurogastroenterol. Motil. Off. J. Eur. Gastrointest. Motil. Soc.* **20**, 818–828 (2008).

111. Hicks, C. W. & Selvin, E. Epidemiology of Peripheral Neuropathy and Lower Extremity Disease in Diabetes. *Curr. Diab. Rep.* **19**, 86 (2019).

112. Grover, M. *et al.* Diabetic and idiopathic gastroparesis is associated with loss of CD206-positive macrophages in the gastric antrum. *Neurogastroenterol. Motil.* **29**, (2017).

113. Harberson, J., Thomas, R. M., Harbison, S. P. & Parkman, H. P. Gastric neuromuscular pathology in gastroparesis: analysis of full-thickness antral biopsies. *Dig. Dis. Sci.* **55**, 359–370 (2010).

114. Wrzos, H. F., Cruz, A., Polavarapu, R., Shearer, D. & Ouyang, A. Nitric oxide synthase (NOS) expression in the myenteric plexus of streptozotocin-diabetic rats. *Dig. Dis. Sci.* **42**, 2106–2110 (1997).

115. Takahashi, T., Nakamura, K., Itoh, H., Sima, A. A. & Owyang, C. Impaired expression of nitric oxide synthase in the gastric myenteric plexus of spontaneously diabetic rats. *Gastroenterology* **113**, 1535–1544 (1997).

116. Grover, M., Farrugia, G. & Stanghellini, V. Gastroparesis: A turning point in understanding and treatment. *Gut* vol. 68 2238–2250 (2019).

117. Du, F., Wang, L., Qian, W. & Liu, S. Loss of enteric neurons accompanied by decreased expression of GDNF and PI3K/Akt pathway in diabetic rats. *Neurogastroenterol. Motil. Off. J. Eur. Gastrointest. Motil. Soc.* **21**, 1229-e114 (2009).

118. Chandrasekharan, B. *et al.* Colonic motor dysfunction in human diabetes is associated with enteric neuronal loss and increased oxidative stress. *Neurogastroenterol. Motil.* **23**, 131-e26 (2011).

119. Choi, K. M. *et al.* CD206-Positive M2 Macrophages That Express Heme Oxygenase-1 Protect Against Diabetic Gastroparesis in Mice. *Gastroenterology* **138**, (2010).

120. Choi, K. M. *et al.* Heme oxygenase-1 protects interstitial cells of Cajal from oxidative stress and reverses diabetic gastroparesis. *Gastroenterology* **135**, 2055–64, 2064.e1–2 (2008).

121. Cipriani, G. *et al.* Change in Populations of Macrophages Promotes Development of Delayed Gastric Emptying in Mice. *Gastroenterology* **154**, 2122-2136.e12 (2018).

122. Cipriani, G. *et al.* Diabetic Csf1op/op Mice Lacking Macrophages Are Protected Against the Development of Delayed Gastric Emptying. *CMGH* (2016) doi:10.1016/j.jcmgh.2015.09.001.

123. Bernard, C. E. *et al.* Association of low numbers of CD206-positive cells with loss of ICC in the gastric body of patients with diabetic gastroparesis. *Neurogastroenterol. Motil.* **26**, 1275–1284 (2014).

124. Chakarov, S. *et al.* Two distinct interstitial macrophage populations coexist across tissues in specific subtissular niches. *Science (80-.).* **363**, (2019).

125. Silva, H. M. *et al.* Vasculature-associated fat macrophages readily adapt to inflammatory and metabolic challenges. *J. Exp. Med.* **216**, 786–806 (2019).

126. Spadoni, I. *et al.* A gut-vascular barrier controls the systemic dissemination of bacteria. *Science (80-.).* **350**, 830 LP – 834 (2015).

127. Mouries, J. *et al.* Microbiota-driven gut vascular barrier disruption is a prerequisite for non-alcoholic steatohepatitis development. *J. Hepatol.* **71**, 1216–1228 (2019).

128. Asano, K., Kikuchi, K. & Tanaka, M. CD169 macrophages regulate immune responses toward particulate materials in the circulating fluid. *J. Biochem.* **164**, 77–85 (2018).

129. Kikuchi, K. *et al.* Macrophages Switch Their Phenotype by Regulating Maf Expression during Different Phases of Inflammation. *J. Immunol.* **201**, 635–651 (2018).

130. Rojo, Ó. P. *et al.* Serum lipopolysaccharide-binding protein in endotoxemic patients with inflammatory bowel disease. *Inflamm. Bowel Dis.* **13**, 269–277 (2007).

131. Gardiner, K. R. *et al.* Significance of systemic endotoxaemia in inflammatory bowel disease. *Gut* **36**, 897–901 (1995).

132. Han, D.-W. Intestinal endotoxemia as a pathogenetic mechanism in liver failure. *World J. Gastroenterol.* **8**, 961–965 (2002).

133. Kamada, N. *et al.* Unique CD14 intestinal macrophages contribute to the pathogenesis of Crohn disease via IL-23/IFN-gamma axis. *J. Clin. Invest.* **118**, 2269–2280 (2008).

134. Ogino, T. *et al.* Increased Th17-inducing activity of CD14+ CD163low myeloid cells in intestinal lamina propria of patients with Crohn's disease. *Gastroenterology* **145**, (2013).

135. Jones, G.-R. *et al.* Dynamics of Colon Monocyte and Macrophage Activation During Colitis. *Front. Immunol.* **9**, 2764 (2018).

136. Grishin, A., Papillon, S., Bell, B., Wang, J. & Ford, H. R. The role of the intestinal microbiota in the pathogenesis of necrotizing enterocolitis. *Semin. Pediatr. Surg.* **22**, 69–75 (2013).

137. Thaiss, C. A. *et al.* Hyperglycemia drives intestinal barrier dysfunction and risk for enteric infection. *Science (80-.).* **359**, 1376–1383 (2018).

138. Kawano, Y. *et al.* Colonic Pro-inflammatory Macrophages Cause Insulin Resistance in an Intestinal Ccl2/Ccr2-Dependent Manner. *Cell Metab.* **24**, 295–310 (2016).

139. Sato, T. *et al.* Paneth cells constitute the niche for Lgr5 stem cells in intestinal crypts. *Nature* **469**, 415–418 (2011).

140. Riba, A. *et al.* Paneth Cell Defects Induce Microbiota Dysbiosis in Mice and Promote Visceral Hypersensitivity. *Gastroenterology* **153**, 1594-1606.e2 (2017).

141. Pull, S. L., Doherty, J. M., Mills, J. C., Gordon, J. I. & Stappenbeck, T. S. Activated macrophages are an adaptive element of the colonic epithelial progenitor niche necessary for regenerative responses to injury. **102**, 99–104 (2005).

142. Seno, H. *et al.* Efficient colonic mucosal wound repair requires Trem2 signaling. *Proc. Natl. Acad. Sci. U. S. A.* **106**, 256–261 (2009).

143. Low, D., Mino-Kenudson, M. & Mizoguchi, E. Recent advancement in understanding colitis-associated tumorigenesis. *Inflamm. Bowel Dis.* **20**, 2115–2123 (2014).

144. Butovsky, O. *et al.* Identification of a unique TGF-β-dependent molecular and functional signature in microglia. *Nat. Neurosci.* **17**, 131–143 (2014).

145. Cahill, T. J. *et al.* Tissue-resident macrophages regulate lymphatic vessel growth and patterning in the developing heart. *Dev.* **148**, (2021).

146. Matcovitch-Natan, O. *et al.* Microglia development follows a stepwise program to regulate brain

homeostasis. *Science* **353**, aad8670 (2016).

147. Munro, D. A. *et al.* Macrophages restrict the nephrogenic field and promote endothelial connections during kidney development. *Elife* **8**, (2019).

148. Fulop, T. *et al.* Immunosenescence and Inflamm-Aging As Two Sides of the Same Coin: Friends or Foes? *Front. Immunol.* **8**, 1960 (2017).

149. Liguori, I. *et al.* Oxidative stress, aging, and diseases. *Clin. Interv. Aging* **13**, 757–772 (2018).

150. Aprahamian, T., Takemura, Y., Goukassian, D. & Walsh, K. Ageing is associated with diminished apoptotic cell clearance in vivo. *Clin. Exp. Immunol.* **152**, 448–455 (2008).

151. van Duin, D. *et al.* Age-Associated Defect in Human TLR-1/2 Function. *J. Immunol.* **178**, 970 LP – 975 (2007).

152. Solana, R. *et al.* Innate immunosenescence: Effect of aging on cells and receptors of the innate immune system in humans. *Semin. Immunol.* **24**, 331–341 (2012).

153. Hammond, T. R. *et al.* Single-Cell RNA Sequencing of Microglia throughout the Mouse Lifespan and in the Injured Brain Reveals Complex Cell-State Changes. *Immunity* **50**, 253-271.e6 (2019).

154. Candlish, M. & Hefendehl, J. K. Microglia Phenotypes Converge in Aging and Neurodegenerative Disease . *Frontiers in Neurology* vol. 12 (2021).

155. Gallegos-Orozco, J. F., Foxx-Orenstein, A. E., Sterler, S. M. & Stoa, J. M. Chronic Constipation in the Elderly. *Am. J. Gastroenterol.* **107**, 18–25 (2012).

156. Bernard, c. e. *et al.* Effect of age on the enteric nervous system of the human colon. *Neurogastroenterol. Motil.* **21**, 746-e46 (2009).

157. Phillips, R. J., Kieffer, E. J. & Powley, T. L. Aging of the myenteric plexus: Neuronal loss is specific to cholinergic neurons. *Auton. Neurosci. Basic Clin.* **106**, 69–83 (2003).

158. Fung, C. & Vanden Berghe, P. Functional circuits and signal processing in the enteric nervous system. *Cell. Mol. Life Sci.* **77**, 4505–4522 (2020).

159. Athow, A. C., Filipe, M. I. & Drake, D. P. Hyperganglionosis mimicking Hirschsprung's disease. *Arch. Dis. Child.* **66**, 1300–1303 (1991).

160. Terra, S. A., De Arruda Lourenção, P. L., Silva, M. G., Miot, H. A. & Rodrigues, M. A. M. A critical appraisal of the morphological criteria for diagnosing intestinal neuronal dysplasia type B. *Mod. Pathol. 2017 307* **30**, 978–985 (2017).

161. Rao, M. & Gershon, M. D. The bowel and beyond: the enteric nervous system in neurological disorders. *Nat. Rev. Gastroenterol. Hepatol.* **13**, 517–528 (2016).

162. Parathan, P., Wang, Y., Leembruggen, A. J., Bornstein, J. C. & Foong, J. P. The enteric nervous system undergoes significant chemical and synaptic maturation during adolescence in mice. *Dev. Biol.* **458**, 75–87 (2020).

163. Vries, P. de, Soret, R., Suply, E., Heloury, Y. & Neunlist, M. Postnatal development of myenteric neurochemical phenotype and impact on neuromuscular transmission in the rat colon. *Am. J. Physiol. Gastrointest. Liver Physiol.* **299**, 539–547 (2010).

164. Nobs, S. P. & Kopf, M. Tissue-resident macrophages: guardians of organ homeostasis. *Trends Immunol.* **42**, 495–507 (2021).

165. Viola, M. F. & Boeckxstaens, G. Niche-specific functional heterogeneity of intestinal resident

macrophages. *Gut* (2020) doi:10.1136/gutjnl-2020-323121.

166. Cipriani, G. *et al.* Muscularis Propria Macrophages Alter the Proportion of Nitrergic but Not Cholinergic Gastric Myenteric Neurons. *Cellular and molecular gastroenterology and hepatology* vol. 7 689-691.e4 (2019).

167. Schafer, D. P., Lehrman, E. K., Heller, C. T. & Stevens, B. An Engulfment Assay: A Protocol to Assess Interactions Between CNS Phagocytes and Neurons. *J. Vis. Exp.* e51482–e51482 (2014) doi:10.3791/51482.

168. Sankowski, R., Monaco, G. & Prinz, M. Evaluating microglial phenotypes using single-cell technologies. *Trends Neurosci.* **45**, 133–144 (2022).

169. Luissint, A.-C., Nusrat, A. & Parkos, C. A. JAM-related proteins in mucosal homeostasis and inflammation. *Semin. Immunopathol.* **36**, 211–226 (2014).

170. La Manno, G. *et al.* RNA velocity of single cells. *Nature* **560**, 494–498 (2018).

171. Aibar, S. *et al.* SCENIC: single-cell regulatory network inference and clustering. *Nat. Methods* **14**, 1083–1086 (2017).

172. Joseph, N. M. *et al.* Enteric glia are multipotent in culture but primarily form glia in the adult rodent gut. *J. Clin. Invest.* **121**, 3398–3411 (2011).

173. Sakata, K., Kunieda, T., Furuta, T. & Sato, A. Selective destruction of intestinal nervous elements by local application of benzalkonium solution in the rat. *Experientia* **35**, 1611–1613 (1979).

174. Sato, A. *et al.* Pathophysiology of aganglionic colon and anorectum: an experimental study on aganglionosis produced by a new method in the rat. *J. Pediatr. Surg.* **13**, 399–435 (1978).

175. Gombash, S. E. *et al.* Intravenous AAV9 efficiently transduces myenteric neurons in neonate and juvenile mice. *Front. Mol. Neurosci.* **7**, 81 (2014).

176. Zöller, T. *et al.* Silencing of TGFβ signalling in microglia results in impaired homeostasis. *Nat. Commun.* **9**, 4011 (2018).

177. Wrana, J. L., Attisano, L., Wieser, R., Ventura, F. & Massagué, J. Mechanism of activation of the TGF-β receptor. *Nat. 1994 3706488* **370**, 341–347 (1994).

178. Pandey, U. & Aich, P. Postnatal intestinal mucosa and gut microbial composition develop hand in hand: A mouse study. *Biomed. J.* (2022) doi:https://doi.org/10.1016/j.bj.2022.03.004.

179. Prinz, M., Masuda, T., Wheeler, M. A. & Quintana, F. J. Microglia and Central Nervous System-Associated Macrophages-From Origin to Disease Modulation. *Annu. Rev. Immunol.* **39**, 251–277 (2021).

180. Masuda, T. *et al.* Novel Hexb-based tools for studying microglia in the CNS. *Nat. Immunol.* **21**, 802–815 (2020).

181. Schafer, D. P. *et al.* Microglia Sculpt Postnatal Neural Circuits in an Activity and Complement-Dependent Manner. *Neuron* **74**, 691–705 (2012).

182. Walton, N. M. *et al.* Microglia instruct subventricular zone neurogenesis. *Glia* **54**, 815–825 (2006).

183. Kierdorf, K. *et al.* Microglia emerge from erythromyeloid precursors via Pu.1- and Irf8-dependent pathways. *Nat. Neurosci.* **16**, 273–280 (2013).

184. Lenz, K. M. & Nelson, L. H. Microglia and Beyond: Innate Immune Cells As Regulators of Brain

Development and Behavioral Function. *Front. Immunol.* **9**, 698 (2018).

185. Orłowski, D., Sołtys, Z. & Janeczko, K. Morphological development of microglia in the postnatal rat brain. A quantitative study. *Int. J. Dev. Neurosci. Off. J. Int. Soc. Dev. Neurosci.* **21**, 445–450 (2003).

186. Parkhurst, C. N. *et al.* Microglia Promote Learning-Dependent Synapse Formation through Brain-Derived Neurotrophic Factor. *Cell* **155**, 1596–1609 (2013).

187. Nelson, L. H. & Lenz, K. M. Microglia depletion in early life programs persistent changes in social, mood-related, and locomotor behavior in male and female rats. doi:10.1016/j.bbr.2016.09.006.

188. Wedel, T. *et al.* Enteric nerves and interstitial cells of Cajal are altered in patients with slow-transit constipation and megacolon. *Gastroenterology* **123**, 1459–1467 (2002).

189. Bassotti, G., Villanacci, V. & Nejad, M. R. Chronic constipation: no more idiopathic, but a true neuropathological entity. *Gastroenterol. Hepatol. From Bed to Bench* **4**, 109 (2011).

190. Chalazonitis, A. & Rao, M. Enteric nervous system manifestations of neurodegenerative disease. *Brain Res.* **1693**, 207 (2018).

191. Niesler, B., Kuerten, S., Demir, I. E. & Schäfer, K.-H. Disorders of the enteric nervous system — a holistic view. *Nat. Rev. Gastroenterol. Hepatol.* **18**, 393–410 (2021).

192. Yona, S. *et al.* Fate mapping reveals origins and dynamics of monocytes and tissue macrophages under homeostasis. *Immunity* **38**, 79 (2013).

193. Hao, M. M. *et al.* Early Emergence of Neural Activity in the Developing Mouse Enteric Nervous System. *J. Neurosci.* **31**, 15352 (2011).

194. Vanden Berghe, P., Kenyon, J. L. & Smith, T. K. Mitochondrial Ca2+ uptake regulates the excitability of myenteric neurons. *J. Neurosci.* **22**, 6962–6971 (2002).

195. Becker, L. *et al.* Age-dependent shift in macrophage polarisation causes inflammation-mediated degeneration of enteric nervous system. *Gut* gutjnl-2016-312940 (2017) doi:10.1136/gutjnl-2016-312940.

196. Picelli, S. *et al.* Full-length RNA-seq from single cells using Smart-seq2. *Nat. Protoc.* **9**, 171–181 (2014).

197. Jurk, D. *et al.* Postmitotic neurons develop a p21-dependent senescence-like phenotype driven by a DNA damage response. *Aging Cell* **11**, 996–1004 (2012).

198. Jiang, Y., Greenwood-Van Meerveld, B., Johnson, A. C. & Travagli, R. A. Role of estrogen and stress on the brain-gut axis. *Am. J. Physiol. Liver Physiol.* **317**, G203–G209 (2019).

199. Phillips, R. J., Walter, G. C., Ringer, B. E., Higgs, K. M. & Powley, T. L. Alpha-synuclein immunopositive aggregates in the myenteric plexus of the aging Fischer 344 rat. *Exp. Neurol.* **220**, 109–19 (2009).

200. Takahashi, M. *et al.* Macrophage lipoprotein lipase modulates the development of atherosclerosis but not adiposity. *J. Lipid Res.* **54**, 1124–1134 (2013).

201. Kim, K. *et al.* Transcriptome Analysis Reveals Nonfoamy Rather Than Foamy Plaque Macrophages Are Proinflammatory in Atherosclerotic Murine Models. *Circ. Res.* **123**, 1127–1142 (2018).

202. Nugent, A. A. *et al.* TREM2 Regulates Microglial Cholesterol Metabolism upon Chronic Phagocytic Challenge. *Neuron* **105**, 837-854.e9 (2020).

203. Cochain, C. *et al.* Single-Cell RNA-Seq Reveals the Transcriptional Landscape and Heterogeneity of Aortic Macrophages in Murine Atherosclerosis. *Circ. Res.* **122**, 1661–1674 (2018).

204. Bain, C. C. *et al.* Rate of replenishment and microenvironment contribute to the sexually dimorphic phenotype and function of peritoneal macrophages. *Sci. Immunol.* **5**, (2020).

205. Viola, M. F. *et al.* Neuro-immune Crosstalk in the Enteric Nervous System from Early Postnatal Development to Adulthood. *bioRxiv* 2022.05.12.491517 (2022) doi:10.1101/2022.05.12.491517.

206. Xia, C., Braunstein, Z., Toomey, A. C., Zhong, J. & Rao, X. S100 Proteins As an Important Regulator of Macrophage Inflammation. *Front. Immunol.* **8**, 1 (2017).

207. Müller, C. *et al.* Reduced expression of C/EBPβ-LIP extends health and lifespan in mice. *Elife* **7**, (2018).

208. Murk, K., Ornaghi, M. & Schiweck, J. Profilin Isoforms in Health and Disease – All the Same but Different . *Frontiers in Cell and Developmental Biology* vol. 9 (2021).

209. Ruggiero, L., Connor, M. P., Chen, J., Langen, R. & Finnemann, S. C. Diurnal, localized exposure of phosphatidylserine by rod outer segment tips in wild-type but not Itgb5-/- or Mfge8-/- mouse retina. *Proc. Natl. Acad. Sci. U. S. A.* **109**, 8145–8148 (2012).

210. Nandrot, E. F. *et al.* Loss of synchronized retinal phagocytosis and age-related blindness in mice lacking alphavbeta5 integrin. *J. Exp. Med.* **200**, 1539–1545 (2004).

211. Allen Reish, H. E. & Standaert, D. G. Role of α-synuclein in inducing innate and adaptive immunity in Parkinson disease. *J. Parkinsons. Dis.* **5**, 1–19 (2015).

212. Cserép, C. *et al.* Microglia monitor and protect neuronal function through specialized somatic purinergic junctions. *Science* **367**, 528–537 (2020).

213. Ganguly, U. *et al.* Alpha-Synuclein as a Biomarker of Parkinson's Disease: Good, but Not Good Enough . *Frontiers in Aging Neuroscience* vol. 13 (2021).

214. Cascella, R., Bigi, A., Cremades, N. & Cecchi, C. Effects of oligomer toxicity, fibril toxicity and fibril spreading in synucleinopathies. *Cell. Mol. Life Sci.* **79**, 174 (2022).

215. Wald, A. *et al.* Gastrointestinal transit: the effect of the menstrual cycle. *Gastroenterology* **80**, 1497–1500 (1981).

216. Nie, X., Xie, R. & Tuo, B. Effects of Estrogen on the Gastrointestinal Tract. *Dig. Dis. Sci.* **63**, 583–596 (2018).

217. Keselman, A., Fang, X., White, P. B. & Heller, N. M. Estrogen Signaling Contributes to Sex Differences in Macrophage Polarization during Asthma. *J. Immunol.* **199**, 1573 LP – 1583 (2017).

218. Dama, A., Baggio, C., Boscaro, C., Albiero, M. & Cignarella, A. Estrogen Receptor Functions and Pathways at the Vascular Immune Interface. *Int. J. Mol. Sci.* **22**, (2021).

219. Kovats, S. Estrogen receptors regulate innate immune cells and signaling pathways. *Cell. Immunol.* **294**, 63–69 (2015).

220. Villa, A., Rizzi, N., Vegeto, E., Ciana, P. & Maggi, A. Estrogen accelerates the resolution of inflammation in macrophagic cells. *Sci. Rep.* **5**, 15224 (2015).

221. Smith, L. C. *et al.* Transforming growth factor beta1 targets estrogen receptor signaling in bronchial epithelial cells. *Respir. Res.* **19**, 160 (2018).

222. Toniolo, A. *et al.* Alternative activation of human macrophages is rescued by estrogen treatment

in vitro and impaired by menopausal status. *J. Clin. Endocrinol. Metab.* **100**, E50-8 (2015).

223. Chen, Q. *et al.* Catalpol Inhibits Macrophage Polarization and Prevents Postmenopausal Atherosclerosis Through Regulating Estrogen Receptor Alpha. *Front. Pharmacol.* **12**, 655081 (2021).

224. Clarke, L. L. A guide to Ussing chamber studies of mouse intestine. *AJP Gastrointest. Liver Physiol.* **296**, G1151–G1166 (2009).

225. Sheldon, R. J., Malarchik, M. E., Burks, T. F. & Porreca, F. Effects of nerve stimulation on ion transport in mouse jejunum: responses to Veratrum alkaloids. *J. Pharmacol. Exp. Ther.* **252**, 636–42 (1990).

226. Korsunsky, I. *et al.* Fast, sensitive and accurate integration of single-cell data with Harmony. *Nat. Methods* **16**, 1289–1296 (2019).

227. Arroyo Portilla, C., Tomas, J., Gorvel, J.-P. & Lelouard, H. From Species to Regional and Local Specialization of Intestinal Macrophages. *Front. cell Dev. Biol.* **8**, 624213 (2020).

228. Nicolás-Ávila, J. A., Hidalgo, A. & Ballesteros, I. Specialized functions of resident macrophages in brain and heart. *J. Leukoc. Biol.* 1–14 (2018) doi:10.1002/JLB.6MR0118-041R.

229. Bayliss, W. M. & Starling, E. H. The movements and the innervation of the large intestine. *J. Physiol.* **26**, 107–118 (1900).

230. Bain, C. C. *et al.* TGFβR signalling controls CD103(+)CD11b(+) dendritic cell development in the intestine. *Nat. Commun.* **8**, 620 (2017).

231. Wang, P. L. *et al.* Peripheral nerve resident macrophages are microglia-like cells with tissue-specific programming. *bioRxiv* 2019.12.19.883546 (2019) doi:10.1101/2019.12.19.883546.

232. Pirzgalska, R. M. *et al.* Sympathetic neuron-associated macrophages contribute to obesity by importing and metabolizing norepinephrine. *Nat. Med.* **23**, 1309–1318 (2017).

233. Kolter, J. *et al.* A Subset of Skin Macrophages Contributes to the Surveillance and Regeneration of Local Nerves. *Immunity* **50**, 1482-1497.e7 (2019).

234. Wade, P. R. & Hornby, P. J. Age-Related Neurodegenerative Changes and How They Affect the Gut. *Sci. Aging Knowl. Environ.* **2005**, pe8–pe8 (2005).

Personal Contribution and Conflict of Interests

Chapter 1: Chapter 1 was adapted from 2 published articles written by Maria Francesca Viola and Guy Boeckxstaens, and a second article written by Maria Francesca Viola, Nathalie Stakenborg and Guy Boeckxstaens. All figures were generated by Maria Francesca Viola. The chapter was corrected by Guy Boeckxstaens.

Chapter 2: Chapter 2 was written by Maria Francesca Viola and corrected by Guy Boeckxstaens.

Chapter 3: Chapter 3 was written by Maria Francesca Viola and corrected by Guy Boeckxstaens. All figures were generated by Maria Francesca Viola. Throughout experiments, we were assisted by Iris Appeltans and Naomi Fabre. Marta Chavero-Pieres performed immunohistochemical analyses, including neuronal quantification shown in Figures 1B-E and 2B. Elodie Modave and Alejandro Sifrim performed analysis of single-cell RNA sequencing data, and generated plots included in Figures 2J-L, 3L., S2F-G, I-J and S3A, E. Nathalie Stakenborg performed BAC experiments with Maria Francesca Viola. Marcello Delfini performed FACS-sorting of cells for data shown in 4C. Tobie Martens performed ex-vivo live-imaging for data shown in 1M. Katy Vandereyken performed HCR experiments. Jan Van Herck prepared the single-cell RNA sequencing library. Phillippe Petry performed tamoxifen injections and genotyping of Cx3cr1CreERT2 TGFBR2flox mice. Simon Verheijden and Sebastiaan De Schepper provided intellectual input. Katrin Kierdorf and Marco Prinz provided Cx3cr1CreERT2 TGFBR2flox mice and intellectual input. Pieter Vanden Berghe and Thierry Voet provided intellectual input. Imaging of HCR experiments was performed by Abril Escamilla-Ayala of the VIB Leuven BioImaging Core. Cell-sorting for Single-cell RNA sequencing experiments was performed by Reena Chinnaraj of the KU Leuven FACS core. Guy Boeckxstaens designed the study together with Maria Francesca Viola.

Chapter 4: Maria Francesca Viola designed experiments, conducted experiments, wrote the manuscript and generated the figures. Elodie Modave and Alejandro Sifrim performed analysis of scRNAseq data and generated plots shown in Figures 2A-B, 3A-B, D-E, S2A-B, S3A-C. Marta Chavero Pieres performed histological analyses shown in 1D-E and analysed muscle strip experiments shown in S1A-B. Javier Aguilera Lizzaraga performed Ussing chamber experiments. Iris Appeltans and Naomi Fabre provided excellent technical support throughout all experiments. NS assisted with scRNAseq experiments. TV provided intellectual input. Guy Boeckxstaens led the project and revised the chapter.

Chapter 5 and 6: Chapters 5 and 6 were written by Maria Francesca Viola and corrected by Guy Boeckxstaens.

There are no conflicts of interests.

Acknowledgements

Six years is a long time (and definitely more than I planned to spend doing my PhD) and I am very much indebted to the people that have put up with me so long.

To begin with, I would like to thank my jury members for finding the time to read this thesis and providing feedback. To Myriam and Schalk, thank you for accompanying me through the years, giving suggestions and challenging our findings, and always looking out for my best interests. Elvira, Kia and Martin; I have had the opportunity of working with you over the years and it is an absolute honour to have scientists I respect so much on board to evaluate my work. And Elvira, thank you for your patience and guidance, and for being a mentor to me from the day that we met!

Guy, you gave me so many opportunities and taught me so many things that it is difficult to narrow it down to a few lines. In the almost 6 years I have been here I co-authored 11 papers with you (maybe another one soon?) and that would never have been possible without the support and trust you placed in me from pretty early in my training. More than anything, I appreciate the freedom you granted me throughout these years, leaving me to explore and make mistakes until I stumbled across something interesting, and then supporting me wherever that interesting thing took me. This freedom, coupled with the fact that I could always knock on your door for advice, is what makes you a truly outstanding mentor in my view, and I am so very grateful for your guidance throughout these years.

To Pieter, thank you for all your support throughout these years. The scientific support was excellent of course, but the psychological support was also key, and you gave me the freedom to vent my frustrations on more than one occasion. Thank you for always lending an ear.

To Simon: you abandoned me early on this path, but you taught me so much in those first 6 months. Thank you for all the ideas!

To Gianluca: Over the years you've given me endless advice and answered so many questions. Thank you for always having time for me!

To Phyllis and Cindy, thank you for your *endless* patience and goodwill when I once again forgot to follow protocol, for chasing down my missing products, organising last-minute anythings and just in general, being there for a chat.

To my TARGID colleagues, thank you for the fun 6 years together. Special thank you to Joran, for our philosophical (and non) chats and for generally trying to solve any problem I had.

To my adoptee lab, the hepato lab: thank you guys for adopting me, putting up with me constantly stealing your things, feeding me and occasionally getting me drunk. Every PhD student should have an adoptee lab to hide in.

To everyone in my lab and the lab of Gianluca, the new ones and the ones that have already left: thank you for the time spent together and for making going to work a pleasure. I wish you all the best of luck in life and in science.

To my 'children': sorry for insisting on calling you that, and thank you for putting up with me. Watching you guys learn and gain confidence has been the best part in all of this.

To Iris: I can't thank you enough. You made so much possible that alone I would never have managed. Thank you for the early mornings, for performing each experiment as if it was your own and always trying to make my life easier, for supporting me and putting up with me in my most negative moments. Working with you was such a joy and I will miss you terribly.

To Naomi: You were my other half for the first 4 years of this PhD and I think half of what is in here would not be here if it had not been for you. Thank you for always being there, for giving so much importance to everything we did together and for being my friend throughout this. If I could cut this title in two and give you the other half I would… but I know you will soon have your own. Thank you for everything.

To Vero: Nessuna frase o paragrafo puo' riassumere cio' che tu sei stata per me in questi ultimi anni. Sei stata la mia roccia e la mia piu' grande sostenitrice, amica piu' intima e fonte di saggezza e forza in ogni momento. Vederti diventare mamma e' stata forse la gioia piu' grande di questi ultimi 6 anni. Non so come sara' la mia vita senza il caffe' con te ogni mattina, ma sappi che ovunque andro', mi portero' dentro un pezzettino di Vero. Grazie per essermi stata accanto in tutti questi anni. Ti voglio bene !

To my girls: thank you for the trips, the dinners, the brunches, the hidden aperos during covid, and just the general chillness of being in a group where everyone is allowed to be weird their own way. I love you all. Ivana: you are sunshine and unicorns and I wish I had all the positive vibes that you have going. Goele: thank you for all our adventures, and for saving me from sleeping under a bridge. Lisse: you are the sweetest human ever and you have been my rock especially the last year. Thank you for being you and for always supporting me. Lena: you were my first little chicken and thank god I had you. You brighten the cloudiest days. And Naomi: you are the most generous soul and you have been my rock from day one. And to Silvia of course: the crazy one that brought us all together. I miss you!

My Marisales: To the longest and craziest experiments, the even longer nights, the many bottles of wine, bowls of nachos, crumbled eggs, alarm clock cats and adventures. Thank you for being my friend, for

helping me along the way and sharing so much of your journey with me. And for answering my random texts with endless wisdom.

To Mattia, Sofia, Eleonora and Lorenzo: Thank you for feeding me on lonely nights and always giving me perspective and advice. I will always be grateful to Mattia for forgetting that Dutch coursebook!

And to my friends that having nothing to do with all of this but have always gamely listened to me and supported me each step along the way, you know who you are. Thank for the time spent together and thank you for keeping me sane.

To Elisa, my first friend in Leuven and the first friend I ever truly lost: I wish I could share this moment with you, like we always said we would.

And finally, I would like to express my endless gratitude to my family. To my parents, for their endless support and encouragement and patience, for hyping me up and celebrating me on my grouchiest days. And to my sisters, who throughout the course of these last years that I have been away have grown into the most badass women that I deeply admire. I have missed you all every single day.

And to end with: Victor. You know it all, the highs and lows, and you have taken it all into stride, despite not having any prior idea really of what you signed up for. Thank you for giving me the love, the joy, and the balance that I was never able to find on my own. I'd do it all again, just to find you along the way.

Curriculum Vitae

Maria Francesca Viola was born in Perth (GB) on the 20th of November 1992. She obtained her Bachelor in Biological Sciences with honours from the University of Bologna in 2014. She performed the research for her master thesis in the laboratory of Prof. John Cryan at the University College Cork, and graduated with honours obtaining the title of Master in Molecular and Cellular Biology in 2016. In March 2017, she began her PhD training under the supervision of Prof. Guy Boeckxstaens in the laboratory for Neuro-Immune Interaction at the KU Leuven in Belgium. Her peer-reviewed publications are listed below.

Publication Record

Chavero-Pieres M*, **Viola MF***, Appeltans I, Abdurahiman S, Gsell W, Matteoli G, Himmelreich U, Boeckxstaens G. Magnetic resonance imaging as a non-invasive tool to assess gastric emptying in mice. Neurogastroenterology and Motility 2022;00:e14490 13 November 2022.

Delfini M*, Stakenborg N*, **Viola MF**, Boeckxstaens G. Macrophages in the gut: Masters in multitasking. Immunity 55(9):1530-1548 13 Sep 2022

Viola MF, Boeckxstaens G. Muscularis macrophages: trained guardians of enteric neurons. Cell Research 32, pages 229–230 (2022)

Aguilera-Lizarraga J*, Florens M*, **Viola MF**, Jain P, Decraecker L, Appeltans I, Cuende-Estevez M, Fabre N, Van Beek K, Perna E, et al. Local immune response to food antigens drives meal-induced abdominal pain. Nature 590(7844):151- 13 Jan 2021

Viola MF, Boeckxstaens G. Niche-specific functional heterogeneity of intestinal resident macrophages. Gut 1-13 (2021)

Stakenborg N, **Viola MF**, Boeckxstaens G. Intestinal neuro-immune interactions: focus on macrophages, mast cells and innate lymphoid cells. Current Opinion In Neurobiology 62:68-75 Jun 2020

Viola MF, Boeckxstaens G. Intestinal resident macrophages: Multitaskers of the gut. Neurogastroenterology and motility 32(8):e13843 28 March 2020

Stakenborg N*, Labeeuw E*, Gomez-Pinilla PJ, De Schepper S, Aerts R, Goverse G, Farro G, Appeltans I, Meroni E, Stakenborg M, **Viola MF** et al. Preoperative administration of the 5-HT4 receptor agonist prucalopride reduces intestinal inflammation and shortens postoperative ileus via cholinergic enteric neurons. Gut 68(8):1406-1416 Aug 2019

Balemans D*, Aguilera-Lizarraga J*, Florens MV, Jain P, Denadai-Souza A, **Viola MF**, Alpizar YA, Van der Merwe S, Vanden Berghe P, Talavera K, et al. Histamine-mediated potentiation of transient receptor potential (TRP) ankyrin 1 and TRP vanilloid 4 signaling in submucosal neurons in patients with irritable bowel syndrome. American Journal Of Physiology-Gastrointestinal And Liver Physiology 316(3):G338-G349 Mar 2019

Meroni E, Stakenborg N, **Viola MF**, Boeckxstaens GE. Intestinal macrophages and their interaction with the enteric nervous system in health and inflammatory bowel disease. Acta Physiologica 225(3):11 pages; e13163 01 Mar 2019

De Schepper S*, Verheijden S*, Aguilera J, **Viola MF**, Boesmans W, Stakenborg N, Voytyuk I, Schmidt I, Boeckx B, Dierckx de Casterlé I, et al. Self-Maintaining Gut Macrophages Are Essential for Intestinal Homeostasis. Cell 175(2):400-415 04 Oct 2018

Moloney GM*, **Viola MF***, Hoban AE, Dinan TG, Cryan JF. Faecal microRNAs: indicators of imbalance at the host-microbe interface? Beneficial Microbes Article number BM2017.0013 21 Dec 2017

Luczynski P*, Tramullas M*, **Viola MF**, Shanahan F, Clarke G, O'Mahony S, Dinan TG, Cryan JF. Microbiota regulates visceral pain in the mouse. Elife 6; e25887 20 Jun 2017

* Authors contributed equally